



Cite this: *Nanoscale Adv.*, 2026, **8**, 361

## Perovskite-based photocatalysis for microbial inactivation: materials, mechanisms, and challenges

Shreya Rawat, S. A. Pranav, Tiana Denny and Manoj Bhaskaran \*

Perovskite nanomaterials have emerged as next-generation photocatalysts for antimicrobial applications due to their exceptional optoelectronic properties, tunable band gaps, and efficient generation of reactive oxygen species (ROS). These features enable visible light-driven microbial inactivation, presenting a promising alternative to conventional, UV-activated photocatalysts. This review offers a comprehensive and interdisciplinary perspective on the structural and compositional diversity of perovskites, encompassing hybrid organic–inorganic, inorganic, layered, and double perovskite systems, as well as their relevance to photoactivated antimicrobial action. Furthermore, we elucidate the mechanisms by which ROS generated by photoexcited perovskites interact with key cellular components, resulting in oxidative stress, membrane disruption, and bacterial cell death. The review highlights strategies to enhance photocatalytic performance, including elemental doping, heterojunction formation, surface passivation, and encapsulation, which optimize charge separation, improve material stability, and minimize toxicity. Additionally, we summarize the efforts made for the real-world deployment of these systems and the factors that need to be optimized and modulated, including the design of photocatalytic systems in the form of suspended or immobilized systems, as well as advanced photoreactor configurations tailored for water disinfection and surface sterilization. We also present a comparative evaluation of perovskite-based photocatalysts with traditional alternatives, demonstrating their superior visible-light responsiveness and ROS generation efficiency. Applications in healthcare, water purification, and smart textiles are discussed, alongside challenges such as lead toxicity, long-term photostability, and environmental safety. This review presents an integrated framework for understanding and advancing perovskite-based photocatalysts, laying the groundwork for translational research and sustainable antimicrobial technologies in diverse settings.

Received 2nd August 2025  
Accepted 6th November 2025

DOI: 10.1039/d5na00737b  
[rsc.li/nanoscale-advances](http://rsc.li/nanoscale-advances)

## 1. Introduction

### 1.1 Historical background and discovery

Perovskites, discovered as a naturally occurring mineral composed of calcium titanate ( $\text{CaTiO}_3$ ) in 1839, have long fascinated material scientists due to their unique properties.<sup>1</sup> The mineral was first discovered in the Ural Mountains by Russian mineralogist Alexander Kämmerer. Its chemical, physical, and structural properties were later analyzed by German mineralogist and crystallographer Gustav Rose, who named it 'perovskite' in honor of Russian politician and mineralogist Lev Perovski.<sup>2</sup> Over the decades, synthetic perovskites have been extensively developed, encompassing a vast class of compounds with the general formula  $\text{ABX}_3$ . Their unique crystal structure and versatile chemical composition quickly made them a focus of material science. In collaboration with his brother Heinrich Rose, Gustav Rose developed the

'crystal chemical mineral system' using the concept of isomorphism. This concept of perovskite structure was a great application of this system, which has also been described in the two classical books on the topic: 'Elemente der Krystallographie, nebst einer tabellarischen Uebersicht der Mineralien nach den Krystallformen' ('Elements of crystallography, in addition to a tabular overview of the minerals according to the crystal forms') in 1833 and 'Das krystallo-chemische Mineralsystem' ('The crystal chemical mineral system') in 1852. Helen Dick Megaw successfully identified the crystalline structure of perovskites in 1945 by using data from X-ray crystallography on barium titanate ( $\text{BaTiO}_3$ ).<sup>3</sup> Initially explored for their remarkable dielectric properties, perovskites gained prominence in the late 20th century with the discovery of high-temperature superconductivity in certain variants, particularly structurally flawed members of the perovskite family, such as the  $\text{La}-\text{Ba}-\text{Cu}-\text{O}$  system with a low critical temperature of 30 K.<sup>4</sup>

More recently, perovskites have gained prominence due to their excellent photophysical properties, including strong visible light absorption, efficient charge generation, and

Christ University, Hosur Road, Bangalore, India. E-mail: [manoj.bhaskaran@christuniversity.in](mailto:manoj.bhaskaran@christuniversity.in)



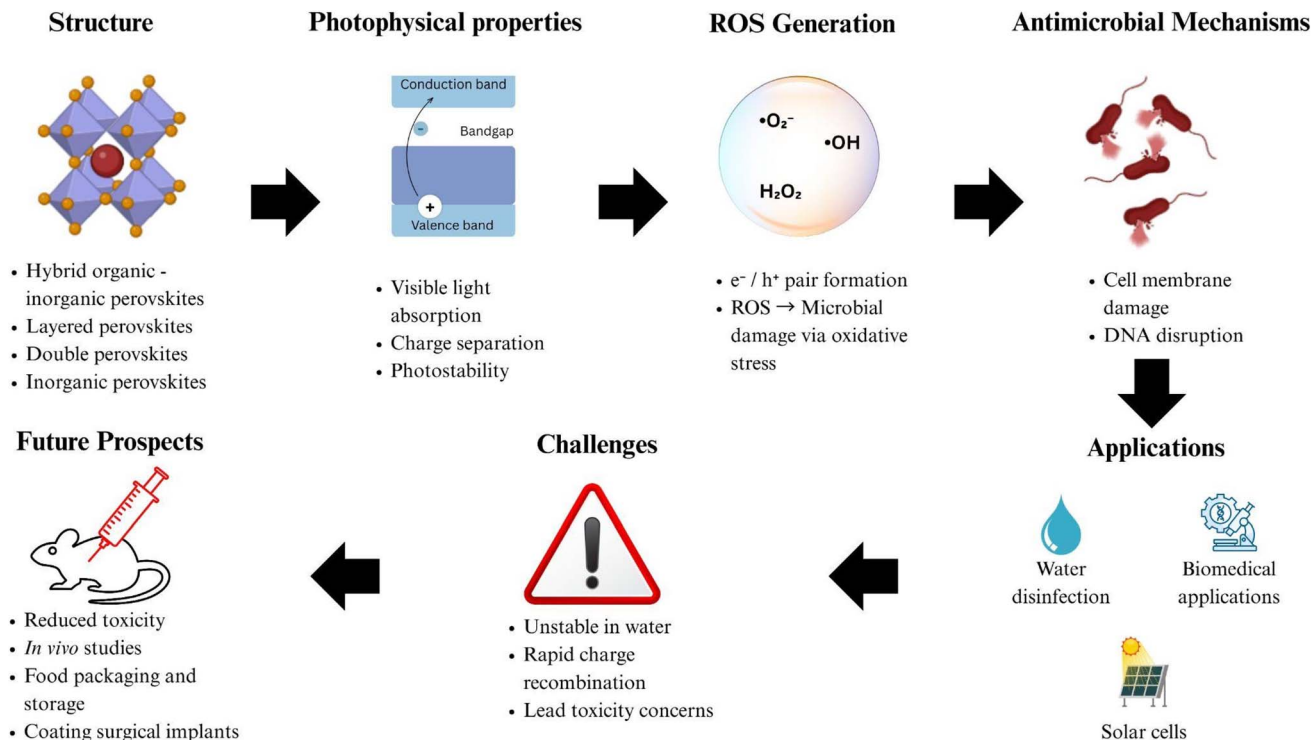


Fig. 1 Overview of the article's contents: from structural and photophysical properties to ROS generation, antimicrobial action, applications, challenges, and future advancements.

tunable bandgap. These properties lead to several key applications, including photovoltaic, fluorescence sensing, photocatalysis, and photoactivated microbial inactivation. In the following section, we summarize the peculiar properties of nanomaterials and particularly perovskites. Subsequently, we shall direct the discussion to elaborate on the focus of this article.

## 1.2. Photoactivation of nanomaterials

Nanomaterials show unique size-dependent photophysical properties that are distinct from their bulk counterparts of the same chemical composition. Nanomaterials exhibit exceptional light-responsive properties, opening many applications in chemical analysis, pharmaceuticals, biosensing, and advanced optical devices. These materials have been employed in biological applications for molecular diagnosis, cancer treatment, biosensing, and photodynamic therapy.<sup>5–7</sup>

Due to their unique properties, nanomaterials offer multiple routes to microbial inactivation. Metal nanoparticles, such as Ag nanoparticles, can release metal ions that interfere with cellular processes and damage microbial cells.<sup>8</sup> Several nanomaterials generate reactive oxygen species (ROS) upon photoactivation and have been utilized for biomedical and environmental applications. ROS-generating nanomaterials are widely used in disease treatment,<sup>9</sup> including central nervous system disorders,<sup>10</sup> and cancer,<sup>11</sup> in theranostics,<sup>12</sup> wound healing,<sup>13</sup> and as anti-inflammatory agents.<sup>14</sup> Specific nanomaterials, particularly inorganic nanomaterials such as  $\text{TiO}_2$ , have also been employed for microbial inactivation. Perovskite

nanomaterials display excellent photoactivation properties and have been used for a range of photocatalytic applications, such as environmental remediation, including organic pollutant degradation,<sup>15</sup>  $\text{CO}_2$  reduction,<sup>16</sup> hydrogen generation by water splitting,<sup>17</sup> organic transformations,<sup>18,19</sup> etc.

This review explores the photocatalyzed microbial inactivation processes driven by perovskite nanomaterials, primarily by ROS generation. We shall introduce the basic structural and functional properties of different classes of perovskites and how they aid in microbial inactivation. Further, we shall explore the mechanisms of microbial inactivation, strategies to enhance their antimicrobial activity, applications, and future directions. The outline of the article is shown below in Fig. 1.

## 1.3. Overview of different types

Perovskites may be synthesized in various compositions owing to the versatility of their structure, which arises as a wide range of elements may occupy the A, B, and X sites. Perovskites are broadly classified based on the nature and composition of these elements, dimensionality, and structural framework, which substantially influence their physical, chemical, and optoelectronic properties. Variations in the A, B, and X components of the  $\text{ABX}_3$  structure give rise to distinct categories such as oxide perovskites, halide perovskites, and hybrid organic-inorganic perovskites. Each type exhibits unique physicochemical properties influencing their stability, electronic behavior, and functional performance. In this section, we provide an overview of the classification of perovskite nanomaterials, based on their



**Table 1** Overview of common synthesis methods for perovskite materials, highlighting the types of perovskites prepared, typical reaction conditions, and key advantages and limitations of each approach

Synthesis method	Perovskite type	Conditions	Advantages	Limitations
Sol-gel method	Lead-based, nanocomposites	Low temp. ( $\sim 80\text{--}100\text{ }^\circ\text{C}$ )	Simple, cost-effective	Hard to scale, purity issues
Hydrothermal	Bismuth-based	High pressure, temp.	Uniform crystal growth	Requires special equipment
Solid-state reaction	Nanocomposites	High temp. ( $\sim 700\text{ }^\circ\text{C}$ )	High crystallinity	Energy-intensive
Spin coating	Thin-film perovskites	Room temp. $-150\text{ }^\circ\text{C}$	Uniform layers, scalable	Needs careful optimization

structure and composition, highlighting their structural characteristics and consequent applications.

**1.3.1. Hybrid organic–inorganic perovskites (HOIPs).** The structural formula of hybrid organic–inorganic perovskites (HOIPs) is  $\text{ABX}_3$ , where A, B, and X represent organic and inorganic ions, respectively. HOIPs show excellent optoelectronic features like strong light absorption, long carrier diffusion lengths, and high charge-carrier mobilities. Such characteristics are essential in achieving high power conversion efficiency in perovskite-based solar cells. Although significant improvements are necessary, the charge transport characteristics of HOIPs are comparable to those of III–V semiconductors, which serve as benchmarks for photovoltaic performance.<sup>20</sup> Hybrid Organic–Inorganic Perovskite Ferroelectrics (HOIPFs), versatile materials that show ferroelectric and piezoelectric properties, find several applications in mechanical energy harvesting, photovoltaics, and light detection.<sup>21</sup> A recent work has utilized passivated organic–inorganic hybrid perovskite quantum dots for photocatalytic antibacterial applications, where short-chain ligands with higher conjugated systems (BODIPY-OH) were used for the surface-regulated synthesis of methyl alkyl ammonium lead bromide perovskites ( $\text{MAPbBr}_3$ ). The peculiar properties of these systems were attributed to the photogenerated carrier transfer between BODIPY-OH and  $\text{MAPbBr}_3$ . The conjugation resulted in enhanced singlet oxygen generation by  $\text{MAPbBr}_3$  quantum dots, which have a potent antibacterial effect on *Escherichia coli*.<sup>22</sup> In 2021, Hachani *et al.* reported a zero-dimensional hybrid organic–inorganic  $\text{CuCl}_4$  perovskite that targeted the peptidoglycan layer in the inner membrane and showed growth inhibition for both Gram-positive (*Staphylococcus aureus* NCTC 6571) and Gram-negative bacteria (*Pseudomonas aeruginosa* SH 38).<sup>23</sup> More recently,  $\text{MAPbBr}_3$  quantum dots were surface-modified using BODIPY-OH, and subsequently encapsulated within a  $\text{SiO}_2$  shell to yield  $\text{SiO}_2@\text{BDP/QDs}$ .<sup>22</sup> The short-chain conjugated ligand enhanced singlet-oxygen generation through a photoinduced charge-transfer process, markedly improving photocatalytic antibacterial performance while maintaining colloidal stability. This work validates ligand-assisted surface engineering as an effective route to boost ROS yield in halide-perovskite nanostructures. Although HOIPs exhibit excellent optical properties, stability issues and toxicity concerns are prominent, mainly due to the presence of lead in many of their compositions. However, research is ongoing to enhance the stability of HOIPs and develop lead-free substitutes, which may mitigate environmental and health risks.

**1.3.2. Layered perovskites.** Layered perovskites comprise perovskite layers interspersed with organic or inorganic spacer cations, resulting in a natural quantum well structure. Layered perovskites can be structurally derived from their 3D counterparts by cutting along specific crystallographic planes. The general formula for the layered structure of perovskites is  $\text{A}_{n-1}\text{B}_n\text{X}_{(3n+1)}$ , where the size of the two-dimensional slabs is indicated by  $n$ . In most layered perovskites, the inorganic component consists of a single sheet ( $n = 1$ ) of corner-sharing metal-halide octahedra separated by organic cation layers. The spacing between layers and the thickness of the inorganic sheets can be modulated by the choice of organic cations.<sup>24</sup> However, these 2D materials generally lack the electronic properties required for efficient solar absorption.  $\text{Ag}^+$ , while highly bactericidal, tends to lose the property over time due to aggregation. Günay *et al.* intercalated  $\text{Ag}^+$  ions in Tm/Er co-doped layered perovskites and their 2D nanosheets to exhibit antibacterial and antibiofilm activities against the human opportunistic pathogens *Escherichia coli* and *Bacillus subtilis* through contact at a concentration of  $100\text{ }\mu\text{g mL}^{-1}$ . The mechanism of bactericidal action has not yet been confirmed, but it is anticipated that  $\text{Ag}^+$  interacts with the DNA of microbes, causing ROS-generated oxidative stress.<sup>25</sup> This study exemplifies how perovskite materials can enhance and sustain the functional properties of other active agents, demonstrating a synergistic effect wherein the perovskite matrix stabilizes  $\text{Ag}^+$  ions and prolongs their antibacterial efficacy. Layered perovskites can be chemically altered to form 2D materials, which generally exhibit less toxicity and greater stability, by separating the host layers and treating them with different lanthanides. The spatial quantum confinement effect is responsible for the various optical and photocatalytic properties of layered perovskites from their bulk form. Another advancement in this technology has been the development of an aqueous-phase dual-function chiral perovskite with applications in  $\text{H}_2\text{S}$  detection and *Escherichia coli* deactivation. Quasi 2-D perovskite nanomaterials,  $\text{Bio}(\text{S-PEA})_2\text{CsPb}_2\text{Br}_7$ , and  $\text{Bio}(\text{R-PEA})_2\text{CsPb}_2\text{Br}_7$ , when dispersed uniformly in the aqueous phase, showed rapid and sensitive fluorescence quenching for  $\text{H}_2\text{S}$ , and their positive charge facilitated cell membrane degradation of *Escherichia coli*, leading to cell death.<sup>26</sup> The electron transfer layer of perovskite solar cells was enhanced by doping zinc oxide nanofibers with  $\text{Mg}^{2+}$ , which improved the charge carrier properties of the overall nanomaterial as well tuned the bandgap from 3.36 eV to 2.8 eV. The doping-induced band tuning resulted in significant improvement in their photocatalytic properties, which were then utilized for making antibacterial textiles, which have risen



in prominence since COVID-19, as photoactive textiles can generate ROS upon illumination and inhibit bacterial proliferation and growth.<sup>27</sup> In addition to these developments, a chiral quasi-two-dimensional perovskite nanomaterial with  $\text{H}_2\text{S}$  responsiveness was recently reported as a proof-of-concept antibacterial platform. The material exhibited selective anti-*Escherichia coli* activity under visible light and demonstrated that chirality can modulate both optical response and biological interactions of layered perovskites.<sup>26</sup> This finding expands the functional landscape of chiral perovskites beyond optoelectronic applications toward biologically responsive antimicrobial systems. To summarize, layered perovskites offer a range of applications, from solar cells to antibacterial textiles, and are a flexible group of materials with highly adjustable characteristics and improved stability, offering solid promise for technological applications.

**1.3.3. Double perovskites.** Double perovskites (DPCs) are compounds that combine two simple perovskite structures,  $\text{ABO}_3$  and  $\text{AB}'\text{O}_3$ , which make up the general formula  $\text{A}_2\text{BB}'\text{O}_6$ . DPCs formed by swapping half the cations of the B site for B', which will give a rock salt structure between the two cations, are reported to show excellent optoelectronic properties.<sup>28</sup> Mehtab and coworkers developed methyl-ammonium lead halide ( $\text{MLH}$ )  $\text{CH}_3\text{NH}_3\text{PbX}_3$  ( $\text{X}$

= Cl, Br, and I) perovskites exhibiting superior optoelectronic properties with a characteristic band gap of 2.78 eV.<sup>29</sup> In 2024, Ghorbani *et al.* synthesized  $\text{Ag}^+$  doped  $\text{Ba}_2\text{FeMoO}_6$  double perovskites (BFMO) using a sol-gel technique. BFMO exhibited antibacterial activity against the Gram-positive bacterium *Staphylococcus aureus*. Ag-doped BFMO to bacterial death.<sup>30</sup> Furthermore, lead-free double perovskites have been investigated for their optoelectronic characteristics, with studies showing that they exhibit adjustable band gaps and high absorption coefficients, positioning them as favorable options for photovoltaic and related applications.<sup>30</sup> Zhang and co-workers reported  $\text{Cs}_2\text{RbTbCl}_6$  microcrystals that showed yellow-green fluorescence with an emission maximum of 547 nm and were highly selective for detecting norfloxacin in an aqueous medium. The perovskite-based sensor showed an excellent detection range of 10–200  $\mu\text{M}$  and serves as a fluorescent test paper detection system under 365 nm UV lamp irradiation.<sup>31</sup> This is considered a breakthrough in perovskite technology for two reasons: (i) aqueous medium detection and (ii) development of a stable lead-free alternative. This broad application range of DPCs and a unique combination of particles have paved the way for developing many new combinations with applications in optoelectronics, nanosensing of antibiotics, antimicrobial activity, *etc.*

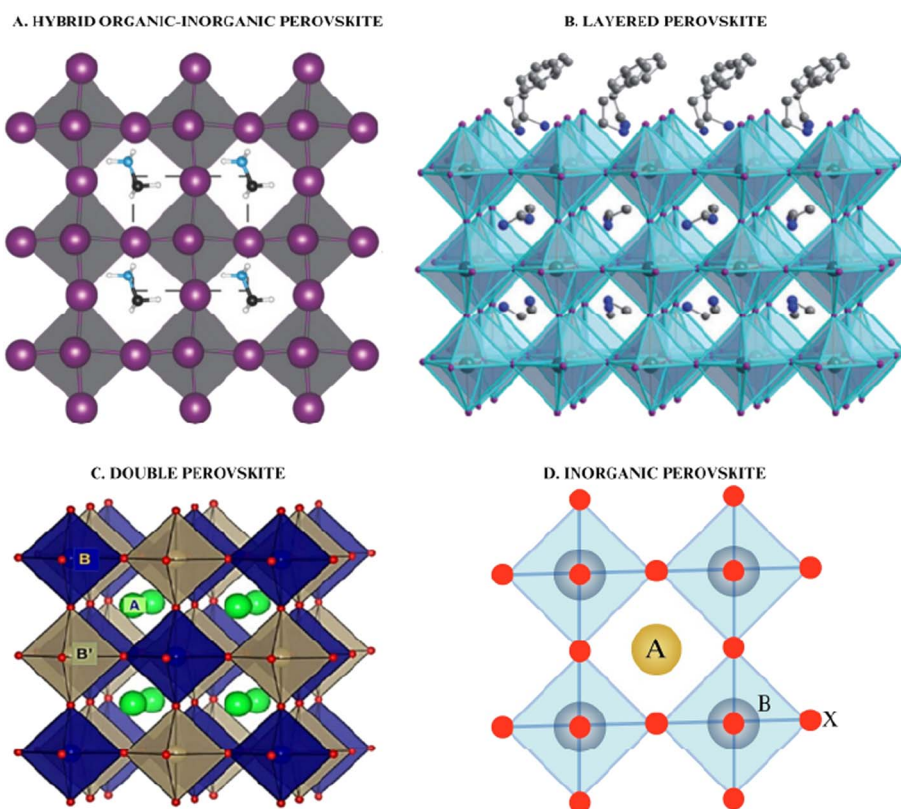


**Fig. 2** Representation of different classes of perovskite materials. (A) Methylammonium lead iodide ( $\text{MAPbI}_3$ ) perovskites. The unit cell is shown by the dashed lines, which show the atoms: carbon (black), nitrogen (blue), iodine (violet), and lead (light grey). Some adjacent unit cells are also shown.<sup>37</sup> (B) Layered perovskite  $(\text{PEA})_2(\text{MA})_2[\text{Pb}_3\text{I}_{10}]$ ;  $\text{PEA} = \text{C}_6\text{H}_5(\text{CH}_2)_2\text{NH}_3^+$ ;  $\text{MA} = \text{CH}_3\text{NH}_3^+$ . 3D structure of the perovskite molecule where the atoms are shown as lead (turquoise), iodine (purple), nitrogen (blue), and carbon (grey).<sup>24</sup> (C) Double perovskite  $\text{A}_2\text{BB}'\text{O}_6$ : A site occupied by alkaline earth metals (Ca, Sr, Ba, *etc.*) or lanthanides (La), B and B' occupied by transition metal elements (Mn, Sc, Co, Ni, *etc.*).<sup>28</sup> (D) Inorganic perovskites ( $\text{ABX}_3$ ); A is a monovalent cation like  $\text{Cs}^+$ ,  $\text{CH}_3^+$ ,  $\text{NH}_3^+$ , *etc.* B is a divalent metal cation like  $\text{Pb}^{2+}$ ,  $\text{Sn}^{2+}$ , *etc.*; X stands for halide anion-  $\text{Cl}^-$ ,  $\text{Br}^-$ , or  $\text{I}^-$ .



**Table 2** Comparative overview of different classes of perovskite materials- hybrid organic–inorganic, layered, double, and inorganic, with respect to their photocatalytic applications, efficiency highlights, advantages, and challenges

	Hybrid organic–inorganic perovskites	Layered perovskites	Double perovskites	Inorganic perovskites
Photocatalytic applications	Photogenerated carrier transfer inactivates <i>E. coli</i> by enhanced singlet oxygen ( ${}^1\text{O}_2$ ) production <sup>22</sup> Dye degradation, $\text{H}_2$ evolution, antimicrobial activity	Detection of $\text{H}_2\text{S}$ and inactivation of <i>E. coli</i> <sup>26</sup> Used for making antibacterial textiles <sup>27</sup>	Antibacterial activity through ROS generation ( ${}^{\cdot}\text{O}_2^-$ , ${}^{\cdot}\text{OH}$ , $\text{H}_2\text{O}_2$ ); $\text{Ag}^+$ doped BFMO for disinfection. <sup>30</sup> Dye degradation, $\text{CO}_2$ reduction	<i>In vitro</i> disinfection; <sup>35</sup> visible-light ROS generation against <i>S. aureus</i> , <i>P. aeruginosa</i> . <sup>36</sup> $\text{CO}_2$ photoreduction, degradation of pollutants
Efficiency highlights	Enhanced ROS generation and microbial inactivation  $\text{MAPbI}_3\text{--NiCoB}$ nanocomposite achieved high $\text{H}_2$ yield. <sup>38</sup>  Mixed-halide systems, such as $\text{MAPbI}_{3-x}\text{Cl}_x$ , allow for bandgap tunability. <sup>42</sup>	Pollutant degradation High fluorescence quenching, visible-light activity, ROS, and $\text{Ag}^+$ contribution Band gap widening and enhanced charge separation <sup>39</sup>  2D/3D interlayers improve stability to moisture and light <sup>43</sup>	Effective antimicrobial action through doping-enhanced ROS activity Lead-free alternatives have a wider band gap <sup>40</sup>  $\text{Cs}_2\text{AgBiBr}_6$ nanocrystals show rapid dye degradation and robust photocatalytic activity <sup>44</sup>	High stability, visible-light activation, and ROS generation in aqueous systems $\text{TiO}_2/\text{CsPbBr}_3$ S-scheme heterojunctions enhance carrier separation and $\text{CO}_2$ reduction <sup>41</sup> $\text{FTO/TiO}_2/\text{CsPbBr}_3$ heterojunction exhibited improved visible-light degradation of the organic dye curcumin <sup>45</sup> Strong visible absorption
Advantages	Increased quantum efficiency Easy bandgap engineering and nanoparticle fabrication	Enhanced environmental stability Better light absorption due to tunable band gap	High environmental compatibility Non-toxic  Enhanced thermal and chemical stability	Efficient charge transport
Challenges	UV photodegradation, leaching of lead, and instability in the presence of water	Lower efficiency due to non-uniform or thick layers	Reduced visible absorption Hysteresis due to trap states Slow charge transport	Partial dissolution in aqueous solutions

**1.3.4. Inorganic perovskites.** Inorganic perovskites have the general formula  $\text{ABX}_3$ , composed entirely of inorganic materials, which sets them apart from HOIPs. In this formula, 'A' is usually a monovalent cation such as cesium ( $\text{Cs}^+$ ), 'B' is a divalent cation like lead ( $\text{Pb}^{2+}$ ) or tin ( $\text{Sn}^{2+}$ ), and 'X' stands for a halide anion ( $\text{Cl}^-$ ,  $\text{Br}^-$ , or  $\text{I}^-$ ). The inorganic nature of these materials leads to significant thermal and chemical stability, which has a range of technological uses. A three-dimensional framework defines the perovskite structure, where the 'B' cation is octahedrally coordinated by six 'X' anions, forming a  $\text{BX}_6$  octahedron. The 'A' cation occupies the spaces between these octahedra, balancing the charge and maintaining structural stability. This structure provides compositional flexibility, enabling property modification through substitutions at the A, B, or X sites.<sup>32</sup> Inorganic perovskites exhibit remarkable optoelectronic properties, including a broad absorption range,<sup>33</sup> high charge carrier mobility, and tunable bandgap.<sup>34</sup> Hydrothermally synthesized  $\text{CeCuO}_3$  perovskites were evaluated as a disinfectant against microorganisms that cause urinary tract infections (UTIs), with the nanoparticles exhibiting *in vitro* disinfecting activity against these microbes.<sup>35</sup> Furthermore, Talebpour *et al.* synthesized  $\text{AgNbO}_3$  perovskites, which prevented the proliferation of microbial cells without itself undergoing corrosion. Antimicrobial activity was checked

against *Staphylococcus aureus* and *Pseudomonas aeruginosa*, and the minimum antimicrobial concentration (MIC) was similar to  $\text{Ag}_2\text{O}$ , but the silver ion release was 60 times less.<sup>36</sup> In contrast to hybrid perovskites, inorganic perovskites exhibit enhanced thermal and environmental stability. The lack of volatile organic elements minimizes degradation caused by heat and humidity, thus improving the durability of devices that utilize these materials. Inorganic perovskites are used in LEDs due to their high photoluminescence quantum yields and tunable emission wavelengths, enabling the development of efficient and color-pure light sources.<sup>32</sup> Despite their advantages, the challenge remains in their development due to Pb toxicity and scalability hurdles, which need to be addressed further and overcome by new techniques and research. Table 1 summarizes various synthetic approaches to designing perovskite nanostructures and their distinct characteristics. Fig. 2 illustrates the structural characteristics of different perovskite classes, and Table 2 summarizes their photocatalytic applications.

## 2. Structural characteristics and unique properties

Among the various classes of perovskites, inorganic perovskites, characterized by the general formula  $\text{ABX}_3$ , stand out due to



their remarkable thermal and chemical stability. Their characteristic set of properties arises not only from their compositional diversity but also from their distinct crystallographic structures. Inorganic perovskites possess a robust crystalline structure that enhances their exceptional physical and chemical characteristics. Their structure comprises a three-dimensional arrangement of corner-sharing  $BX_6$  octahedra, where the B-site cation (such as  $Pb^{2+}$  or  $Sn^{2+}$ ) is surrounded by halide anions ( $Cl^-$ ,  $Br^-$ , or  $I^-$ ) in an octahedral coordination. The A-site cation, usually a monovalent ion like  $Cs^+$ , fills the spaces within the octahedral framework, maintaining charge neutrality and contributing to structural integrity. The stability of this lattice depends on the Goldschmidt tolerance factor  $t$ , which is given by the following eqn (1).

$$t = \frac{(r_A + r_O)}{[\sqrt{2}(r_B + r_O)]} \quad (1)$$

where  $r_A$ ,  $r_B$ , and  $r_O$  indicate the radius of cation A, cation B, and the anion, respectively. Values near 1 indicate a stable perovskite structure, and deviations in  $t$  can lead to structural distortions, such as tilting of octahedra, which affect material properties.<sup>32,46</sup> Ajjouri and colleagues synthesized inorganic and hybrid organic-inorganic monohalide perovskites and reported their tunable band gaps ranging from 1.7 eV to 1.9 eV.<sup>47</sup>  $CsPbX_3$  ( $X = Cl, Br, I$ ) based mixed halide perovskite QDs with tunable emission from 408 to 694 nm was reported by changing the halide composition. The material reported in this study showed excellent photostability, which facilitates its applications in several photovoltaic devices, such as LEDs and solar cells.<sup>48</sup> Mixed-cation hybrid lead halide perovskites, with easy-to-process tunable band gaps that boost their commercialization potential, have demonstrated remarkable progress within a short span, particularly in their application to photovoltaic technologies.<sup>49</sup> More research is required to extend the absorption to longer wavelengths by band gap tuning through composition engineering and to address the stability issues. Schwartz *et al.* investigated the all-inorganic mixed metal perovskite system  $CsPb_xSnBr_3$  prepared by thermal evaporation. With increasing lead content, the shape changed from cubic to tetragonal and orthorhombic without phase segregation, and a band gap range from 1.82 eV to 2.37 eV, which is essential for photovoltaic applications.<sup>50</sup> The combination of excellent photophysical properties, structural stability, and tunability makes them an excellent candidate for antimicrobial applications.

A key factor contributing to the antibacterial properties of perovskites is their photocatalytic activity, which stems from their ability to absorb light and generate reactive oxygen species (ROS) such as hydroxyl radicals, superoxide anions, and singlet oxygen. These ROS play a crucial role in disrupting bacterial cell structures and functions, leading to effective microbial inhibition, causing intracellular component damage, microbial cell membrane disruption, and cell death.<sup>51</sup> Long-lasting antibacterial action is guaranteed by the intrinsic structural and chemical stability of inorganic perovskites, even in adverse circumstances like moisture, heat, or extended exposure to microbiological habitats. By optimizing ROS generation under visible light, the tunable bandgap lowers the need for UV light

sources. Also, their inherent property to withstand photodegradation and the leaching of harmful ions may guarantee their safe application in food packaging, water purification systems, and medical equipment.<sup>52</sup> Much attention has been paid to doping techniques and surface modifications to increase their antibacterial effectiveness while reducing any possible harmful effects on human cells, which also proves their adaptability and flexibility for use in biomedical applications. The following section summarizes the mechanisms by which photoactivation of perovskites can result in antimicrobial action.

### 3. Molecular mechanisms of photoactivated antimicrobial effects

Photocatalysis involves harnessing photon energy to drive chemical reactions on non-adsorbing substrates through single-electron transfer, energy transfer, or atom transfer.<sup>53</sup> Zhang *et al.* described photocatalysis as "a light-driven catalytic process". In essence, it refers to the acceleration of a chemical reaction facilitated by photocatalysts under light irradiation.<sup>54</sup> Fujishima and Honda in 1972 reported the phenomenon of photocatalytic water splitting on a  $TiO_2$  electrode under UV light.<sup>55</sup> The development paved the way for extensive research in photocatalysis exploiting the mechanism for numerous applications like disinfection of water<sup>56</sup> removal of metallic and inorganic pollutants,<sup>57,58</sup> purification and disinfection of air,<sup>59</sup> energy generation using photo fuel cells<sup>60</sup> and offer potential applications in medical implants,<sup>61</sup> chemical compounds delivery and food packaging.<sup>62</sup> The production of reactive species that cause fatal harm to microbial cells is essential for the photocatalyzed microbial inactivation process.

Due to their unique structural and electrical characteristics, perovskite materials have recently become robust photocatalysts in antimicrobial applications. Upon light activation, perovskites produce ROS such as hydroxyl radicals ( $^{\bullet}OH$ ), superoxide radicals ( $^{\bullet}O_2^-$ ), hydrogen peroxide ( $H_2O_2$ ), and singlet oxygen ( $^1O_2$ ), which play a crucial role in disrupting bacterial membranes, proteins, and genetic material, leading to microbial inactivation. The photoinduced electron-hole separation will initiate reduction at the valence band, forming  $^{\bullet}OH$ . In contrast, oxidation takes place in the conduction band, leading to the formation of superoxide and peroxide radicals. In a study, it was proven that the singlet oxygen, hydrogen peroxide ( $H_2O_2$ ), and photo-generated electrons contributed to the inactivation of *Escherichia coli* species by causing leakage of potassium ions, leading to consecutive cell membrane disruption and DNA degradation, inactivating the bacteria.<sup>63</sup> A schematic representation of perovskite-mediated ROS generation and subsequent antimicrobial effect is shown in Fig. 3 below.

The general steps involved in photocatalytic antimicrobial action are as follows:<sup>64</sup>

#### 3.1. Photon absorption

The photocatalyst absorbs light energy ( $h\nu$ ) equal to or greater than its band gap energy, exciting electrons ( $e^-$ ) from the



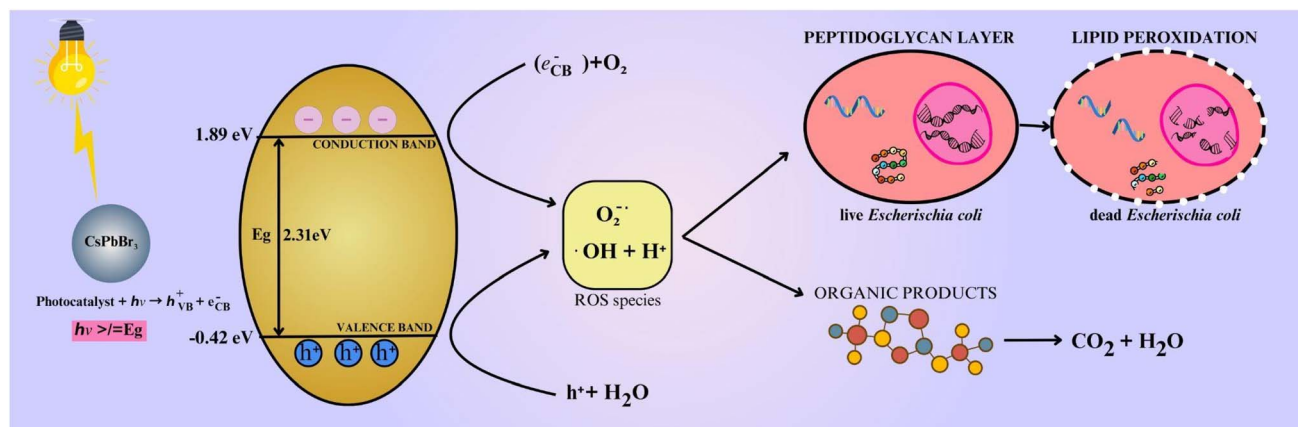
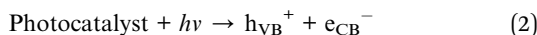


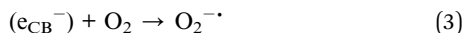
Fig. 3 Schematic representation of ROS-mediated antibacterial action of  $\text{CsPbBr}_3$  perovskite under visible light irradiation. Upon photoexcitation ( $E_g = 2.31 \text{ eV}$ ), photogenerated electrons and holes facilitate the generation of reactive oxygen species ( $\text{O}_2^{\cdot-}$ ,  $\cdot\text{OH}$ ), which disrupt the peptidoglycan layer and induce lipid peroxidation, leading to *Escherichia coli* cell death and mineralization of organic products to  $\text{CO}_2$  and  $\text{H}_2\text{O}$ .

valence band to the conduction band ( $e_{\text{CB}}$ ), leaving behind holes ( $h_{\text{VB}}^+$ ) in the valence band.<sup>65</sup> The photocatalytic activity of conventional perovskites in the visible spectrum (420–800 nm) remains low due to their wide bandgap. This presents a significant challenge in the commercial adoption of perovskite-based photocatalysts.<sup>66</sup> Perovskites (band gaps in brackets) such as  $\text{SrTiO}_3$  (3.2 eV) and  $\text{BaTiO}_3$  (3.0 eV) require high-energy UV ( $\lambda < 400 \text{ nm}$ ) for activation, with their strong photocatalytic activity stemming from their high oxidative potential. These materials lack practicality for extensive applications because UV light makes up only approximately 5% of the solar spectrum.<sup>67</sup> Materials like  $\text{BiFeO}_3$  (2.2 eV),  $\text{LaFeO}_3$  (2.1 eV), and  $\text{Cs}_3\text{Bi}_2\text{I}_9$  (2.35 eV) absorb visible light more efficiently.  $\text{CsSnI}_3$  (1.8 eV) is a near-infrared (NIR)-activated perovskite, which can absorb photons beyond 700 nm. However, the lower energy of NIR photons limits overall photocatalytic efficiency due to reduced redox potential.<sup>67</sup>

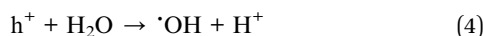


#### Generation of reactive species:

Reduction reaction: conduction band electrons ( $e_{\text{CB}}$ ) reduce molecular oxygen ( $\text{O}_2$ ) adsorbed on the catalyst's surface to form superoxide anion.



Oxidation reaction: valence band holes oxidize water ( $\text{H}_2\text{O}$ ) or hydroxide ions ( $\text{OH}^-$ ) to produce hydroxyl radicals.



The generated reactive species exhibit distinct reactivities and biological effects, targeting specific components of microbial cells. At the cellular level, the biological targets of ROS may include proteins, DNA, RNA, and lipids. Hydroxide ions are among the most important free radicals in various antibiotic pathways to eliminate causative agents. Kohanski *et al.* explained bacterial cell death *via* antibiotics, providing evidence

of ROS-driven bactericidal action formed by a Fenton-like reaction with hydroxide as the key free radical.<sup>68</sup> The supply of hydroxyl radicals leads to irreversible cell damage by oxidising protein and membrane lipid peroxidation. Hydroxyl radical formation is a convergent mechanism responsible for cell death, as it connects metabolic stress, redox imbalance, disruption of iron homeostasis, and DNA damage into a single cell-death cascade. Naturally, the mitochondrial electron transport chain is the primary source of superoxide anion radicals; however, other enzymes, such as cytochrome P450 and NADPH oxidase, also reduce molecular oxygen to superoxide.<sup>69</sup> The superoxide anion is a weaker oxidative agent, but it can trigger oxidative injury, and it is the main byproduct of the mitochondrial respiratory chain. It has low membrane permeability due to its charge, thereby using inefficient anion channels, and it is susceptible to accumulation in chambers. Superoxide is mainly toxic because it damages proteins with Fe-S centres like succinate dehydrogenase, NADH ubiquinone oxidoreductase, *etc.* Furthermore, it produces other oxidative species far more harmful than itself (hydroxyl, hyperoxide, *etc.*).<sup>70</sup> Exposure to external superoxide anions near the membrane, where the pH is much lower than the cytoplasm, generates its protonated form (hyperoxide), which triggers a cell destruction cascade. Hydrogen peroxide ( $\text{H}_2\text{O}_2$ ) is known to cause cellular death *via* many mechanisms, like autolysis, autophagy, necrosis, ferroptosis, *etc.*, depending on the cell type and concentration of peroxide.<sup>71</sup> Lower concentration (1 mM) leads to cell death by DNA damage, whereas concentrations  $> 10 \text{ mM}$  kill due to damage to all macromolecules.<sup>72</sup>  $\text{H}_2\text{O}_2$  plays a vital role in photocatalytic antimicrobial action due to its relative stability and ability to diffuse across bacterial membranes. Unlike charged or highly reactive ROS such as superoxide ( $\text{O}_2^{\cdot-}$ ) or hydroxyl radicals ( $\cdot\text{OH}$ ),  $\text{H}_2\text{O}_2$  is uncharged and sufficiently stable to traverse lipid bilayers, allowing it to accumulate within microbial cells. Once inside, it can directly oxidize vital biomolecules, including proteins, especially those containing thiol groups, leading to enzyme inactivation and structural degradation. Moreover, it targets Fe-S cluster-



containing enzymes, which are essential for bacterial respiration and DNA synthesis. This damage impairs cellular metabolism and releases free ferrous ions ( $\text{Fe}^{2+}$ ), leading to further ROS generation through Fenton-like chemistry.<sup>68</sup> In the presence of ferrous iron,  $\text{H}_2\text{O}_2$  serves as a substrate for the Fenton reaction, wherein it is catalytically converted to hydroxyl radicals. Therefore, peroxide not only acts as a direct oxidative agent but also as a mobile, transmembrane precursor that can generate other oxidative species, causing ROS stress and eventual cell death through various mechanisms. Singlet oxygen plays a vital role in cellular stress by signaling to initiate programmed cell death or directly providing toxicity. It is a very strong electrophile, enabling it to undergo various biochemical reactions. One of the primary targets of oxidative damage is polyunsaturated fatty acids, one of the main components of cellular membranes. It leads to a peroxidation reaction, which can form kinks in the hydrophobic fatty acid tails, disrupting membrane ultrastructure.<sup>73</sup> Besides,  $^1\text{O}_2$  can oxidize DNA bases, especially guanine, to create products like 8-oxoguanine, leading to mutations, base mismatches, and even DNA strand breaks.<sup>74</sup> These oxidative lesions interfere with DNA replication and transcription, hampering bacterial survival and division. Furthermore, the damage becomes lethal if the DNA repair systems are overwhelmed or inhibited. Together, these ROS form a synergistic oxidative network that disrupts microbial

homeostasis at multiple levels, such as membrane integrity, protein function, metabolic activity, and genomic stability, ultimately converging on irreversible cell death and establishing photocatalytic ROS generation as a potent antimicrobial strategy.

When proteins are exposed to ROS, the polypeptide side chains are modified, leading to functional disorders and an altered 3D structure. This may deem the essential amino acids dysfunctional or participate in side reactions, which are dangerous to cell survival.<sup>75</sup> The sulphur in cysteine and methionine makes them most susceptible to degradation.<sup>76</sup> The high levels of lipids in cellular and organelle membranes are usually targeted for microbial inactivation. Lipids are highly vulnerable to ROS damage by a phenomenon that targets the carbon–carbon double bonds of polyunsaturated fatty acids (PUFAs), known as lipid peroxidation. Research shows that lipid peroxidation caused by ROS can send cell death signals and induce autophagy or apoptosis.<sup>77</sup> Lipid peroxidation exerts its effect by altering the assembly, structure, composition, and dynamics. It can cause a cascade reaction producing even more ROS, which can cause crosslinking of DNA and proteins.<sup>78</sup> DNA and RNA are susceptible to ROS oxidation, but single-stranded RNA, with its bases directly exposed and less associated with proteins, is highly susceptible.<sup>79</sup> RNA molecules can be oxidized by  $^{\bullet}\text{OH}$ , forming several oxidation adducts, namely 8-oxo-7,8-

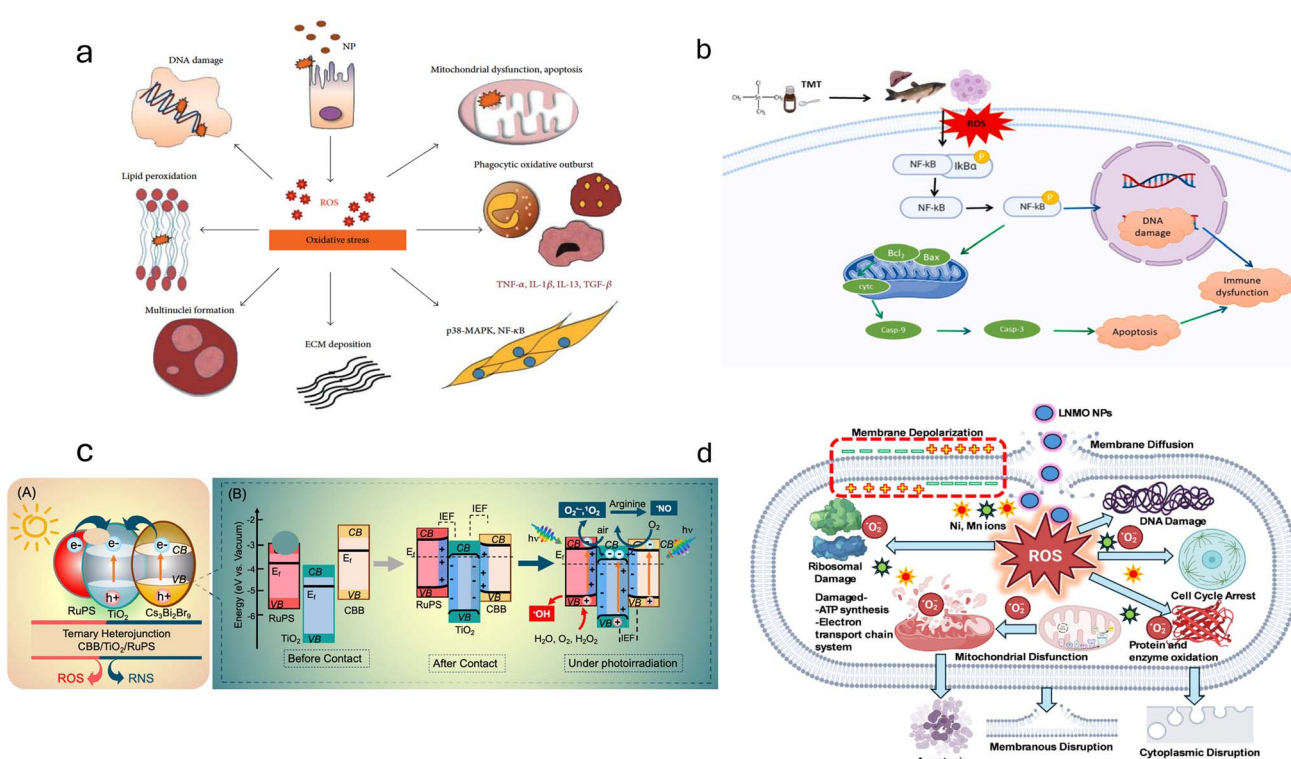


Fig. 4 (a) Summary of pathways leading to cell damage via ROS generation (reproduced from ref. 83 with permission from Hindawi, Copyright 2013). (b) Mechanism of DNA damage by ROS (Reproduced from ref. 84 with permission from Elsevier, copyright 2023) (c and d) Mechanism of antimicrobial activity in selected perovskite-based systems. (c) ROS/RNS generation after photoexcitation in a ternary heterojunction formed by  $\text{Cs}_3\text{Bi}_2\text{Br}_9$  perovskite-TiO<sub>2</sub> in the presence of a photosensitizer (Reproduced from ref. 85 with permission from American Chemical Society, Copyright 2023) and (d) mechanism of antibacterial and antifungal activity of La<sub>2</sub>NiMnO<sub>6</sub> double perovskite nanoparticles (Reproduced from ref. 86 with permission from Royal Society of Chemistry, Copyright 2025).

dihydroguanosine (8-oxo-G), 8-oxo-7,8-dihydroadenosine (8-oxo-A), 5-deoxyuridine (5-HO-U), and 5-hydroxylsine (5-HO-C).<sup>80,81</sup> The most common oxidation lesion in cells is 8-oxo-G, as guanosine has the lowest reduction potential. This modification causes mutations in the open reading frame (ORF), leading to a reduced rate of peptide-bond formation, impairing protein synthesis.<sup>82</sup> Fig. 4 provides an overview of pathways to cell damage *via* ROS generation. From the discussion, it is evident that the antimicrobial activity of perovskites depends on ROS-induced molecular disruption, and strategies to boost ROS production are vital for improving their efficacy.

## 4. Engineering and deployment strategies for perovskite-based antimicrobial photocatalysis

Perovskite materials have garnered significant attention due to their exceptional optoelectronic properties. Their structural flexibility allows precise tuning of band gap energies, making them highly efficient for visible light-driven photoactivated processes. This offers a distinct advantage over conventional photocatalysts, which rely on UV light for activation. The general photoexcitation mechanism follows similar principles to  $\text{TiO}_2$ -based photocatalysis but is enhanced due to the high charge carrier mobility, tunable bandgap, and strong visible-light absorption of perovskites.<sup>87,88</sup> The mechanisms of lead-halide and lead-free perovskite-based environmental and antimicrobial applications have been extensively studied (*vide infra*).

Optimizing their photocatalytic performance through strategic material engineering and system design is essential to harness the full potential of perovskite materials for antimicrobial applications. This involves tailoring structural, electronic, and surface properties to enhance light absorption, charge separation, and ROS generation. Moreover, the practical deployment of these materials in real-world environments requires thoughtful consideration of their configuration as well as the design of efficient photocatalytic reactors. The efficiency of photocatalysis depends on the effective separation and migration of the charge carriers to the surface of the perovskite material. Structural defects and grain boundaries can act as recombination centres, reducing efficiency. Engineering the perovskite structure to minimize such defects is crucial for enhancing its photocatalytic performance.

### 4.1. Methods to enhance ROS generation: doping, heterostructure formation, and surface modification

The application of perovskites in antimicrobial photocatalysis is well justified by their key advantages, including tunable band gaps, suppressed electron–hole recombination, and efficient generation of reactive oxygen species (ROS). Among these, band gap engineering is one of the most critical and impactful modifications, particularly for photovoltaic and optoelectronic applications. The band gap of perovskites can be significantly tailored through compositional substitution. Two competing mechanisms were identified by examining the influence of the

A-site cation in tin- and lead-iodide semiconductor perovskites with the  $\text{AMX}_3$  structure: tilting of the  $\text{MX}_6$  octahedra leads to an increase in the band gap, whereas isotropic lattice contraction causes its reduction. This cation-based band gap tuning in 3D metal halide perovskite nanoparticles holds promise for optoelectronic applications.<sup>99</sup> The band gap tuning can be crystal size induced,<sup>90</sup> by a sequential deposition process,<sup>91</sup> spin-coating deposition,<sup>92</sup> etc. Compositional doping leading to modification in the bandgap of perovskite materials is illustrated in Fig. 5 below.

While doping is a popular optimization method, photocatalytic properties can be further improved by combining perovskites with other semiconductors *via* a heterojunction. Hybrid inorganic or organic perovskites have emerged as efficient light absorbers and important nanomaterials in third-generation photovoltaics.  $\text{CH}_3\text{NH}_3\text{PbI}_3$ , employed in a planar heterojunction configuration, yielded a power conversion efficiency of 12.1%.<sup>96</sup> The material was initially fabricated as thin film solid semiconductors and has since been modified and modulated to form high-efficiency nanostructured devices. Type II heterojunctions, such as  $\text{SrTiO}_3/\text{g-C}_3\text{N}_4$  composites, promote directional electron transfer from one semiconductor's conduction band to another with a lower energy level, while holes migrate in the opposite direction. These structural modifications significantly enhance hydrogen evolution reactions and organic pollutant degradation, with some composites demonstrating nearly 99% removal efficiency of contaminants within 90 minutes of light exposure.<sup>97</sup>

Additionally, heterojunction-type photocatalysts such as  $\text{CsPbBr}_3/\text{TiO}_2$ , synthesized by ligand-assisted reprecipitation (LARP), have shown enhanced visible-light absorption, improved carrier separation, and elevated photocatalytic activity, resulting from the formation of interfacial Pb–O bonds that promote efficient charge separation, suppress recombination, and enhance structural stability.<sup>98</sup> Furthermore, Zhao *et al.* reported that Cl-exchange at the surface of  $\text{CsPbBr}_3$  led to the formation of  $\text{CsPbBr}_{3-x}\text{Cl}_{x}/\text{TiO}_2$  heterojunctions, which showed enhanced photocatalytic performance and achieved a benzaldehyde production rate of  $1874 \mu\text{mol g}^{-1} \text{h}^{-1}$ , by the oxidation of toluene (4 times higher than that of naked  $\text{CsPbBr}_3$ ).<sup>99</sup> Such heterojunctions find application in hybrid Perovskite Solar Cells (PSCs) with a theoretical maximum power-conversion efficiency of 31%.<sup>100</sup> The standard device structure is based on a p-i-n heterojunction where the perovskite film is between an electron transporter (*e.g.*,  $\text{TiO}_2$ ) and a hole transporting layer (*e.g.*, spiro-OMeTAD).<sup>101</sup> However, efforts are being made to make the entire heterojunction perovskite-based to reduce the lattice mismatch between different crystal structures.

The potential of such perovskite-based heterojunctions in antimicrobial applications has also been explored. Methicillin-resistant *Staphylococcus aureus* (MRSA) biofilm infections are the primary causes of orthopedic implant failure and sepsis. Oxide perovskite-based P–N heterojunction-calcium titanate, when placed on the titanium implant surface, eradicated MRSA biofilms with an efficacy of  $99.42\% \pm 0.22\% \text{ in vivo}$ , crucial in the context of ever-increasing antibiotic resistance.<sup>102</sup> A ternary heterojunction material derived from a Bi-based perovskite-

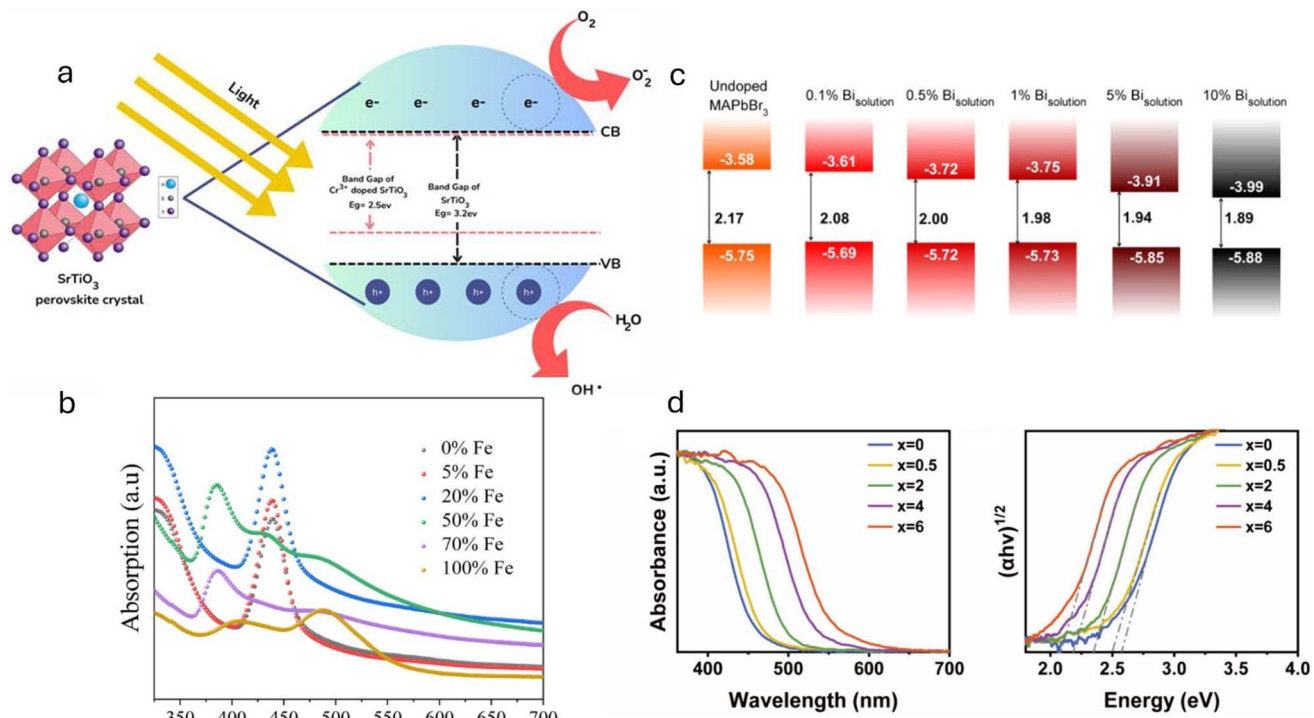


Fig. 5 Illustration of the effect of doping on the band structure and resulting optical properties in different perovskites. (a) A schematic diagram illustrating the electronic band structures for SrTiO<sub>3</sub> upon Cr<sup>3+</sup> doping. Doping with Cr<sup>3+</sup> introduces new electronic states within the bandgap, which can significantly improve its photocatalytic efficiency upon irradiation. (b) Variation in the bandgap alignment of CH<sub>3</sub>NH<sub>3</sub>PbBr<sub>3</sub> crystals with change in Bi% (Reproduced from ref. 93 with permission from American Chemical Society, Copyright 2016) (c) shift in the UV-vis absorption upon Fe incorporation in Cs<sub>3</sub>Bi<sub>2</sub>Br<sub>9</sub> (Reproduced from ref. 94 with permission from Royal Society of Chemistry, Copyright 2024). (d) UV-vis absorption spectra and corresponding Tauc plots of Cs<sub>2</sub>AgBiCl<sub>6-x</sub>Br<sub>x</sub> with varying concentration of Br (Reproduced from ref. 95 with permission from American Chemical Society, Copyright 2025).

TiO<sub>2</sub> hybrid and [Ru(2,2'-bpy)<sub>2</sub>(4,4'-dicarboxy-2,2'-bpy)]<sup>2+</sup>, (2,2'-bpy, 2,2'-bipyridyl) was shown to eradicate antibiotic-resistant bacterial films, upon photosensitization. The inactivation mechanism was attributed to the generation of reactive oxygen/nitrogen species, and the material maintained a high level of biocompatibility. The same group developed a metal halide perovskite nanocrystal heterojunction by *in situ* capping the nanocrystals with a NO-releasing derivative and an OH-releasing phenothiazine ligand. The heterostructure demonstrated efficient biofilm inactivation, as confirmed by both *in vitro* and *in vivo* investigations.<sup>103</sup>

Perovskites in their pristine state are highly susceptible to environmental stresses like humidity, temperature, pH, etc., and are toxic.<sup>104</sup> Encapsulation techniques are continuously being explored to overcome personnel and product safety deficiencies. One such encapsulation method is to etch them within macroscale polymer matrices. Raja *et al.* encapsulated colloidal CsPbBr<sub>3</sub> quantum dots into a high molecular weight, hydrophobic macroscale matrix, which protected the perovskite from environmental stress and prevented Pb leakage into the surroundings. Notably, the resulting quantum dots showed no lowering in photoluminescence quantum yield even after four months of continuous immersion in water.<sup>105</sup> Other surface functionalization techniques to enhance perovskite stability

and reduce ion-leakage induced toxicity include strategies such as silica-coating, which will be discussed later.

The effectiveness of perovskite-based antimicrobial action depends on ROS generation and how these materials are integrated into functional systems. These systems may operate in suspended or immobilized states, each offering distinct advantages and challenges in practical applications. Furthermore, the design of the photoreactor plays a crucial role in determining the overall efficiency of photocatalytic antimicrobial processes. Photoreactor configurations have been developed to enhance light utilization, material stability, and microbial inactivation rates. These aspects are discussed in detail in the following sections.

#### 4.2. Suspended vs. immobilized systems

Suspended systems (colloidal and slurry-based) involve dispersing perovskite nanoparticles within a liquid medium, forming colloidal or slurry mixtures. This setup ensures intimate contact between the photocatalyst and microbial contaminants, enhancing antimicrobial efficacy. The high surface area-to-volume ratio of perovskite nanoparticles facilitates efficient light absorption and ROS generation upon illumination. However, their intrinsic instability in aqueous conditions poses a serious problem for suspended systems. These difficulties are overcome by employing immobilized



systems that involve anchoring the perovskite materials onto solid substrates, forming thin films, coatings, or composites. Additionally, such systems offer advantages like ease of separation from treated media, reusability, and enhanced structural stability, which are crucial for practical applications and green synthesis. Various fabrication techniques have been employed to create immobilized perovskite systems.

Sol-gel processing techniques have been widely employed in transitioning a liquid 'sol' into a solid 'gel' phase to deposit perovskite films onto substrates. The versatility of such systems has been exploited for unconventional yet compelling applications, such as removing radioactive waste. Zhao and co-workers synthesised sol-gel ceramics using the sol-gel technique to synthesize perovskite-type  $\text{Ba}_{1-x}(\text{La, Cs})_x\text{ZrO}_3$  ( $x = 0, 0.1, 0.2, 0.3, 0.4$ ). Using a leaching test, they investigated the structural and chemical properties of these particles. Radioactive Cs crystalline ceramics are safer forms of nanomaterials for energy generation. Unlike other methods of immobilizing radioactive crystalline Cs ceramics, which usually require very high temperatures ( $>1000^\circ\text{C}$ ) that can destroy the Cs itself, the sol-gel method was carried out at  $800^\circ\text{C}$  and provided excellent thermal stability. The resulting films exhibit uniform thickness and strong adhesion, essential for consistent photocatalytic performance.<sup>106</sup>

Increasing recalcitrant organic pollutants (ROPs) in water poses a significant challenge, as conventional methods like flocculation, reverse osmosis, or filtration do not effectively remove them. The widespread use of nanoparticles in powdered form for water treatment has been identified as a significant contributing factor. In a 2020 study, thin films of C-N-TiO<sub>2</sub> were prepared by dynamic spin coating of a C-N-TiO<sub>2</sub> sol-gel on a glass support. The spin-coating ensured even distribution of thin films on solid support and provided precise control over film thickness. This was followed by an annealing process to further stabilize the layer, which can then be used for photocatalytic purposes, like the reduction of orange II dye. Its reasonable power conversion efficiency (9%) provided a feasible way for engineering C-N-TiO<sub>2</sub> films for wastewater remediation.<sup>107</sup> Such strategies can be extended to perovskite-based systems for advanced photocatalytic applications.

In dip-coating immobilization, substrates are immersed in a perovskite precursor solution and withdrawn at a controlled rate, which facilitates the deposition of a thin film. Some studies aim to produce scalable quantities of perovskite nanoparticles to remove antibiotics from polluted sources. One such study utilizes the incorporation of BiFeO<sub>3</sub> (BFO) perovskites with boron nitride quantum dots (BNQD) and immobilizing them on a commercial polyester filter *via* the dip-coating method (BFO/BNQD@PE). This resolved and restricted the disadvantages of using the powder form of crystals by immobilizing them on a filter. Furthermore, the system displayed an increased photodegradation efficiency (91.3%) as the immobilization provided more active sites for targeting TC-HCL molecules, and particles were reusable.<sup>108</sup> Immobilized perovskite systems are continuously being explored for various antimicrobial applications, like perovskite coatings on medical devices, which can prevent biofilm formation and reduce infection rates.<sup>105,109</sup>

Additionally, nanoparticle-based catalytic coatings such as TiO<sub>2</sub> and ZnO on water purification membranes have demonstrated the ability to inactivate bacteria upon light exposure, photo-generating ROS like hydroxyl radicals, singlet oxygen, and superoxide anion radicals, leading to bactericidal effects and thereby enhancing the water treatment processes.<sup>110</sup> The immobilization of perovskite materials improves their durability and minimizes the potential release of nanoparticles into the environment, addressing ecological concerns associated with nanomaterials. Fig. 6 illustrates the employment of a photocatalyst in suspended and immobilized configurations for wastewater treatment.

#### 4.3. Photocatalytic reactors for antimicrobial action

The performance of suspended and immobilized systems is influenced by the nature of the photocatalytic reactors, which are specifically engineered structures that facilitate the interaction between light, photocatalysts, and microbial contaminants. The design and configuration of these reactors are essential for optimizing the photocatalytic process for antimicrobial applications. A photocatalytic setup, regardless of its scale, comprises reagents, a light source, the reactor, and its operating system.<sup>111</sup> These should also be versatile to properly

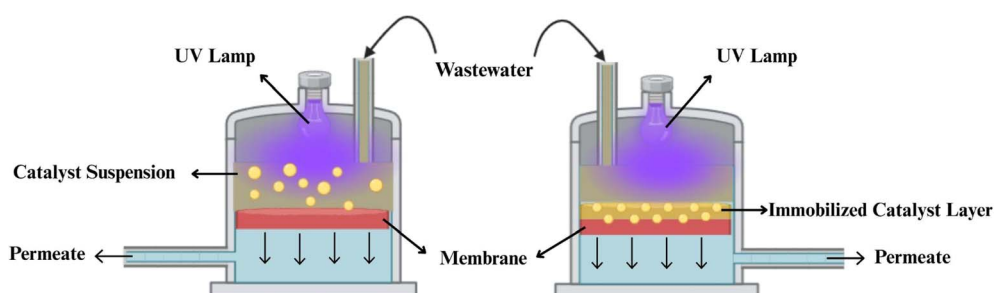


Fig. 6 Schematic illustration of a photocatalytic membrane reactor with suspended (left) and immobilized (right) perovskite-based systems for wastewater treatment. In suspended systems, perovskite nanoparticles are dispersed in the medium to enhance contact with contaminants. In contrast, immobilized systems involve anchoring the catalyst onto a solid support, enabling improved stability, ease of separation, and reusability during photocatalytic processes.



function with various materials. Several reactor designs have been explored for perovskite-based photocatalytic antimicrobial applications.

Batch reactors, also called closed system reactors, ensure only a fixed volume of contaminated fluid is treated with the suspended or immobilized perovskite photocatalyst under controlled light exposure. More of the contaminated fluid can be added only after the first batch is removed from the reactor. The reactors are simple to build and are equipped with pH probes, foaming probes, temperature monitors, *etc.*, making them suitable for laboratory-scale studies and small-scale applications. However, these cannot be utilized for large-scale applications due to long reaction times and limitations with scaling up that require specialized continuous flow reactors. In this regard, continuous flow systems offer advantages such as scalability and adaptability for industrial applications. Studies have shown that lead-free perovskite photocatalysts integrated into continuous-flow reactors enhanced disinfection efficiency against *Pseudomonas aeruginosa* and *Legionella pneumophila* due to sustained ROS production and improved catalyst stability.<sup>112</sup> Recent advancements in microfluidics have enabled the development of compact photocatalytic reactors with enhanced mass

transfer and photon utilization.<sup>113</sup> Microfluidic reactors employ perovskite thin films or nanoparticles confined within microchannels, where precise control over light exposure and fluid dynamics enhances microbial inactivation. The use of microfluidic perovskite reactors guarantees the adequate mixing of the precursor ions, the swift nucleation of crystal seeds in the antisolvent, and controlled crystal growth of the doped perovskite along the flow direction, which could further enhance the quality and quantity of dopant in halide perovskite.<sup>114</sup> For large-scale environmental applications, floating perovskite photocatalysts have been developed to treat surface water contamination. These systems utilize buoyant photocatalyst supports, ensuring optimal light exposure and enhanced photocatalytic activity.<sup>115</sup> Floating perovskite composites have the potential to overcome the disadvantages of traditional photocatalysts due to their lower bandgap, enabling them to harness visible light irradiation instead of relying solely on UV irradiation.<sup>116</sup> Photocatalytic applications primarily hinge on how the catalyst responds to light activation. It is essential to understand the effect of modulations in the light source can impact the properties of the catalyst. In the following section, we briefly discuss this aspect.

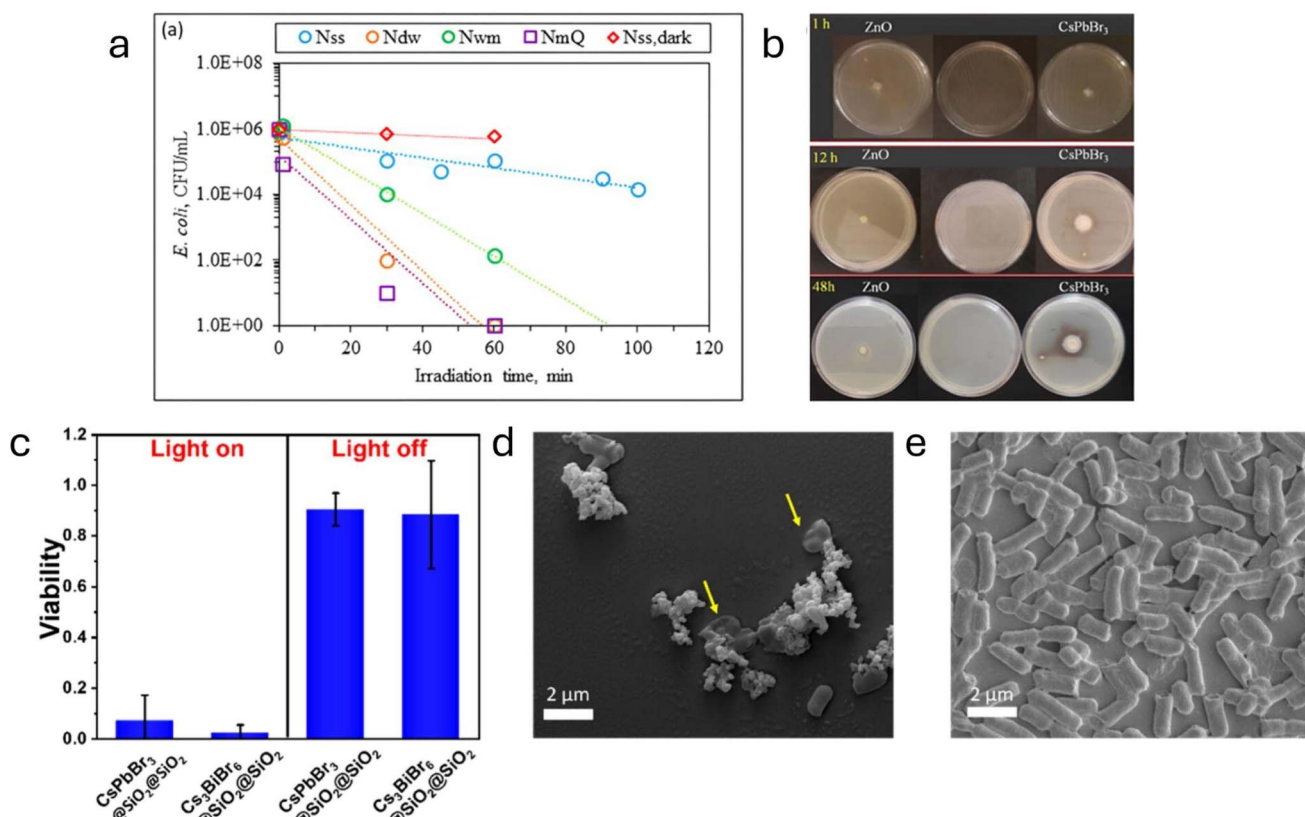


Fig. 7 (a) Photocatalytic inactivation of *Escherichia coli* ( $\sim 10^7$  CFU  $\text{mL}^{-1}$ ) under simulated solar light ( $\sim 100$  mW  $\text{cm}^{-2}$ , Xe lamp) with LaFeO<sub>3</sub> (0.5 mg  $\text{mL}^{-1}$ ) in different water matrices: saline (Nss), distilled (NdW), ion-rich (Nwm), and Milli-Q (NmQ). Bacterial counts declined nearly linearly over 60 minutes. No significant inactivation was observed in dark controls (Nss, dark). (Reproduced from ref. 117 with permission from MDPI, Copyright 2021). (b) Comparative antibacterial activity of CsPbBr<sub>3</sub> perovskite and ZnO nanoparticles against *Escherichia coli* under visible light irradiation. (Reproduced from ref. 118 with permission from Springer, Copyright 2019). (c-e) Disinfection performance of PNCs@SiO<sub>2</sub>@SiO<sub>2</sub> after six hours of visible light irradiation. (c) *Escherichia coli* viability was determined using the plate count method. (d) SEM image of bacteria after the photocatalytic reaction by CsPbBr<sub>3</sub>@SiO<sub>2</sub>@SiO<sub>2</sub>. The yellow arrows in the SEM image indicate the deformation and structural collapse of the bacteria. (e) The SEM image shows intact bacteria. (Reproduced from ref. 119 with permission from American Chemical Society, Copyright 2024).



## 5. Influence of light intensity, duration, and source on perovskites

The success of photocatalytic reactors hinges on how effectively light is utilized within these systems. The rate of charge carrier generation is directly proportional to the light intensity, which directly translates to increased ROS generation, such as hydroxyl radicals and superoxide anions, which are essential for photocatalysis. Beyond an optimal intensity, excessive photon absorption can lead to increased electron–hole (exciton) recombination, reducing the overall efficiency of the process.  $\text{LaFeO}_3$ -based perovskites have shown that optimal light intensities between 50–150  $\text{mW cm}^{-2}$  yield the highest ROS production rates, while intensities beyond this threshold cause a decline in photocatalytic efficiency.<sup>117</sup>

Prolonged irradiation allows continuous charge carrier generation, leading to sustained photocatalytic activity. In halide perovskites such as  $\text{CH}_3\text{NH}_3\text{PbI}_3$ , excessive exposure can lead to photocorrosion and catalyst degradation. While UV light-activated perovskites offer limited practical applications, visible-light-responsive perovskites (band gap energy in brackets) such as  $\text{BiFeO}_3$  (2.2 eV),  $\text{LaFeO}_3$  (2.1 eV), and  $\text{Cs}_3\text{Bi}_2\text{I}_9$  (2.35 eV) are particularly suited for solar-driven photocatalysis, self-cleaning surfaces, and water disinfection. Some modified perovskites, such as  $\text{CsSnI}_3$  (1.8 eV), exhibit absorption in the near-infrared (NIR) region. While this extends their operational range, the lower energy of NIR photons limits ROS generation.<sup>117</sup> To evaluate the real-world performance of engineered photocatalytic systems, it is crucial to assess their antimicrobial efficacy under environmental conditions. Beyond the intrinsic properties of the photocatalyst and the reactor design, the nature of the water matrix and the specific application context, such as bacterial inactivation, are critical in determining overall effectiveness. Fig. 7 highlights how environmental conditions and material properties strongly influence the antimicrobial performance of perovskite-based photocatalytic systems. The study demonstrates that the surrounding water matrix can significantly alter photocatalytic disinfection efficiency, emphasizing the need to consider real-world conditions when designing such systems. The figure also cites an example in which cell viability assays and microscopic analysis were performed to study the photocatalyzed antimicrobial action of perovskite nanocrystals. These findings underscore the potential of perovskites as efficient antimicrobial agents with tunable activity and also emphasize the critical interplay between photocatalyst selection, operating conditions, and the surrounding medium, reinforcing the importance of integrating system design with realistic deployment scenarios for optimal antimicrobial performance.

## 6. Types of perovskites displaying antimicrobial activity

### 6.1. Lead-based perovskites

Lead-based perovskites, specifically their halide variants, such as  $\text{CsPbI}_3$ , have been found to possess unique structural and

electronic properties, making them suitable for a wide range of photocatalytic applications. These perovskites have a crystalline structure with a general formula of  $\text{ABX}_3$ , where A is a cation (such as Cs), B is usually lead (Pb), and X is a halide (Cl, Br, or I). Due to an appropriate band gap energy (1.9 eV for  $\text{CsPbI}_3$ ), these materials can efficiently absorb visible light. Moreover, they exhibit a high degree of crystallinity and enhanced electron–hole separation, which improves the catalytic performance. Modifications like incorporating graphene oxide into lead-based perovskite structures have enhanced stability and photocatalytic performance.<sup>120,121</sup>

### 6.2. Lead-free alternatives

Despite their advantages, lead-based perovskites exhibit high toxicity levels due to the presence of lead and lack stability in aqueous conditions. To overcome these limitations, the development of lead-free perovskites has gained a lot of interest over the past few years, especially bismuth and antimony-based compounds. These materials preserve the core structure and optoelectronic properties of conventional perovskites while overcoming their shortcomings. As with conventional lead-based perovskites, their photocatalytic properties directly correlate with their structure, visible light stability, and capability to generate reactive oxygen species.<sup>122</sup>

Bismuth-based systems are stable in aqueous systems compared to their lead-based counterparts, and show exceptional stability and photocatalytic efficiency, particularly in aqueous environments like hydriodic acid (HI) solutions.<sup>121</sup> For instance,  $\text{Cs}_3\text{Bi}_2\text{I}_9$ , possesses a broad absorption range in the visible spectrum, maximizing light usage and providing efficacy over various wavelengths. Their wide band gap (~2.0 eV) allows for the generation of electron–hole pairs that subsequently react with water and oxygen, resulting in the formation of ROS. The stability of these structures is attributed to the inert nature of the  $\text{Bi}^{3+}$ , which possesses a fully filled 6s orbital, which confers resistance to oxidative degradation and enhances structural robustness. The material also shows higher rates of hydrogen evolution, a parallel reaction in ROS generation, and increases the efficiency of ROS generation.<sup>122</sup> The formation of heterojunctions, which prevents recombination losses by facilitating efficient charge separation and transfer of electrons, can further improve the performance of bismuth-based perovskites. Coupling  $\text{Cs}_3\text{Bi}_2\text{I}_9$  with graphitic carbon nitride creates heterojunctions that align the conduction and valence bands of the two semiconductors.<sup>97</sup> This facilitates the transfer of the photogenerated electrons of  $\text{Cs}_3\text{Bi}_2\text{I}_9$  into the conduction band of the graphitic carbon nitride while holes move in the reverse direction. The presence of nanoparticles such as Pt, Pd, or Au as a co-catalyst enhances the activity of bismuth-based perovskites. Platinum shows superior electrical conductivity, high catalytic activity, and strong hydrogen adsorption capabilities, and is often the preferred co-catalyst. When photogenerated electrons move towards the conduction band, Pt provides a surface to combine with protons to generate hydrogen. The extracted electrons from the photocatalyst are transferred to protons, ensuring that the holes left behind in the valence band



**Table 3** Comparison of antimicrobial and photocatalytic properties of lead-based, lead-free (bismuth-based), and perovskite nanocomposite materials. The table summarizes key parameters, including band gap, structural modifications, stability, reactive oxygen species (ROS) generation mechanisms, and antimicrobial efficacy under visible-light irradiation

Type	Example(s)	Band gap (eV)	Modifications/enhancements	Stability	Mechanism of ROS generation	Antimicrobial performance	References
Lead-based perovskites	$\text{CsPbI}_3$	~1.73	Graphene oxide incorporation	Low (especially in aqueous media)	Light absorption → $e^-/h^+$ separation → ROS formation	Effective against microbes <i>via</i> oxidative stress (qualitative)	125 and 126
Lead-free (bismuth-based) perovskites	$\text{Cs}_3\text{Bi}_2\text{I}_9$ , $\text{MA}_3\text{Bi}_2\text{I}_9$	~2.1 ( $\text{Cs}_3\text{Bi}_2\text{I}_9$ ), ~2.22 ( $\text{MA}_3\text{Bi}_2\text{I}_9$ )	Heterojunctions with $\text{g-C}_3\text{N}_4$ ; hybrid organic-inorganic structures; compositional engineering	High in aqueous media; thermally stable (~420 °C); stable over multiple photocatalytic cycles	Visible-light-induced electron-hole separation → $e^-$ transfer <i>via</i> $\text{g-C}_3\text{N}_4$	High ROS yield; efficient visible-light photocatalytic degradation; 98% rhodamine B removal in 3 h (proxy for antimicrobial potential)	127–130
Perovskite nanocomposites	$\text{LaCoO}_3/\text{Ag}_3\text{PO}_4$	Variable	Heterojunction with $\text{Ag}_3\text{PO}_4$ ; enhanced visible-light absorption; improved $e^-/h^+$ separation	Stable under visible-light irradiation; functional stability confirmed by MIC values	Visible-light-induced ROS <i>via</i> heterojunction electron-hole separation; $\text{Ag}^+$ release; oxidative stress; glutathione oxidation	MIC against <i>E. coli</i> : 0.1 mg mL; MIC against <i>S. aureus</i> : 0.15 mg mL; antibacterial rate under visible light (20 min): <i>E. coli</i> 99.9%, <i>S. aureus</i> 98.3%	131

remain active for oxidation reactions, thereby limiting recombination losses and increasing the ROS generation.<sup>121,122</sup>

### 6.3. Perovskite nanocomposites

Perovskite nanocomposites can integrate the superior optoelectronic properties of perovskites with enhanced stability and charge separation mechanisms offered by secondary materials, making them a popular material for photocatalytic applications. Structurally, these composites retain the fundamental perovskite  $\text{ABO}_3$  framework, where the A-site is occupied by alkaline earth or rare-earth metal cations, and the B-site consists of transition metal cations coordinated with oxygen octahedra.<sup>65,123</sup> The incorporation of nanomaterials such as carbon-based compounds (*e.g.*, graphene oxide), noble metals (*e.g.*, Pt, Au, Ag), or secondary semiconductors (*e.g.*,  $\text{TiO}_2$ ,  $\text{g-C}_3\text{N}_4$ ,  $\text{ZnO}$ ) modifies the electronic structure of perovskites, leading to enhanced charge separation and photocatalytic performance.<sup>123</sup> The photocatalytic mechanism of perovskite nanocomposites is governed by their ability to generate and manipulate charge carriers under light irradiation. Rapid electron-hole recombination in conventional perovskites is a limiting factor in their photocatalytic applications. As discussed in the previous section, incorporating secondary materials in perovskite nanocomposites mitigates this issue by forming heterojunctions, which act as charge transfer interfaces and enhance ROS generation. Hydroxyl radicals and superoxide anions exert oxidative stress on bacterial membranes, leading to lipid peroxidation, protein denaturation, and DNA fragmentation.<sup>65,123</sup> Studies on  $\text{LaCoO}_3/\text{Bi}_4\text{Ti}_3\text{O}_{12}$  nanocomposites have demonstrated a remarkable 87.8% degradation efficiency against tetracycline-resistant

bacterial strains. A related strategy employing surface-ligand regulation was demonstrated for  $\text{CsPbBr}_3$  nanocrystals self-assembled using  $\text{NH}_4\text{PF}_6$  as a ligand. The resulting positively charged nanoparticles acted as efficient visible-light photocatalytic antibacterial agents, generating reactive oxygen species while the quaternary chitosan shell provided synergistic electrostatic inhibition of *E. coli*.<sup>124</sup> This study illustrates how ligand engineering can couple photophysical activity with biological targeting, offering a dual ROS-mediated and charge-driven microbial suppression mechanism. A table summarizing these aspects is given below (Table 3).

## 7. Factors affecting photocatalytic antimicrobial efficiency

As discussed in the previous sections, the interaction between perovskite materials and the subsequent charge separation is the most significant factor influencing their photocatalytic properties. However, these interactions vary considerably among perovskites of the same subtype. Variations in structural composition, stability, and other environmental conditions lead to substantial differences in antimicrobial behavior. Considering all these parameters, the effectiveness of perovskite-based antimicrobial systems is discussed below.

### 7.1. Composition

The composition of the perovskite materials is crucial in determining their optical, electronic, and structural properties. A great deal of literature demonstrates how modifications with ligands, elements, and even changes to the shape of the



materials are necessary for the best performance of perovskite-based antimicrobial systems. Functionalized hybrid halide perovskite (PeV) nanocrystals with nitric oxide (NO) releasing ligands showed increased exciton migration, which enhanced the photocatalytic generation of cytotoxic molecules like  $\cdot\text{OH}$  and  $\text{NO}^{\cdot}$ .<sup>132</sup> It was reported that the photocatalytic performance of  $\text{Bi}_4\text{NbO}_8\text{Cl}$  perovskite nanosheets depended mainly on the solute concentration and the calcination temperature. The degradation of tetracycline antibiotics under visible light illumination became possible after optimizing the composition parameters through fine-tuning methods.<sup>133</sup> Due to oxygen vacancy composition, the photocatalytic characteristics of  $\text{CaCu}_3\text{Ti}_4\text{O}_{12}$  perovskites differed significantly between octahedral and nanorod-shaped materials. Antimicrobial performance enhancement through defect engineering resulted from different charge carrier separations and surface property modifications.<sup>134</sup>  $\text{CsPbI}_3$  perovskite nanostructures synthesized through hydrothermal methods showed efficient photocatalytic degradation of organic dyes and bactericidal action against clinically important bacteria, *Pseudomonas aeruginosa* and *Escherichia coli*.<sup>135</sup> It was reported that the Ag doping of  $\text{BiVO}_4$  perovskites suppressed electron-hole recombination, generating extra reactive species that increased oxidative stress on bacterial cells.<sup>136</sup>

## 7.2. Morphology and size

The antimicrobial photocatalytic properties of perovskite nanostructures depend heavily on their morphological characteristics and dimensions, as these parameters are crucial in controlling their carrier dynamics, surface interactions, and cell contact. Recent research has shown that photocatalytic performance depends on the shape and morphology of the particle, which leads to differences in light absorption, charge separation, and surface reactivity levels.  $\text{CaCu}_3\text{Ti}_4\text{O}_{12}$  perovskites synthesized in different morphologies: cubes, polyhedra, nanorods, and octahedra, using molten salt synthesis, showed morphology-dependent photocatalytic performance due to elevated oxygen vacancy density, stronger charge separation ability, and larger surface area.<sup>137</sup>  $\text{Bi}_4\text{NbO}_8\text{Cl}$  nanosheets under various synthesis conditions exhibited varying morphology and photocatalytic functions. The visible light-induced photocatalytic antimicrobial action was enhanced by optimized synthesis parameters, resulting in 82.07% destruction of oxytetracycline.<sup>138</sup> Cubic  $\text{CsPbI}_3$  perovskite nanostructures synthesized *via* hydrothermal reaction techniques demonstrated excellent antimicrobial effects against *Escherichia coli* and *Pseudomonas aeruginosa* through superior light absorption capabilities and enhanced charge carrier mobility, leading to increased ROS creation.<sup>139</sup> Biofilm disruption receives additional influence from morphology-related factors. The size of hybrid halide perovskite nanoparticles modified with NO-releasing ligands determines biofilm infiltration ability, which generates localized ROS/RNS to kill bacteria effectively. Modern biofilm inactivation processes benefit from NTFA@PeV@BA-PTZ@ $\text{SiO}_2$  nanocomposites with dimensions within 100–150 nanometers, which help them pass through biofilm pores.<sup>85</sup>

## 7.3. Environmental factors

Environmental conditions determine the final photocatalytic antimicrobial capacity because they affect the behavior of charge carriers, the production of reactive oxygen species, and the interaction of microbial cells with surfaces. The efficacy of perovskite-based antimicrobial photocatalysts depends on significant factors such as pH, ionic strength, temperature, light intensity, and both organic and inorganic contaminants present during operation.  $\text{LaFeO}_3$  perovskite nanoparticles exhibited their maximum tetracycline degradation efficiency under slightly acidic to neutral pH values (pH 5–7) because this range fostered a superior carrier separation mechanism and ROS formation. High sulfate and chloride levels in wastewater negatively affected photocatalysis because they caused nanoparticles to cluster together and reduced the accessible surface sites.<sup>140</sup> The antimicrobial properties of perovskites also depend on temperature through their influence on charge carrier kinetic energy and ROS distribution mechanisms. The photo-induced hydrogen evolution capacity of  $\text{Cs}_2\text{SnI}_6$  perovskites increased when the temperature reached moderate ranges between 25–50 °C. Excessive heat exposure caused the materials to degrade structurally, which decreased the effectiveness of photocatalysis.<sup>141</sup> Similar temperature effects were reported in  $\text{CH}_3\text{NH}_3\text{PbI}_3$  perovskite thin films synthesized through sol–gel methods.<sup>142</sup> The activity of perovskite photocatalysts in aqueous systems is severely affected by the presence of both organic substances and inorganic pollutants. Zhou *et al.* discovered that  $\text{SiO}_2$  coatings on halide perovskite nanocrystals increased water resistance, avoided biological solution degradation, and enabled efficient microbial inactivation through  ${}^1\text{O}_2$  production.<sup>141</sup> Perovskite– $\text{TiO}_2$  heterojunctions containing bismuth elements produce more ROS/RNS under solar irradiation, leading to efficient biofilm destruction.<sup>143</sup> It is established that the perovskite durability and antiseptic capabilities in multi-functional environments strongly rely on surface modifications. In these cases, the photocatalytic efficiency is influenced by two interrelated factors: hydrodynamic effects and substrate interactions, which impact operational efficiency in practical applications. Stable  $\text{LaFeO}_3$  photocatalysts immobilized onto commercial polystyrene resin promoted visible light absorption capability alongside better stability for wastewater treatment applications. The controlled method of substrate fixation produced antimicrobial activity gains by lowering agglomeration patterns and maximizing charge carrier efficiency.<sup>144</sup> Material engineering strategies must be implemented to ensure consistent catalytic performance across diverse environmental conditions.

## 8. Comparative assessment of perovskites and traditional photocatalysts for antimicrobial applications

Perovskite-based antimicrobial strategies offer several advantages over traditional antimicrobial methods. Unlike



Table 4 A table summarizing these differences between traditional photocatalysts and perovskite-based photocatalysts

Feature	Traditional photocatalysts	Perovskite photocatalysts
Light absorption efficiency	Primarily absorb UV light; limited solar spectrum utilization	Broad absorption across the visible and near-infrared spectrum; better solar utilization
Charge carrier dynamics	Rapid electron-hole recombination; limited ROS generation	High carrier mobility, long diffusion lengths, low trap recombination, enhanced ROS generation
Key photogenerated species	Mainly $^{\bullet}\text{OH}$ and $^{\bullet}\text{O}_2^-$ radicals	$^{\bullet}\text{OH}$ , $^{\bullet}\text{O}_2^-$ , and singlet oxygen ( $^1\text{O}_2$ ); broader spectrum of oxidative species
Structural and compositional tunability	Limited ability to tune bandgap or electronic structure	Highly tunable <i>via</i> halide substitution, doping, and hybrid structures
Stability in aqueous environments	Generally stable, but $\text{ZnO}$ may leach toxic $\text{Zn}^{2+}$ ions	Intrinsically less stable in moisture; improved by surface engineering and encapsulation
Environmental impact	$\text{ZnO}$ may release harmful ions	Can be designed for better compatibility; composites reduce leaching
Antimicrobial mechanism efficiency	Lower ROS yield; slower kinetics	Higher ROS production, faster, and more diverse inactivation mechanisms
Photoreactor compatibility	Compatible with conventional UV-based reactors	Well-suited for visible-light-based and advanced photoreactor designs

conventional systems that rely on the continuous release of biocidal agents (*e.g.*, silver ions, organic antimicrobials), perovskite photocatalysts deliver on-demand, light-activated ROS generation at the surface, thereby minimizing unwanted diffusion into the food matrix. Their tunable band structure and defect engineering allow optimization of visible-light absorption and selective ROS profiles, providing flexibility that static antimicrobial agents lack. Moreover, the mechanism of antimicrobial action by perovskites is broad and simultaneous (membranes, proteins, nucleic acids), which substantially eliminates the likelihood of developing microbial resistance. Additionally, when properly immobilized and encapsulated, perovskite systems can achieve strong surface disinfection under ordinary illumination while limiting migration of active species- a subtle balance often lacking in free-release antimicrobials.

Given these capabilities, it is necessary to assess how perovskites compare to traditional photocatalysts. While traditional photocatalysts such as titanium dioxide ( $\text{TiO}_2$ ) and zinc oxide ( $\text{ZnO}$ ) have been widely utilized for photocatalytic antimicrobial applications, perovskite materials offer distinct advantages that position them as superior alternatives. Conventional photocatalysts, such as  $\text{TiO}_2$ , primarily absorb ultraviolet light, whereas perovskite materials exhibit broad absorption across the visible and near-infrared spectrum. This extended absorption capability enables perovskite photocatalysts to harness a larger portion of the solar spectrum, resulting in higher antimicrobial efficiency under ambient lighting conditions.<sup>145</sup> Traditional photocatalysts suffer from rapid electron-hole recombination, limiting their ROS generation potential. Perovskite-based photocatalysts, particularly those incorporating heterojunction structures, exhibit superior charge separation efficiency due to their high carrier mobility and tunable band structures. This property enhances ROS production, leading to more effective microbial inactivation.<sup>146</sup> Perovskites, particularly halide perovskites, possess exceptional charge carrier properties, show low trap-related recombination rates,<sup>147</sup> long diffusion lengths ( $\sim 1 \mu\text{m}$ ),<sup>148</sup> high mobility ( $\sim 10$

$\text{cm}^2 \text{ V}^{-1} \text{ s}^{-1}$ ), and prolonged lifetimes ( $\sim$ microseconds to milliseconds).<sup>149</sup> These properties contribute to a significantly higher probability of charge separation, leading to increased production of hydroxyl radicals ( $^{\bullet}\text{OH}$ ), superoxide radicals ( $^{\bullet}\text{O}_2^-$ ), and singlet oxygen ( $^1\text{O}_2$ ) – the primary agents responsible for bacterial and viral inactivation.<sup>150</sup>

Modifying the composition of perovskite materials, such as by substituting halides or incorporating dopants, allows for precise control over their photocatalytic properties.<sup>151</sup> In contrast, conventional metal oxide photocatalysts have limited tunability, restricting their adaptability for specific antimicrobial applications. A key drawback of perovskite materials is their susceptibility to degradation in humid or aqueous environments. However, recent advancements in surface engineering, encapsulation techniques, and composite fabrication have significantly improved their stability. Compared to  $\text{ZnO}$ , which can undergo leaching and release potentially toxic  $\text{Zn}^{2+}$  ions,  $\text{ZnO}$  layered with perovskite materials, when appropriately stabilized, demonstrates better environmental compatibility.<sup>152</sup> Both conventional and perovskite photocatalysts use ROS to inactivate bacteria. However, perovskites produce more ROS and distinct photogenerated species, enabling them to exhibit better antibacterial kinetics. Photogenerated  $^{\bullet}\text{OH}$  and  $^{\bullet}\text{O}_2^-$  radicals disrupt bacterial membranes by peroxidation of lipid bilayers, leading to intracellular leakage and cell lysis. However, in the case of conventional  $\text{AgI}/\text{ZnO}$ -based systems, the efficiency is often low due to slow ROS production kinetics and limited visible-light absorption.<sup>153</sup> In addition to  $^{\bullet}\text{OH}$  and  $^{\bullet}\text{O}_2^-$ , perovskites generate singlet oxygen ( $^1\text{O}_2$ ), selectively oxidizing biomolecules, disrupting nucleic acids and proteins, increasing their efficiency. The key differences between conventional catalysts and perovskite-based systems are summarized below in Table 4.

## 9. Applications and future prospects

The ability of perovskites to generate a broad spectrum of ROS and integrate into heterojunction and core-shell systems



highlights that their performance is superior to conventional materials such as  $\text{TiO}_2$  and  $\text{ZnO}$ . However, the actual value of these materials is best realized when translated into real-world applications. Recent developments have leveraged these capabilities to address critical issues in healthcare and environmental management. From suppressing biofilm formation on surgical instruments to dual-action water disinfection units, perovskite-based photocatalysts are evolving in numerous industries where microbial control is crucial. The following sections outline the versatile role of perovskite-based photocatalysts across diverse domains, particularly in healthcare and environmental remediation. Fig. 8 provides a concise overview of their wide-ranging applications.

### 9.1. Antimicrobial applications in healthcare

Microbial contamination and biofilm formation pose serious challenges across healthcare and related sectors, contributing to increased infection rates, treatment complications, and antimicrobial resistance. Traditional approaches to controlling these infections, such as antibiotic coatings or metal-based agents, are increasingly limited by issues of toxicity and reduced effectiveness. In this context, perovskite materials have gained attention as a new class of photocatalytic antimicrobial agents. Their ability to effectively generate ROS under visible light exposure, combined with tunable structural and chemical properties (*vide supra*), boosts their prospects in self-sterilizing surfaces, coatings, and medical applications. By integrating perovskites into antimicrobial systems, it is possible to develop

more effective, stable, and sustainable strategies for preventing and controlling infections.

Infections due to microbial colonization and biofilm are one of the significant concerns in orthopedic implants since they are usually associated with high morbidity and mortality rates.<sup>154</sup> Integrating perovskite materials into photocatalytic antimicrobial systems represents a transformative advancement in microbial control strategies.<sup>155</sup> Perovskite-based antimicrobial coatings on hospital surfaces, surgical instruments, and personal protective equipment can significantly reduce the risk of healthcare-associated infections. Various methods, such as antibiotic-loaded cement, silver-based coatings, and hydrogels, have been employed in orthopedic surgery to prevent implant infections. However, the cytotoxic nature of the incorporated metal ions, such as silver, and the emergence of multidrug-resistant bacteria have brought on the need to search for alternative solutions.<sup>154,156</sup> Perovskite materials, such as  $\text{SrTiO}_3$ , can inhibit the growth of both Gram-positive and Gram-negative bacteria under visible light irradiation. Hydrogels embedded with  $\text{SrTiO}_3$  nanoparticles were particularly effective against *Staphylococcus aureus* and *Escherichia coli* under visible light irradiation. Antimicrobial coating on surgical instruments is vital in reducing the risk of hospital-acquired infections. Light exposure can activate photocatalytic coatings, providing a self-sterilizing effect.<sup>156</sup>

Hybrid halide perovskites show effective antibacterial properties from their optimal exciton migration and charge separation mechanisms. An effective antibacterial process driven by

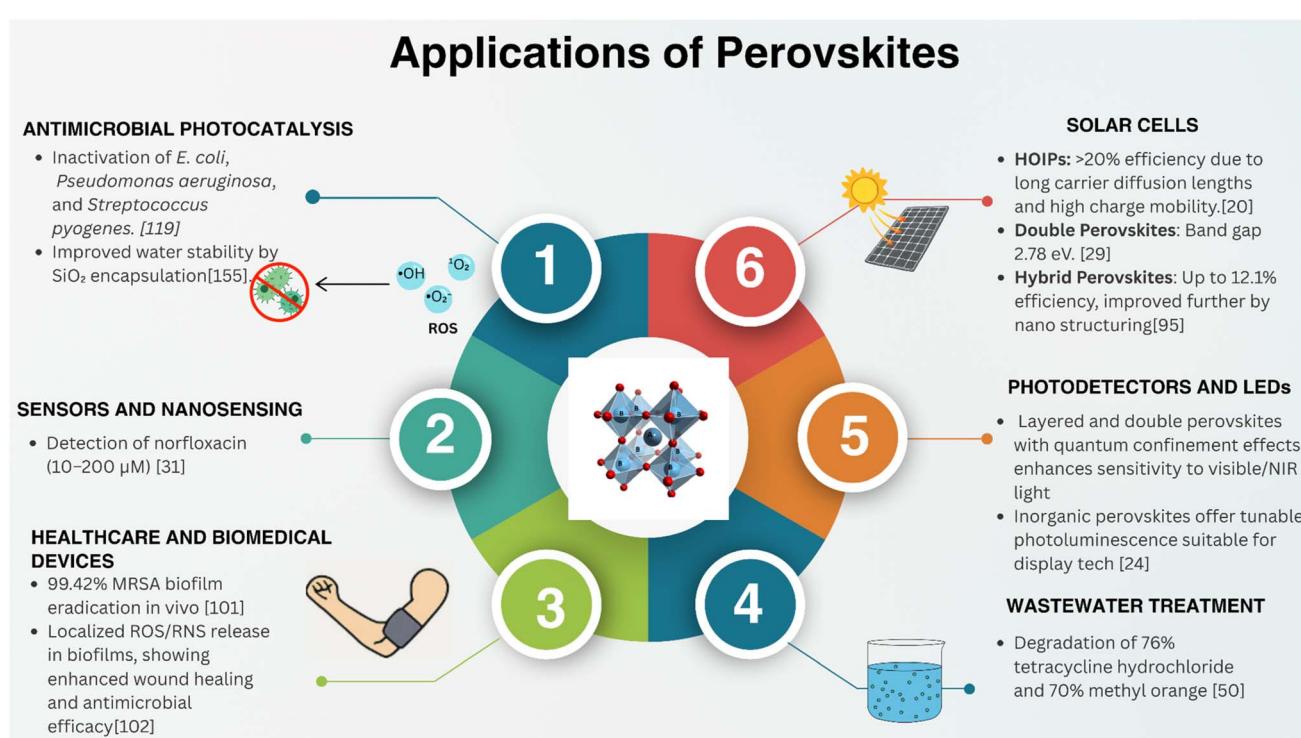


Fig. 8 Overview of the diverse applications of perovskite materials, including antimicrobial photocatalysis, sensors and nanosensing, healthcare and biomedical devices, wastewater treatment, photodetectors and LEDs, and solar cells, enabling their application in both energy and environmental technologies.



ROS/RNS generation was recently demonstrated using a heterojunction system composed of bismuth-based perovskite integrated with  $\text{TiO}_2$  and a Ru(II) polypyridyl photosensitizer. Effective exciton dissociation occurred due to the heterojunction's aligned band structures, which enhance the photocatalytic antimicrobial action and preserve satisfactory biocompatibility levels above  $1 \text{ mg mL}^{-1}$ .<sup>103</sup> Integrating perovskite materials into photocatalytic antimicrobial systems represents a transformative advancement in microbial control strategies. Mao *et al.* designed a novel antibiotic-free antibacterial perovskite-based nanofilm (Ti-CTO/RP) by integrating calcium titanate (CTO) and fibrous red phosphorus (RP) on a titanium implant surface. The P-N heterojunction and internal electric field at the interface facilitated efficient charge separation and transfer under near-infrared light, significantly enhancing photocatalytic MRSA biofilm eradication ( $99.42\% \pm 0.22\% \text{ in vivo}$ ) via ROS generation. Furthermore, the charge transfer-induced hyperthermia aids in biofilm removal. Beyond its antibacterial properties, the biocompatible and osteoconductive CTO/RP perovskite nanofilm promotes mesenchymal stem cell proliferation and osteogenic differentiation, supporting implant-to-bone osseointegration post-biofilm eradication.<sup>102</sup>

Aqueous stability is an essential condition determining how well perovskite materials perform as antimicrobial materials. A double-layer  $\text{SiO}_2$  coating implemented to HPNCs interlaces structural preservation with optical stability while maintaining active photocatalytic functions. The material showed a 90% inactivation rate towards *Escherichia coli* under visible light illumination for six hours, indicating its capability to develop antimicrobial hospital surface and medical device coatings.<sup>119</sup> The use of perovskite-based coatings demonstrates effectiveness against different strains of antibiotic-resistant bacteria.  $\text{CsPbI}_3$  nanostructures, synthesized through the hydrothermal method, demonstrated high antimicrobial properties against *Pseudomonas aeruginosa*, *Escherichia coli*, and *Streptococcus pyogenes*. The dual application potential of nanostructures for environmental and biomedical disinfection became evident after achieving an 81.7% organic dye degradation rate under visible light illumination.<sup>121</sup>

The anti-microbial coatings from perovskites demonstrate practical bacterial killing abilities and healing benefits. The antibacterial action of perovskite-based photocatalysts is primarily governed by the generation of reactive oxygen species upon light activation, which is crucial to their applications in healthcare. These ROS disrupt the bacterial membrane structure, oxidize proteins, and denature nucleic acids, leading to irreversible cell damage and death. Fig. 9 illustrates the underlying photocatalytic mechanism using  $\text{Ag/LaTiO}_3$  perovskite electrospun fibers as an example. Engineering hybrid halide perovskite with NO-releasing ligands alongside phenothiazine derivatives, producing  $\cdot\text{OH}$  radicals, improved bacterial penetration throughout biofilms while leading to complete elimination. A silica shell encapsulation raised its biocompatibility and made it suitable for placement in wound dressings, promoting healing and infection prevention.<sup>103</sup> The development of Bi-doped  $\text{BaBiO}_3$  perovskite oxides represents recent

advancements in perovskite materials as suitable substances for antimicrobial use. The materials demonstrate potent antibacterial effects against *Staphylococcus aureus*, leading to growth inhibition reaching 96.23% and proving highly effective as antioxidants. Integrating materials designed for antimicrobial coatings enables passive defense against bacterial infections and oxidative stress when used on surgical instruments, medical prosthetics, and medical textiles.<sup>157</sup> Despite their promising results, challenges such as their long-term stability, photo corrosion, and potential cytotoxicity persist. The use of lead-free perovskites, such as bismuth and antimony-based perovskites, offers an alternative. 3-D printing and scaffold creation using such photocatalytic antimicrobial materials is an exciting focus area.<sup>157</sup>

## 9.2. Wastewater treatment

The water instability of halide perovskites remains a fundamental issue that prevents their usage for wastewater treatment processes. Recent research has shown that encapsulation methods can create substantial improvements in the stability of perovskites in aqueous media.<sup>119</sup> Perovskite cores embedded within  $\text{SiO}_2$  shells simultaneously prevent hydrolysis damage and optimize the energy transfer between core and shell components needed to generate the potent antimicrobial agent,  $^1\text{O}_2$ . Hydrothermal synthesis enables high-performance photocatalytic wastewater treatment using  $\text{CsPbI}_3$  perovskite nanostructures. The materials demonstrate high antibacterial properties in addition to their effective degradation of organic dyes. Visible light irradiation produced the most efficient results when using methyl violet because it led to an 81.7% decolorization rate in the study.<sup>121</sup> The wastewater purification applications for  $\text{CsPbI}_3$  nanoparticle nanostructures have become more promising because these materials can remove organic contaminants while killing bacteria during photocatalytic reactions. Zhang *et al.* investigated strontium titanate ferrite ( $\text{STF}_x$ ) nanoparticles as a potent antibacterial agent, particularly for water purification.  $\text{STF}_x$  nanoparticles ( $x = 0\text{--}1$ ) were synthesized using high-energy ball milling and tested against *Escherichia coli* in water. The  $\text{STF}_{0.8}$  type demonstrated complete bacterial death ( $\sim 10^5 \text{ CFU mL}^{-1}$ ) within 15 minutes under both light and dark conditions, indicating a non-photocatalytic mechanism. Surface charge analysis, fluorescence microscopy, and SEM analysis revealed that the positive surface charge, high pH,  $\text{Sr}^{2+}$  release, and nanoscale size collectively contribute to its strong antibacterial effect, highlighting  $\text{STF}_x$  as a promising material for microbial elimination in water purification applications.<sup>156</sup> Under visible light illumination,  $\text{CsPbBr}_3$  quantum dot photocatalysts degraded 76% of tetracycline hydrochloride while removing 70% of methyl orange from organic solutions within 30 minutes.<sup>51</sup>

The durability and wastewater treatment capacity can be enhanced through ligand modifications and core-shell architectural designs, which alleviate moisture sensitivity. Introducing co-doping elements into perovskite crystal structures improves their operational performance for photocatalysis operations. Nb/N co-doped  $\text{Sr}_2\text{TiO}_4$  perovskites efficiently



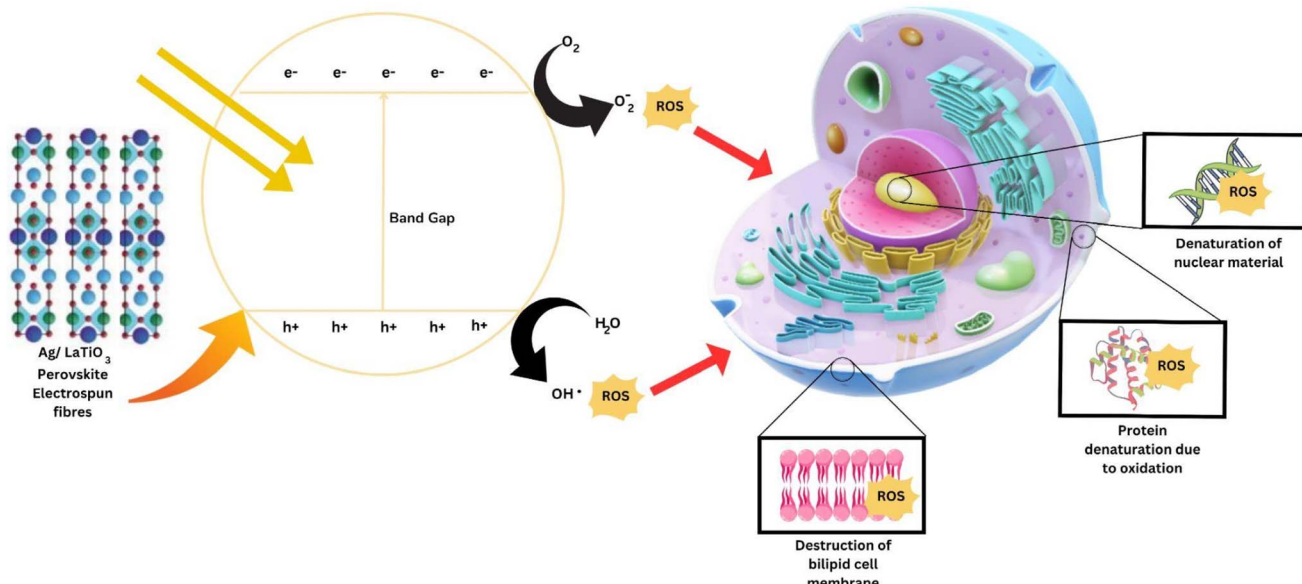


**Fig. 9** Schematic representation of the photocatalytic antibacterial mechanism of perovskite materials. Upon light irradiation, electron–hole pairs are generated across the band gap of  $\text{Ag/LaTiO}_3$  perovskite electrospun fibers, which subsequently generate ROS, including superoxide ( $\text{O}_2^{\cdot-}$ ) and hydroxyl radicals ( $\text{OH}^{\cdot}$ ). These ROS attack bacterial cells by disrupting the lipid bilayer membrane, denaturing proteins, and damaging nucleic acids, ultimately leading to cell death. [Reproduced from ref. 154 with permission from MDPI, Copyright 2020].

absorb visible light and exhibit excellent charge carrier separation, which results in efficient tetracycline antibiotic degradation.<sup>158</sup> Co-doping changes the material's band gap, enhancing light absorption ability and decreasing electron–hole pairing. These materials exhibit excellent recyclability features, which allow high photocatalytic activity retention through multiple cycles, making them suitable candidates for sustaining wastewater treatment processes. Oxide and oxyhalide perovskites have been compared to halide perovskites for their long-term stability while effectively treating wastewater. Perovskite-based compounds, including  $\text{LaFeO}_3$  and  $\text{BaBiO}_3$ , have shown high potential for chemical oxidation, which allows the breakdown of complex organic substances and microbial organisms. The materials showed low leaching behavior under aqueous conditions, thus making them useful for industrial wastewater processing facilities.<sup>159</sup>

### 9.3. Antimicrobial food packaging and storage

Lately, there has been a growing interest in developing active packaging materials and storage systems that can enhance the safety and shelf life of food products. Conventional preservation techniques, such as refrigeration and chemical preservatives, possess limitations, including high energy consumption, potential toxicity, and ineffectiveness against certain microbes. In this regard, perovskites are an effective alternative, due to their ability to produce ROS under light irradiation.

Besides efficiently generating ROS under visible light exposure, perovskites also exhibit tunable band gaps, which make them active contenders for incorporation into active food packaging systems.<sup>160</sup> Studies have shown that incorporating photocatalytic materials such as nano- $\text{TiO}_2$  into polymer

matrices enhances their antimicrobial activity.<sup>161</sup> Perovskite-modified films exhibited enhanced bactericidal effects against *Escherichia coli* and *Staphylococcus aureus* under visible light exposure. Perovskite-based nanocomposites in food packaging can provide antimicrobial functions and control the release of beneficial agents. Perovskite nanocomposite systems can combine multiple functionalities, including antimicrobial activity, oxygen scavenging, and controlled release of antioxidants. This enhances the protective ability of packaging films and increases the shelf life of food products.<sup>160</sup> However, the application of perovskites in food packaging may face challenges regarding safety and stability. The potential toxicity of lead-based perovskites limits their application in the food storage industry.<sup>162</sup> Developing lead-free perovskites, such as those based on bismuth and antimony, may offer a promising alternative. Table 5 below summarises notable studies demonstrating the diverse antimicrobial and environmental remediation applications of perovskite-based materials and their composites.

### 9.4. Research and development priorities

For research directed towards the antimicrobial properties of perovskites to be translatable, there is a need to understand the research and development priorities for industries. Addressing challenges such as toxicity, large-scale synthesis, scalable coating methods, and long-term stability of these materials under fluctuating temperature and humidity conditions is vital for their real-world applications.

Common strategies for obtaining perovskite nanocrystals include using the hot-injection or ligand-assisted reprecipitation methods. They are typically helpful for milligram-scale



**Table 5** Summary of representative applications of perovskite-based materials and composites in antimicrobial and environmental remediation. The table outlines the types of perovskites used, their underlying mechanisms, target microbes or pollutants, quantitative outcomes, and key remarks on performance and stability

Application	Perovskite type/composite	Mechanism	Target microbes/pollutants	Quantified outcome/efficiency	Remarks	References
Dual-action antibacterial film	Ti-CTO/RP nanofilm on Ti implants	P-N heterojunction + NIR-induced ROS + hyperthermia	MRSA biofilms	99.42% eradication ( <i>in vivo</i> )	Synergistic ROS + hyperthermia; promotes osteogenesis and osseointegration	102
Visible-light active coatings	SiO <sub>2</sub> -coated halide perovskites	Structural protection + ROS generation	<i>E. coli</i>	90% inactivation in 6 h	SiO <sub>2</sub> shell confers water stability; effective under mild visible light	119
Antibacterial nanostructures	CsPbI <sub>3</sub> perovskite nanostructures	Visible-light photocatalysis	<i>P. aeruginosa</i> , <i>S. pyogenes</i> , <i>E. coli</i>	81.7% dye degradation; antimicrobial	Hydrothermal synthesis; morphology and capping-agent dependent	121
Wound healing dressing	Hybrid PeV NCs with NO donor + phenothiazine	ROS + NO delivery	Biofilms	Complete elimination; tissue repair	Multimodal ROS/NO therapy; <i>in vivo</i> biocompatibility	103
Bi-doped oxide perovskite	Bi-BaBiO <sub>3</sub>	Oxidative stress + ROS	<i>S. aureus</i>	96.23% inhibition	Sol-gel synthesis; enhanced antibacterial and antioxidant activity	157
Water purification/antibacterial agent	SrTi <sub>1-x</sub> Fe <sub>x</sub> O <sub>3</sub> (STF <sub>x</sub> , x = 0–1); optimal STF <sub>0.8</sub>	Surface charge, high pH, Sr <sup>2+</sup> release, nanoscale effects (non-photocatalytic)	<i>E. coli</i> (~10 <sup>5</sup> CFU mL <sup>-1</sup> )	Complete inactivation within 15 min (light & dark)	Tunable bandgap (1.9–3.1 eV); further cytotoxicity study required	156
Organic pollutant degradation	CsPbBr <sub>3</sub> QDs	Visible-light photocatalysis <i>via</i> O <sub>2</sub> <sup>·-</sup>	Tetracycline hydrochloride (TC-HCl), methyl orange (MO)	76% TC-HCl, 70% MO degradation in 30 min	Active in ethanol; stable; complete mineralization; water instability noted	51
Wastewater treatment/antibiotic degradation	Nb/N co-doped Sr <sub>2</sub> TiO <sub>4</sub> (2 at% Nb)	Visible-light photocatalysis <i>via</i> O <sub>2</sub> <sup>·-</sup>	Tetracycline (TC)	99% degradation in 60 min (vs. 40% pristine)	Nb/N co-doping enhances visible-light absorption, charge separation, stability, and recyclability	158

synthesis that uses an organic solvent and, often, an inert atmosphere. However, these methods are impractical for bulk production, such as incorporation into polymers as perovskite films or 3D-printed scaffolds. To address practical applications, several research groups have adopted solid-state or solvent-minimized synthetic and hydrothermal routes that include mechanochemical methods, or the annealing of precursor salts at low temperatures, where a minimum quantity of solvents is used. Solventless or solid-state methods are cost-effective, environmentally friendly, and enable batch synthesis of powders that can be extruded or cast with polymers. Jiang *et al.* described a scalable solid-state route capable of multi-gram batches of CsCuX (X = Cl, Br) nanocrystals, with high photoluminescence quantum yields (~95%) and air stability of over two years, indicating good compatibility for incorporation into antimicrobial polymer composites.<sup>163</sup>

Another obstacle to the practical utilization of perovskites for their antimicrobial properties is their susceptibility to degradation from hydrolysis, ion migration, and thermal phase transitions. When exposed to ambient conditions or high

humidity, perovskites rapidly lose their ROS-generating activity. The instability of perovskites presents significant challenges for usage in food packaging exposed to refrigeration cycles and fluctuating humidity conditions. To mitigate these issues, scientists have considered polymer encapsulation techniques. Encapsulation layers, such as poly (methyl methacrylate) (PMMA), polyurethane (PU), or hybrid inorganic-organic barriers, which allow only moderate light penetration for critical photocatalytic activation, have proven to provide effective barriers to moisture and oxygen. PMMA and PU are widely used FDA- and EU-approved polymers in medical devices, dental materials, food contact coatings, and packaging. Raman *et al.* demonstrated that PMMA/PU bilayer coatings could maintain perovskite photocatalytic activity for over 1500 hours under 80% relative humidity, but still exhibited adequate light-driven performance.<sup>164</sup> A recent study by Bonomo *et al.* found that PU encapsulation of perovskite films reduced humidity-induced degradation and increased the stability and durability of perovskites subjected to repeat wet-dry cycling, which is an



essential requirement for applications in biomedical or packaging fields.<sup>165</sup>

For broad commercial applications, such as antimicrobial packaging films, liners, or hospital surfaces, there is a need for large-area, continuous deposition techniques to replace conventional spin-coating methods, which are the most common method of perovskite deposition. It produces high-quality films with smooth and controllable thicknesses and excellent crystallinity, essential for favorable optoelectronic properties. However, it also leads to a significant loss of raw materials. Baker *et al.* found that while spin-coating can use approximately 240 mL m<sup>-2</sup> of solution, methods like slot-die or blade coating can be as efficient as 5 mL m<sup>-2</sup>.<sup>166</sup> Moreover, spin-coating can only be done on smaller, rigid substrates (<100 cm<sup>2</sup>), with uniformity being compromised for large surface area films. Furthermore, spin-coating is incompatible with flexible or curved form factor materials used in medical tools such as surgical instruments and flexible packaging.<sup>167</sup> Methods such as spray and slot-die coating have addressed these shortcomings. Spray coating uses an atomizing nozzle to generate precursor solution droplets that coalesce into a uniform film, which undergoes crystallization when the solvent evaporates. This

technique is ideal for curved and flexible substrates, where control over drop impact and drying conditions can be used to tune film thickness and porosity. Heo *et al.* demonstrated spray-coated CH<sub>3</sub>NH<sub>3</sub>PbI<sub>3</sub> films with power conversion efficiencies as high as 19.4%-clearly demonstrating not only the quality of the films but also that the processes can be scaled.<sup>168</sup> In contrast, slot-die coating offers the benefit of precision and continuous roll-to-roll deposition well-suited to large-area applications. A pre-metered “ink” is extruded through a narrow slot onto a moving substrate that affords excellent control over the thickness of the deposit and near full-use of the deposited material (~95–100%). Slot-die-coated perovskite films with nontoxic solvents have achieved lab-scale solar cell efficiencies of 13.9%, comparable to spin-coated perovskite films.<sup>169</sup> Although these are predominantly used in solar cells, their applications in the domain of microbial inactivation may still be considered. A figure summarizing these aspects is given below (Fig. 10).

The production of halide perovskites, particularly for applications such as food packaging or medical implants, is limited by the health risks and environmental impacts. These concerns are further discussed in the next section. Intense research

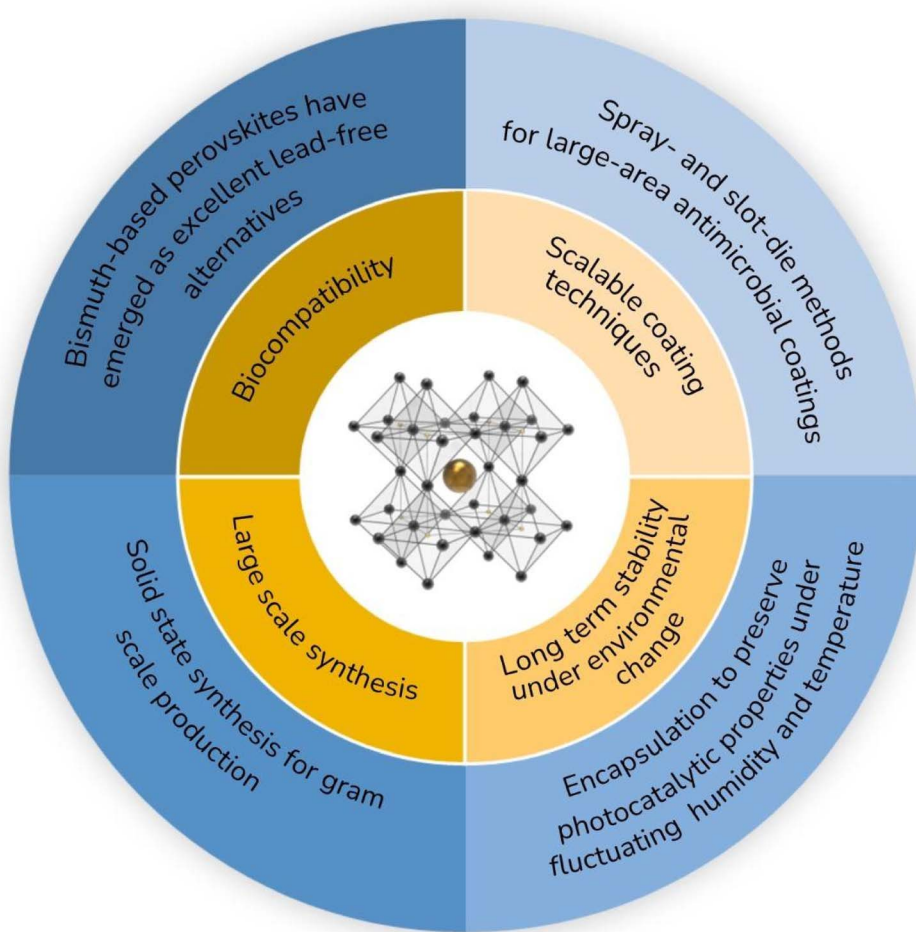


Fig. 10 Research and development priorities for advancing scalable synthesis and application of perovskites as antimicrobial materials.



efforts are taking place to find lead-free alternatives, mainly bismuth- and antimony-based perovskites, which retain excellent visible-light absorption and photocatalytic ROS generation without the significant cytotoxic effects.

## 10. Limitations and environmental concerns

While developments continue to help streamline scalable synthesis, protective encapsulation, and protective large-area coating methods, which have significantly elevated the practicality of perovskite-based antimicrobial technologies, considerable challenges remain. The innate instability of perovskites in aqueous and biological solutions frequently hinders the transition from lab-scale efficiency to functioning in the real world. These drawbacks are discussed in the following sections.

**Table 6** Summary of reported toxicological effects of various lead- and tin-based perovskite materials on different biological models, highlighting key observations such as oxidative stress, organ-specific toxicity, reproductive effects, bioavailability, and cellular responses, emphasizing the dose- and exposure-dependent nature of perovskite toxicity

Perovskite material	Test model	Toxic effects observed	Key findings
Lead-halide perovskites (e.g., $\text{CsPbBr}_3$ )	Lung epithelial cells (BEAS-2B), ICR mice	<ul style="list-style-type: none"> <li>• <math>\text{Pb}^{2+}</math> ions trigger the release of reactive oxygen species, causing excessive oxidative stress and apoptosis</li> <li>• Epithelial-mesenchymal transition is observed</li> <li>• Risk of pulmonary inflammation &amp; fibrosis</li> </ul>	<ul style="list-style-type: none"> <li>• Toxicity increases with exposure concentration and duration<sup>174</sup></li> </ul>
Lead ( $\text{Pb}^{2+}$ ), tin ( $\text{Sn}^{2+}$ , $\text{Sn}^{4+}$ ) and bismuth ( $\text{Bi}^{3+}$ )	Mice (lung, liver, brain, kidney, spleen, heart, and reproductive assessment)	<ul style="list-style-type: none"> <li>• <math>\text{Pb}^{2+}</math> and <math>\text{Sn}^{2+}</math> show more severe impacts (thickened alveolar walls) than <math>\text{Sn}^{4+}</math> and <math>\text{Bi}^{3+}</math></li> <li>• Only moderate levels of hepatocyte stenosis are observed in all of the mouse groups, showing low liver toxicity</li> <li>• No significant effects are observed when analysing the hippocampus, cornu ammonis one, and dentate gyrus (DG) regions in the brain</li> <li>• The mortality rate of the larvae exposed to the perovskite nanoparticles was similar to (or lower than) the mortality rate in the larvae exposed to lead nitrate</li> <li>• Uptake of Pb into hepatic cells was seen</li> <li>• Only a limited change in the gut microbiota of the zebrafish adults was observed</li> <li>• Decrease in area and thickness of the neural retina</li> <li>• The nanoparticles induced endoplasmic reticulum stress, leading to apoptosis</li> </ul>	<ul style="list-style-type: none"> <li>• In mouse models, <math>\text{Pb}^{2+}</math> and <math>\text{Sn}^{2+}</math> ions showed severe organ damage compared to <math>\text{Sn}^{4+}</math> and <math>\text{Bi}^{3+}</math></li> <li>• On assessing the reproductive health of the mice, it was found that the exposed female mice showed dose-dependent toxicity, causing a decrease in body weight and an increase in fetal mortality<sup>175</sup></li> <li>• Bioavailability of Pb in hepatic tissues was proved through the activation of mt2 and reduction of ala-d expression levels</li> <li>• The limited gut microbiota alteration shows the potential role of probiotic species in Pb detoxification<sup>172</sup></li> <li>• <math>\text{CsPbBr}_3</math> nanoparticles were found to be less toxic when compared to <math>\text{Pb}(\text{AC})_2</math> when exposed to hEROS</li> <li>• Pb-based perovskite particles affect early retinal development<sup>176</sup></li> </ul>
Pb-based perovskites	Zebra fish larvae and adults		
Pb-based perovskites ( $\text{CsPbBr}_3$ nanoparticles and $\text{Pb}(\text{AC})_2$ )	Human embryonic stem cell-derived three-dimensional floating retinal organoids (hEROS)		



exposure can occur *via* ingestion, inhalation, or direct skin contact, which can lead to severe neurodegeneration, renal failure, disruption of blood cell formation, and even increased cancer risk. Pb leaching is of great concern as the half-life of Pb is about 20–30 years after integrating into bones and teeth. Using Pb-based perovskites in photovoltaic systems can cause bioaccumulation as it produces Pb in a water-soluble form, like  $\text{PbI}$ , which breaks down into  $\text{Pb}^{2+}$  ions. The ionic form has a far greater chance of being introduced into the food chain through aquatic life.<sup>172</sup> A recent study by Zhu *et al.* systematically investigated the toxicity effects of perovskite-related materials ( $\text{PbI}_2$ , FAI, FAPbI<sub>3</sub>). Pb concentration in zebrafish gradually increased with increasing Pb-based perovskite materials, causing reduced survival rate, deformity, and Pb accumulation. Further, the Pb absorption capacity of plants embedded with FAPbI<sub>3</sub> perovskites was higher than that of plants planted with  $\text{PbI}_2$ .<sup>173</sup> These aspects are comprehended in Table 6 below. Fig. 11 below summarizes the perovskite nanocrystal-induced toxicity in the human body.

A more recent cytotoxicity study on Pb-based ( $\text{CsPbBr}_3$  and  $\text{CsPbI}_3$ ) and lead-free ( $\text{Cs}_2\text{AgBiBr}_6$ ) perovskite nanocrystals revealed that both Pb and Bi exhibit mitogenic effects and oxidative stress in liver cells, cytotoxicity in pulmonary cells, and a dose-dependent hemolytic effect.<sup>177</sup>

Various encapsulation strategies, such as polymer encapsulation and  $\text{SiO}_2$  coating, have been adopted to improve the stability of the nanocrystals and to prevent  $\text{Pb}^{2+}$  leakage (Fig. 12). It has also been established that such encapsulation strategies enhance the durability of nanocrystals, and this aspect will be discussed in detail in the subsequent section. Water-soluble PQDs reproducibly synthesized *via* encapsulating  $\text{CsPbBr}_3$  PQDs into triblock copolymers showed enhanced robustness, photostability, and reduced toxicity, resulting in improved biocompatibility.<sup>178</sup> A recent report investigated the cytotoxicity of  $\text{CsPbBr}_3/\text{CsPb}_2\text{Br}_5@\text{SiO}_2\text{-Brij58}$  on HeLa cells using the 3-(4,5-dimethylthiazol-2-yl)-2,5-diphenyltetrazolium bromide (MTT) assay. The results showed that even at

a material concentration of  $32 \mu\text{g mL}^{-1}$ , the cell viability rate was 94.2%, indicating the improved biocompatibility of the  $\text{SiO}_2$  encapsulated nanocrystals.<sup>179</sup> Such silica-coated perovskites have also shown excellent fluorescence and antibacterial activity.  $\text{Cs}_3\text{Bi}_2\text{Br}_9$  QDs@ $\text{SiO}_2$  grafted on cotton fibers exhibited excellent antibacterial capability against *Staphylococcus aureus* and *Escherichia coli*.<sup>180</sup>

## 10.2. Reusability

Perovskite-based photocatalysts experience severe limitations in terms of their reusability. Typical photocatalytic materials lack durability under continuous exposure to light and lose functionality for repeated usage in practical applications. Surface modification techniques such as silica encapsulation are employed to enhance the durability of these materials.  $\text{SiO}_2$  coating applied to halide perovskite nanocrystals results in better water resistance and sustained optical function, and thereby superior antimicrobial output.<sup>119</sup> The modifications added to photocatalysts typically bring synthesis challenges while reducing interface charge transfer capabilities, resulting in lower overall efficiency. Rapid electron–hole recombination subtracts from the available active charge carriers, reducing ROS and RNS production. Combining co-doping methods with heterojunction development techniques and band structure engineering provides solutions. Incorporating Nb/N into  $\text{Sr}_2\text{TiO}_4$  perovskites enhances charge separation, leading to improved degradation of antibiotic pollutants.<sup>158</sup> Developing practical applications of these materials requires improving doping concentration and material stability. Perovskite-based antimicrobial photocatalysts are sensitive to three critical external variables: light intensity level, pH, and the concentration of both inorganic and organic compounds in the surrounding media. The surface charge behavior of perovskites is sensitive to pH change because it determines membrane interactions with bacteria and ultimately affects antimicrobial function. The poisoning of active species by organic materials

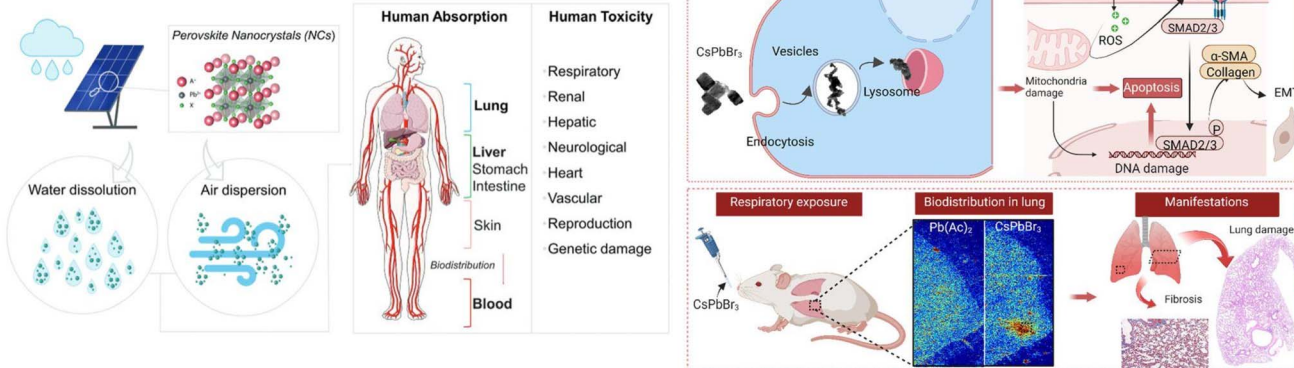


Fig. 11 Diagram illustrating the potential absorption and distribution of lead (Pb) halide perovskite nanocrystals in the human body. [Reproduced from ref. 177 with permission from Wiley, Copyright 2025]. Schematic illustration of  $\text{CsPbBr}_3$  nanoparticle uptake and toxicity.  $\text{CsPbBr}_3$  induces ROS generation and activates TGF- $\beta$ 1/Smad signaling, leading to apoptosis and EMT *in vitro*, and causes lung damage and fibrosis upon respiratory exposure *in vivo* (Reproduced from ref. 174 with permission from American Chemical Society, Copyright 2023).



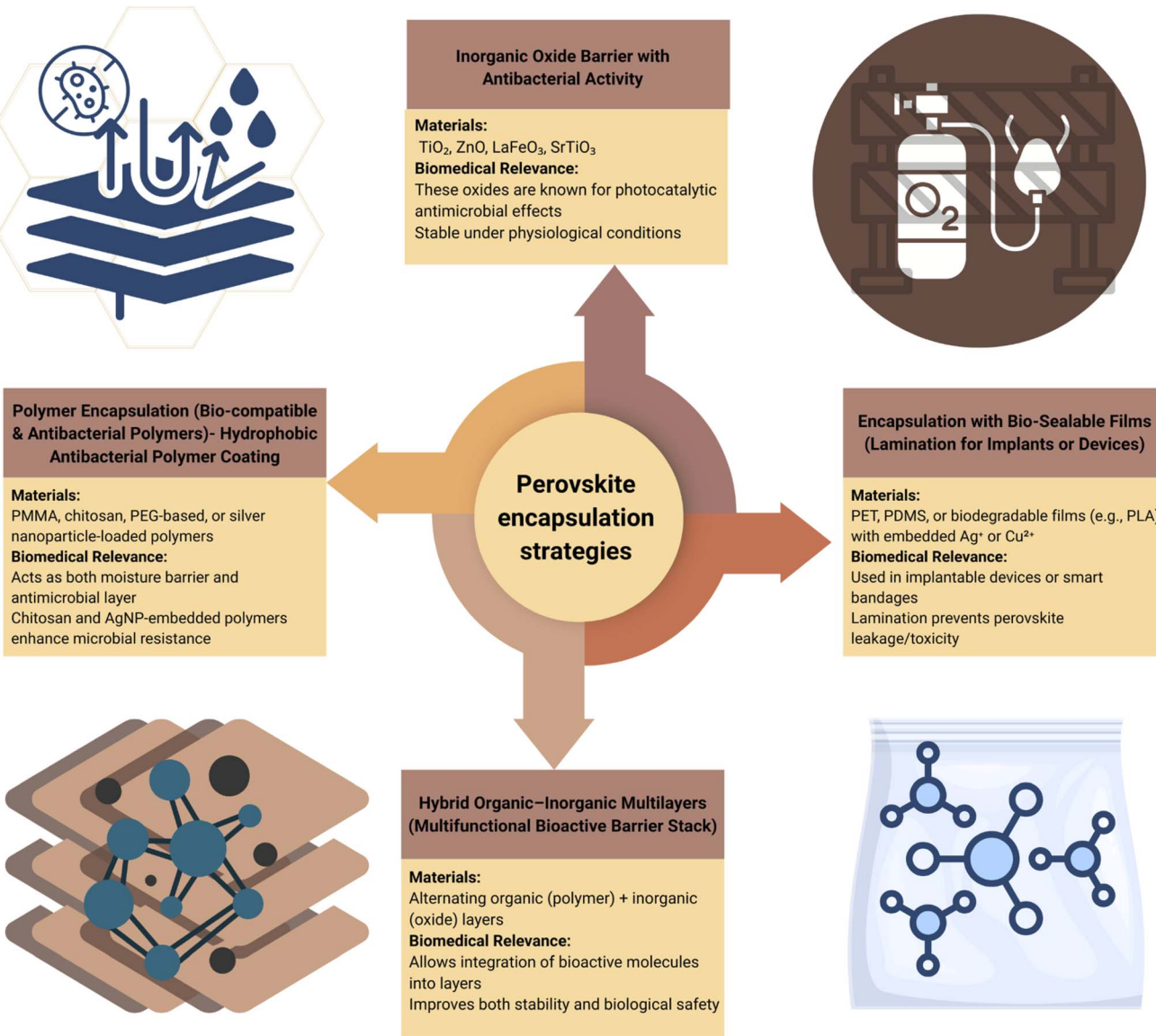


Fig. 12 Figure summarizing various encapsulation strategies employed in perovskite nanocrystals.

found in wastewater or biological fluids reduces the success rate of disinfection using photocatalytic systems.<sup>159</sup>

### 10.3. Stability and degradation

The effectiveness of perovskites in photocatalytic antimicrobial operations depends on material stability because it regulates structural preservation, ROS generation mechanisms, and charge-carrying properties. The antimicrobial and photocatalytic performances of perovskites decrease when exposed to water and humidity, temperature changes, and chemical agents, leading to their degradation. The light absorption and the charge carrier mobility benefits of lead-based perovskites are affected by the materials undergoing rapid breakdown in aqueous and biological systems. As reported by Zhu *et al.*,<sup>18</sup> water and biological fluids degrade halide perovskite nanocrystals, which diminishes their antimicrobial photocatalyst performance.

Encapsulation of perovskites into  $\text{SiO}_2$  is an effective strategy, especially for antimicrobial applications, as it provides an inert protective layer that shows no interference in the fluorescent quenching of nanomaterials (for detection-based assays) or ROS production (for antibacterial effects). Fig. 13 depicts a commonly employed synthetic strategy for the silica coating of perovskites. The coating of  $\text{CsPbBr}_3$  with  $\text{SiO}_2$  resulted in a significant increase in photoluminescence intensity. Since these particles are non-toxic, they are helpful for *in vitro* cell imaging of HeLa cells, paving the way for new biomedical applications.<sup>181</sup> Jiang *et al.* demonstrated the synthesis of environmentally friendly  $\text{Cs}_2\text{AgBiBr}_6$  embedded in  $\text{TiO}_2$  mesoporous matrix through an S-scheme heterostructure for enhanced carrier separation and efficient extraction. The composite structure maintained stable performance by preserving its structural characteristics for more than 500 days under air exposure. A 92.83% degradation of rifampicin



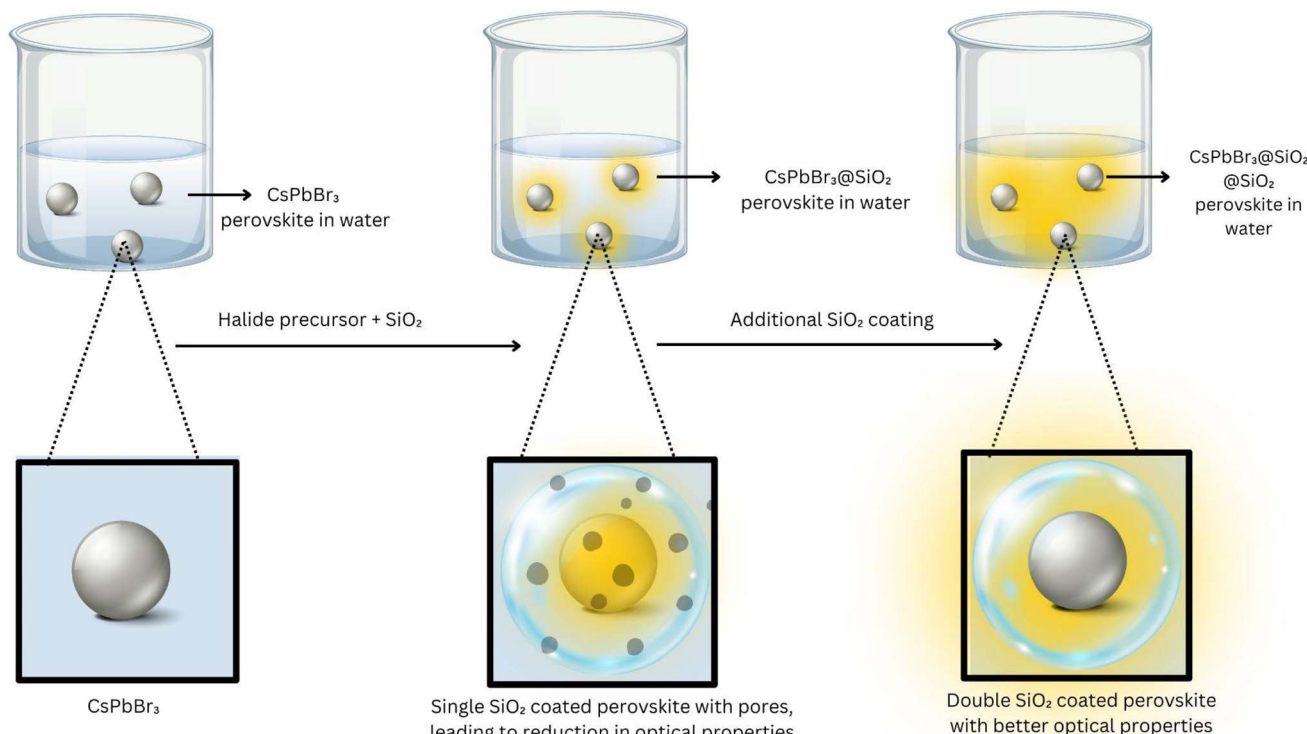
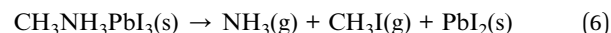


Fig. 13 Schematic diagram showing double  $\text{SiO}_2$ -coated perovskites.

antibiotics occurred within 80 minutes under simulated sunlight, thanks to the improved charge carrier dynamics, proving that perovskite stability promotes persistent photocatalytic antimicrobial activity.<sup>182</sup> Yang *et al.* focused on understanding potassium-doped lanthanum manganese perovskite oxides ( $\text{La}_{1-x}\text{K}_x\text{MnO}_3$ ) as photo-fenton systems for antibiotic degradation. Maximum electron–hole separation, as well as minimal activity decline over many photocatalytic cycles, occurred in  $\text{La}_{0.95}\text{K}_{0.05}\text{MnO}_3$  (LKMO-5). It has been established that proper doping approaches enhance perovskite stability through fundamental changes to the band configuration and surface character, thereby extending their antimicrobial capabilities.<sup>183</sup> Extensive research has been done on perovskite degradation paths to investigate components affecting photocatalytic efficiency. The quantum dots exhibit strong capabilities for tetracycline hydrochloride and methyl orange breakdown in organic solutions before their photocatalytic activity decreases when placed in water. The material composition of perovskite and the surrounding environment play vital roles in its degradation process, so researchers must develop application-specific stabilization techniques.<sup>51</sup> Due to hygroscopic ammonium and/or  $\text{Pb}(\text{II})$  salts, perovskites are susceptible to chemical decomposition from moisture. Moisture instability remains a constant worry for perovskite solar cells, and comprehensive solutions are necessary to address this issue.<sup>37,184</sup>



Lead iodide ( $\text{PbI}_2$ ) is water-insoluble but can dissolve under certain conditions, posing an environmental hazard. In terms of stability research, the thermal stability of halide PSCs remains a hurdle for commercialization.<sup>185</sup>



The heat deterioration of three pristine perovskite single-crystal surfaces ( $\text{MAPbI}_3$ ,  $\text{MAPbBr}_3$ , and  $\text{FAPbBr}_3$ ) was studied with synchrotron-based photoelectron spectroscopy, which revealed that the nature of the halide has a significant impact on thermal stability.<sup>185</sup> The photodegradation of perovskites affects both photocatalytic performance and the working of perovskite solar cells, where light-induced degradation is highly possible due to continuous exposure to the sun, causing a significant reduction in their efficiency and stability.<sup>186</sup> Another concern is oxygen exposure, as it can degrade perovskite materials, especially when combined with light, leading to the formation of superoxide and other ROS that erode the perovskite lattice and create charge traps, ultimately reducing stability, efficiency, and even the entire structure.<sup>187</sup> Defect engineering techniques aim to stabilize perovskites under biological conditions to aid antimicrobial research. Wang *et al.* demonstrated that Nb/N co-doping of  $\text{Sr}_2\text{TiO}_4$  perovskites led to 99% tetracycline destruction under 60-minute processing while maintaining five consecutive reactions thanks to its charge compensation system, which shows stability enhancement.<sup>188</sup> Alpay *et al.* embedded  $\text{LaFeO}_3$  perovskite nanoparticles on commercial polystyrene resin by deploying them as a catalyst base, which simultaneously prevented agglomeration and



boosted charge transfer kinetics. The researchers implemented this method to enhance tetracycline degradation under visible light and simultaneously developed a scale-up solution to support perovskite stabilization in actual wastewater treatment applications.<sup>188</sup>

## 11. Challenges and prospects

Perovskite-based photocatalytic antimicrobial systems are at an exciting juncture: material advances have produced candidate compositions and device formats with excellent light absorption and ROS-generation properties, yet translation to robust, safe, and scalable technologies remains incomplete. In this section, we summarize the unmet challenges categorically, along with recommended future directions for translation.

Halide perovskites are highly sensitive to moisture, oxygen, thermal cycles, and ionic migration, which remains the single most significant barrier to the practical applications of perovskites, including antibacterial activity. Future research will focus on designing compositions with intrinsic resistance to hydrolysis and photodegradation, such as all-inorganic formulations, ordered double-perovskite frameworks, or defect-tolerant stoichiometries that suppress adverse ion motion. Parallel theoretical screening to predict moisture- and ion-migration-resistant chemistries can accelerate discovery. Replacing Pb in halide perovskites remains essential for many biomedical and food-related uses. Bismuth-, antimony-, tin-, and specific double-perovskite chemistries show promise but frequently suffer from poor charge separation and optical properties. Systematic approaches such as alloying, controlled doping, and heterostructure formation with co-catalysts (Pt, Au, conductive carbons) are necessary to improve ROS yields while ensuring negligible leaching and acceptable environmental profiles. Comprehending lead-free candidates against standard metrics (quantum yields, ROS spectrum, and leaching) is required.

Maximizing ROS production without accelerating photodegradation requires tailored interfaces: passivating surface traps, building type-II/Z-scheme heterojunctions that effectively separate charges, and introducing shallow states that facilitate charge extraction. The stability and leaching issues can be addressed by adopting novel encapsulation strategies. Encapsulation must serve three simultaneous goals: (i) block moisture/oxygen that cause degradation, (ii) prevent release of toxic ions (e.g.,  $Pb^{2+}$ ), and (iii) allow photon flux and mass transport of  $O_2/H_2O$  so ROS generation is maintained. Recent bilayer polymer encapsulation and polymer-nanoparticle composite strategies have demonstrated extended operational lifetimes under harsh humidity conditions. These promising scalable strategies should be adapted and tested specifically for antimicrobial applications and in aqueous/food-contact environments, coupled with standardized leaching protocols.

Citing recent studies, we have shown that perovskites are most effectively deployed as immobilized coatings for practical applications. Research should develop deposition approaches compatible with large-area, flexible, and curved substrates to ensure uniformity and adhesion without degrading the

perovskite during processing. Because many perovskite syntheses use halides, organic solvents, and rare metals, large-scale use demands life-cycle assessment (LCA) to compare environmental costs *vs.* benefits. Green synthetic routes (mechanical, solvent-minimized hydrothermal) and solventless or low-solvent synthetic methods should be prioritized and benchmarked in LCA studies. Perovskite-based photocatalysts combine tunable photophysics with strong ROS-generation capacity and therefore represent a promising route to self-sterilizing surfaces and water-treatment modules. However, future research should focus on achieving coordinated progress on stability, safe-by-design composition, encapsulation that preserves activity while preventing release, and rigorous mechanistic and ecotoxicological characterization. Interdisciplinary collaborations paired with standardized reporting will be essential to move perovskite photocatalysis from attractive demonstrations to safe, regulated, and impactful technologies.

## 12. Conclusion

Perovskite materials, with their exceptional optoelectronic properties, offer conveniently tunable band gaps and excellent visible light absorption, as well as the ability to photogenerate reactive oxygen species, making them key materials for antimicrobial applications. Perovskites offer structural and compositional tunability, allowing tailored modifications to enhance photocatalytic efficiency, stability, and biocompatibility. While challenges such as toxicity, moisture sensitivity, and environmental degradation remain, advances in lead-free alternatives, heterojunction formation, and encapsulation strategies have significantly improved their performance and sustainability. Compared to conventional photocatalysts such as  $TiO_2$  and  $ZnO$ , perovskites offer broader light absorption, enhanced charge separation, and superior antimicrobial activity, making them promising candidates for healthcare, wastewater treatment, and environmental remediation applications. Efforts are being made to enhance the stability of perovskite nanomaterials, particularly in aqueous media, with the goal of minimizing toxicity by developing lead-free materials. A significant challenge lies in scaling up their production for real-world applications. Nevertheless, perovskite-based materials offer immense potential as antimicrobials and can transform disinfection strategies, contributing to sustainable technological advancements.

## Conflicts of interest

There are no conflicts to declare.

## Data availability

No new data were created or analyzed in this study. All data supporting the findings of this work are available within the published literature cited throughout the manuscript.



## References

1 R. M. Hazen, Perovskites, *Sci. Am.*, 1988, **258**(6), 74–80, DOI: [10.1038/scientificamerican0688-74](https://doi.org/10.1038/scientificamerican0688-74).

2 E. A. Katz, Perovskite: Name puzzle and German-Russian Odyssey of Discovery, *Helv. Chim. Acta*, 2020, e2000061, DOI: [10.1002/hlca.202000061](https://doi.org/10.1002/hlca.202000061).

3 Crystal structure of barium titanate," *Nature*, vol. **155**, no. 3938, pp. 484–485, Apr. 1945, doi: DOI: [10.1038/155484b0](https://doi.org/10.1038/155484b0).

4 J. G. Bednorz and K. A. Müller, Possible high Tc superconductivity in the Ba-La-Cu-O system, *Z. Phys. B Condens. Matter*, 1986, **64**(2), 189–193, DOI: [10.1007/bf01303701](https://doi.org/10.1007/bf01303701).

5 S. George, in *Nanomaterial Properties: Implications for Safe Medical Applications of Nanotechnology*, Springer eBooks, 2015, pp. 45–69, DOI: [10.1007/978-3-319-13575-5\\_4](https://doi.org/10.1007/978-3-319-13575-5_4).

6 S. Kumar, *et al.*, Optically Active Nanomaterials and Its Biosensing Applications—A Review, *Biosensors*, 2023, **13**(1), 85, DOI: [10.3390/bios13010085](https://doi.org/10.3390/bios13010085).

7 P. C. Ray, Size and shape dependent second order nonlinear optical properties of nanomaterials and their application in biological and chemical sensing, *Chem. Rev.*, 2010, **110**(9), 5332–5365, DOI: [10.1021/cr900335q](https://doi.org/10.1021/cr900335q).

8 E. Urnukhsaikhan, B.-E. Bold, A. Gunbileg, N. Sukhbaatar and T. Mishig-Ochir, Antibacterial activity and characteristics of silver nanoparticles biosynthesized from *Carduus crispus*, *Sci. Rep.*, 2021, **11**(1), 21047, DOI: [10.1038/s41598-021-00520-2](https://doi.org/10.1038/s41598-021-00520-2).

9 C. Zhang, X. Wang, J. Du, Z. Gu and Y. Zhao, Reactive Oxygen Species-Regulating Strategies based on nanomaterials for disease treatment, *Adv. Sci.*, 2021, **8**(3), 2002797, DOI: [10.1002/advs.202002797](https://doi.org/10.1002/advs.202002797).

10 Z. An, J. Yan, Y. Zhang and R. Pei, Applications of nanomaterials for scavenging reactive oxygen species in the treatment of central nervous system diseases, *J. Mater. Chem. B*, 2020, **8**(38), 8748–8767, DOI: [10.1039/d0tb01380c](https://doi.org/10.1039/d0tb01380c).

11 Y. Li, J. Yang and X. Sun, Reactive Oxygen Species-Based nanomaterials for cancer therapy, *Front. Chem.*, 2021, **9**, 650587, DOI: [10.3389/fchem.2021.650587](https://doi.org/10.3389/fchem.2021.650587).

12 K. S. Kim, D. Lee, C. G. Song and P. M. Kang, Reactive Oxygen Species-Activated nanomaterials as theranostic agents, *Nanomedicine*, 2015, **10**(17), 2709–2723, DOI: [10.2217/nmm.15.108](https://doi.org/10.2217/nmm.15.108).

13 A. Joorabloo and T. Liu, Recent advances in reactive oxygen species scavenging nanomaterials for wound healing, *Exploration*, 2024, **4**(3), 20230066, DOI: [10.1002/exp.20230066](https://doi.org/10.1002/exp.20230066).

14 X. Huang, D. He, Z. Pan, G. Luo and J. Deng, Reactive-oxygen-species-scavenging nanomaterials for resolving inflammation, *Mater. Today Bio*, 2021, **11**, 100124, DOI: [10.1016/j.mtbio.2021.100124](https://doi.org/10.1016/j.mtbio.2021.100124).

15 K. Wei, Y. Faraj, G. Yao, R. Xie and B. Lai, Strategies for improving perovskite photocatalysts reactivity for organic pollutants degradation: A review on recent progress, *Chem. Eng. J.*, 2021, **414**, 128783, DOI: [10.1016/j.cej.2021.128783](https://doi.org/10.1016/j.cej.2021.128783).

16 Q. Wang, *et al.*, Research progress on photocatalytic CO<sub>2</sub> reduction based on perovskite oxides, *Small*, 2023, **19**(38), 2301892, DOI: [10.1002/smll.202301892](https://doi.org/10.1002/smll.202301892).

17 S. A. Ali and T. Ahmad, Treasure trove for efficient hydrogen evolution through water splitting using diverse perovskite photocatalysts, *Mater. Today Chem.*, 2023, **29**, 101387, DOI: [10.1016/j.mtchem.2023.101387](https://doi.org/10.1016/j.mtchem.2023.101387).

18 X. Zhu, Y. Lin, J. S. Martin, Y. Sun, D. Zhu and Y. Yan, Lead halide perovskites for photocatalytic organic synthesis, *Nat. Commun.*, 2019, **10**(1), 2843, DOI: [10.1038/s41467-019-10634-x](https://doi.org/10.1038/s41467-019-10634-x).

19 J. S. Martin, N. Dang, E. Raulerson, M. C. Beard, J. Hartenberger and Y. Yan, Perovskite photocatalytic CO<sub>2</sub> reduction or Photoredox organic transformation, *Angew. Chem., Int. Ed.*, 2022, **61**(39), e202205572, DOI: [10.1002/anie.202205572](https://doi.org/10.1002/anie.202205572).

20 T. M. Brenner, D. A. Egger, L. Kronik, G. Hodes and D. Cahen, Hybrid organic–inorganic perovskites: low-cost semiconductors with intriguing charge-transport properties, *Nat. Rev. Mater.*, 2016, **1**(1), 15007, DOI: [10.1038/natrevmats.2015.7](https://doi.org/10.1038/natrevmats.2015.7).

21 T. Zhang, *et al.*, Ferroelectric hybrid organic–inorganic perovskites and their structural and functional diversity, *Natl. Sci. Rev.*, 2023, **10**(2), 1–18, DOI: [10.1093/nsr/nwac240](https://doi.org/10.1093/nsr/nwac240).

22 J. Liu, *et al.*, In situ ligand passivated organic–inorganic hybrid perovskite quantum dots for photocatalytic antibacterial applications, *J. Colloid Interface Sci.*, 2025, **688**, 630–640, DOI: [10.1016/j.jcis.2025.02.167](https://doi.org/10.1016/j.jcis.2025.02.167).

23 A. Hachani, I. Dridi, A. Othmani, T. Roisnel, H. Stephane and K. Riadh, A zero dimensional hybrid organic–inorganic perovskite CuCl<sub>4</sub> based: Synthesis, crystal structure, vibrational, optical properties, DFT and TDFT calculations, dielectric properties and biological activity, *J. Mol. Struct.*, 2020, **1229**, 129838, DOI: [10.1016/j.molstruc.2020.129838](https://doi.org/10.1016/j.molstruc.2020.129838).

24 I. C. Smith, E. T. Hoke, D. Solis-Ibarra, M. D. McGehee and H. I. Karunadasa, A Layered Hybrid Perovskite Solar-Cell Absorber with Enhanced Moisture Stability, *Angew. Chem., Int. Ed.*, 2014, **53**(42), 11232–11235, DOI: [10.1002/anie.201406466](https://doi.org/10.1002/anie.201406466).

25 B. Günay, H. Döger, Z. F. Karagonlar and Ö. Sağlam, Ag-intercalation of Tm<sup>3+</sup>/Er<sup>3+</sup> Co-doped layered perovskites and their exfoliated 2D nanosheets with an enhanced antibiofilm and antibacterial activity, *Mater. Today Commun.*, 2022, **33**, 104972, DOI: [10.1016/j.mtcomm.2022.104972](https://doi.org/10.1016/j.mtcomm.2022.104972).

26 J. Zhang, *et al.*, Aqueous-phase dual-functional chiral perovskites for hydrogen sulfide (H<sub>2</sub>S) detection and antibacterial applications in *Escherichia coli*, *J. Colloid Interface Sci.*, 2024, **661**, 740–749, DOI: [10.1016/j.jcis.2024.01.207](https://doi.org/10.1016/j.jcis.2024.01.207).

27 Z. Arshad, *et al.*, Enhanced charge transport characteristics in zinc oxide nanofibers via Mg<sup>2+</sup> doping for electron transport layer in perovskite solar cells and antibacterial textiles, *Ceram. Int.*, 2022, **48**(17), 24363–24371, DOI: [10.1016/j.ceramint.2022.05.018](https://doi.org/10.1016/j.ceramint.2022.05.018).



28 M. U. Rehman, Q. Wang and Y. Yu, Electronic, magnetic and optical properties of double perovskite compounds: a first principle approach, *Crystals*, 2022, **12**(11), 1597, DOI: [10.3390/crust12111597](https://doi.org/10.3390/crust12111597).

29 N. Mehtab-Ur-Rehman, X. Jin, Q. Wang and A. M. Jadoon, Opto-Electronic Properties of Methyl-Ammonium lead halide: A first principle approach, *J. Phys. Conf.*, 2020, **1622**(1), 012105, DOI: [10.1088/1742-6596/1622/1/012105](https://doi.org/10.1088/1742-6596/1622/1/012105).

30 Z. Ghorbani and M. H. Ehsani, Viability and antibacterial properties of  $BA_2-x$   $AGXFEMOO_6$ ( $x=0.0, 0.05$ ) double perovskite oxides, *Heliyon*, 2024, **10**(20), e38869, DOI: [10.1016/j.heliyon.2024.e38869](https://doi.org/10.1016/j.heliyon.2024.e38869).

31 H.-C. Zhang, *et al.*, An all-inorganic lead-free metal halide double perovskite for the highly selective detection of norfloxacin in aqueous solution, *Microchim. Acta*, 2024, **191**(3), 1–9, DOI: [10.1007/s00604-024-06198-3](https://doi.org/10.1007/s00604-024-06198-3).

32 X. Li, *et al.*, All inorganic halide perovskites nanosystem: synthesis, structural features, optical properties and optoelectronic applications, *Small*, 2017, **13**(9), 1603996, DOI: [10.1002/smll.201603996](https://doi.org/10.1002/smll.201603996).

33 J. S. Manser, J. A. Christians and P. V. Kamat, Intriguing optoelectronic properties of metal halide perovskites, *Chem. Rev.*, 2016, **116**(21), 12956–13008, DOI: [10.1021/acs.chemrev.6b00136](https://doi.org/10.1021/acs.chemrev.6b00136).

34 K. Chen, S. Schünemann, S. Song and H. Tüysüz, Structural effects on optoelectronic properties of halide perovskites, *Chem. Soc. Rev.*, 2018, **47**(18), 7045–7077, DOI: [10.1039/c8cs00212f](https://doi.org/10.1039/c8cs00212f).

35 S. Soren, *et al.*, Evaluation of the antimicrobial potential of cerium-based perovskite ( $CeCuO_3$ ) synthesized by a hydrothermal method, *New J. Chem.*, 2022, **46**(40), 19147–19152, DOI: [10.1039/d2nj03646k](https://doi.org/10.1039/d2nj03646k).

36 C. Talebpour, F. Fani, M. Ouellette, H. Salimnia and H. Alamdari, Nondegradable antimicrobial Silver-Based perovskite, *ACS Sustain. Chem. Eng.*, 2022, **10**(15), 4922–4928, DOI: [10.1021/acssuschemeng.1c08181](https://doi.org/10.1021/acssuschemeng.1c08181).

37 B. P. Kore, M. Jamshidi and J. M. Gardner, The impact of moisture on the stability and degradation of perovskites in solar cells, *Mater. Adv.*, 2024, **5**(6), 2200–2217, DOI: [10.1039/d3ma00828b](https://doi.org/10.1039/d3ma00828b).

38 L. Jiang, *et al.*, Amorphous NiCoB-coupled MAPbI<sub>3</sub> for efficient photocatalytic hydrogen evolution, *Dalton Trans.*, 2021, **50**(48), 17960–17966, DOI: [10.1039/d1dt03633e](https://doi.org/10.1039/d1dt03633e).

39 G. Grancini, *et al.*, One-Year stable perovskite solar cells by 2D/3D interface engineering, *Nat. Commun.*, 2017, **8**(1), 15684, DOI: [10.1038/ncomms15684](https://doi.org/10.1038/ncomms15684).

40 Z. Zhang, *et al.*, *Stable and Highly Efficient Photocatalysis with Lead-Free Double-Perovskite of  $Cs_2AgBiBr_6$* , Wiley Online Library, 2019, DOI: [10.1002/anie.201900658](https://doi.org/10.1002/anie.201900658).

41 F. Xu, K. Meng, B. Cheng, S. Wang, J. Xu and J. Yu, Unique S-scheme heterojunctions in self-assembled TiO<sub>2</sub>/CsPbBr<sub>3</sub> hybrids for CO<sub>2</sub> photoreduction, *Nat. Commun.*, 2020, **11**(1), 4613, DOI: [10.1038/s41467-020-18350-7](https://doi.org/10.1038/s41467-020-18350-7).

42 C. C. Stoumpos and M. G. Kanatzidis, The renaissance of halide perovskites and their evolution as emerging semiconductors, *Acc. Chem. Res.*, 2015, **48**(10), 2791–2802, DOI: [10.1021/acs.accounts.5b00229](https://doi.org/10.1021/acs.accounts.5b00229).

43 L. Mao, C. C. Stoumpos and M. G. Kanatzidis, Two-Dimensional Hybrid Halide Perovskites: Principles and promises, *J. Am. Chem. Soc.*, 2018, **141**(3), 1171–1190, DOI: [10.1021/jacs.8b10851](https://doi.org/10.1021/jacs.8b10851).

44 L. Zhou, Y. Xu, B. Chen, D. Kuang and C. Su, Synthesis and photocatalytic application of stable Lead-Free CS<sub>2</sub>AGBIBR<sub>6</sub> perovskite nanocrystals, *Small*, 2018, **14**(11), 1703762, DOI: [10.1002/smll.201703762](https://doi.org/10.1002/smll.201703762).

45 J. R. Gonzalez-Moya, C.-Y. Chang, D. R. Radu and C.-Y. Lai, Photocatalytic deposition of nanostructured CSPBBr<sub>3</sub> perovskite Quantum Dot films on mesoporous TiO<sub>2</sub> and their enhanced Visible-Light photodegradation properties, *ACS Omega*, 2022, **7**(30), 26738–26748, DOI: [10.1021/acsomega.2c03089](https://doi.org/10.1021/acsomega.2c03089).

46 C. Wang, *et al.*, Phase Regulation Strategy of Perovskite Nanocrystals from 1D Orthomorphic NH<sub>4</sub>PbI<sub>3</sub> to 3D Cubic (NH<sub>4</sub>)<sub>0.5</sub>Cs<sub>0.5</sub>Pb(10.5Br0.5)<sub>3</sub> Phase Enhances Photoluminescence, *Angew. Chem., Int. Ed.*, 2019, **58**(34), 11642–11646, DOI: [10.1002/anie.201903121](https://doi.org/10.1002/anie.201903121).

47 Y. E. Ajjouri, A. M. Igual-Muñoz, M. Sessolo, F. Palazon and H. J. Bolink, Tunable Wide-Bandgap Monohalide perovskites, *Adv. Opt. Mater.*, 2020, **8**(17), 2000423, DOI: [10.1002/adom.202000423](https://doi.org/10.1002/adom.202000423).

48 Y. Su, *et al.*, Highly Controllable and Efficient Synthesis of Mixed-Halide CsPbX<sub>3</sub> (X = Cl, Br, I) Perovskite QDs toward the Tunability of Entire Visible Light, *ACS Appl. Mater. Interfaces*, 2017, **9**(38), 33020–33028, DOI: [10.1021/acsami.7b10612](https://doi.org/10.1021/acsami.7b10612).

49 F. Xu, T. Zhang, G. Li and Y. Zhao, Mixed cation hybrid lead halide perovskites with enhanced performance and stability, *J. Mater. Chem. A*, 2017, **5**(23), 11450–11461, DOI: [10.1039/c7ta00042a](https://doi.org/10.1039/c7ta00042a).

50 H. A. Schwartz, *et al.*, Band-Gap tuning in All-Inorganic CSPBXSN<sub>1</sub>-xBr<sub>3</sub> perovskites, *ACS Appl. Mater. Interfaces*, 2021, **13**(3), 4203–4210, DOI: [10.1021/acsami.0c20285](https://doi.org/10.1021/acsami.0c20285).

51 X. Qian, *et al.*, Perovskite cesium lead bromide quantum dots: A new efficient photocatalyst for degrading antibiotic residues in organic system, *J. Clean. Prod.*, 2019, **249**, 119335, DOI: [10.1016/j.jclepro.2019.119335](https://doi.org/10.1016/j.jclepro.2019.119335).

52 T. Gulin-Sarfraz, *et al.*, Inorganic nanocarriers for encapsulation of natural antimicrobial compounds for potential food packaging application: A comparative study, *Nanomaterials*, 2021, **11**(2), 379, DOI: [10.3390/nano11020379](https://doi.org/10.3390/nano11020379).

53 F. Mohamadpour and A. M. Amani, Photocatalytic systems: reactions, mechanism, and applications, *RSC Adv.*, 2024, **14**(29), 20609–20645, DOI: [10.1039/d4ra03259d](https://doi.org/10.1039/d4ra03259d).

54 L. Zhang, P. Kuang and J. Yu, in *Introductory Chapter: Fundamentals of Photocatalysis and Electrocatalysis*, Elsevier eBooks, 2022, pp.1–30, DOI: [10.1016/b978-0-12-824526-2.00001-5](https://doi.org/10.1016/b978-0-12-824526-2.00001-5).

55 A. Fujishima and K. Honda, Electrochemical photolysis of water at a semiconductor electrode, *Nature*, 1972, **238**(5358), 37–38, DOI: [10.1038/238037a0](https://doi.org/10.1038/238037a0).

56 D. A. Keane, *et al.*, Solar photocatalysis for water disinfection: materials and reactor design, *Catal. Sci. Technol.*, 2014, **4**(5), 1211–1226, DOI: [10.1039/c4cy00006d](https://doi.org/10.1039/c4cy00006d).



57 H. K. Khalilova, S. A. Hasanova and F. G. Aliyev, Photocatalytic Removal of Organic Pollutants from Industrial Wastewater Using  $\text{TiO}_2$  Catalyst, *J. Environ. Prot.*, 2018, **09**(06), 691–698, DOI: [10.4236/jep.2018.96043](https://doi.org/10.4236/jep.2018.96043).

58 C.-C. Wang, J.-R. Li, X.-L. Lv, Y.-Q. Zhang and G. Guo, Photocatalytic organic pollutants degradation in metal-organic frameworks, *Energy Environ. Sci.*, 2014, **7**(9), 2831–2867, DOI: [10.1039/c4ee01299b](https://doi.org/10.1039/c4ee01299b).

59 H. Ren, P. Koshy, W.-F. Chen, S. Qi and C. C. Sorrell, Photocatalytic materials and technologies for air purification, *J. Hazard. Mater.*, 2016, **325**, 340–366, DOI: [10.1016/j.jhazmat.2016.08.072](https://doi.org/10.1016/j.jhazmat.2016.08.072).

60 R. Michal, S. Sfaelou and P. Lianos, Photocatalysis for renewable energy production using PhotoFuelCells, *Molecules*, 2014, **19**(12), 19732–19750, DOI: [10.3390/molecules191219732](https://doi.org/10.3390/molecules191219732).

61 M. Lilja, J. Forsgren, K. Welch, M. Åstrand, H. Engqvist and M. Strømme, Photocatalytic and antimicrobial properties of surgical implant coatings of titanium dioxide deposited through cathodic arc evaporation, *Biotechnol. Lett.*, 2012, **34**(12), 2299–2305, DOI: [10.1007/s10529-012-1040-2](https://doi.org/10.1007/s10529-012-1040-2).

62 H. Xu, *et al.*, Progress in the development of photoactivated materials for smart and active food packaging: Photoluminescence and photocatalysis approaches, *Chem. Eng. J.*, 2021, **432**, 134301, DOI: [10.1016/j.cej.2021.134301](https://doi.org/10.1016/j.cej.2021.134301).

63 J. Ma, *et al.*, Inactivation mechanism of *E. coli* in water by enhanced photocatalysis under visible light irradiation, *Sci. Total Environ.*, 2023, **866**, 161450, DOI: [10.1016/j.scitotenv.2023.161450](https://doi.org/10.1016/j.scitotenv.2023.161450).

64 P. Ganguly, C. Byrne, A. Breen and S. C. Pillai, Antimicrobial activity of photocatalysts: Fundamentals, mechanisms, kinetics and recent advances, *Appl. Catal., B*, 2017, **225**, 51–75, DOI: [10.1016/j.apcatb.2017.11.018](https://doi.org/10.1016/j.apcatb.2017.11.018).

65 O. V. Nkwachukwu and O. A. Arotiba, Perovskite Oxide-Based Materials for Photocatalytic and Photoelectrocatalytic Treatment of Water, *Front. Chem.*, 2021, **9**, 634630, DOI: [10.3389/fchem.2021.634630](https://doi.org/10.3389/fchem.2021.634630).

66 M. Irshad, *et al.*, Photocatalysis and perovskite oxide-based materials: a remedy for a clean and sustainable future, *RSC Adv.*, 2022, **12**(12), 7009–7039, DOI: [10.1039/D1RA08185C](https://doi.org/10.1039/D1RA08185C).

67 H. Wang, Q. Zhang, M. Qiu and B. Hu, Synthesis and application of perovskite-based photocatalysts in environmental remediation: A review, *J. Mol. Liq.*, 2021, **334**, 116029, DOI: [10.1016/j.molliq.2021.116029](https://doi.org/10.1016/j.molliq.2021.116029).

68 M. A. Kohanski, D. J. Dwyer, B. Hayete, C. A. Lawrence and J. J. Collins, A common mechanism of cellular death induced by bactericidal antibiotics, *Cell*, 2007, **130**(5), 797–810, DOI: [10.1016/j.cell.2007.06.049](https://doi.org/10.1016/j.cell.2007.06.049).

69 J. Fujii, T. Homma and T. Osaki, Superoxide radicals in the execution of cell death, *Antioxidants*, 2022, **11**(3), 501, DOI: [10.3390/antiox11030501](https://doi.org/10.3390/antiox11030501).

70 C. M. C. Andrés, J. M. P. De La Lastra, C. A. Juan, F. J. Plou and E. Pérez-Lebeña, Superoxide Anion Chemistry—Its role at the core of the innate immunity, *Int. J. Mol. Sci.*, 2023, **24**(3), 1841, DOI: [10.3390/ijms24031841](https://doi.org/10.3390/ijms24031841).

71 T. Chidawanyika and S. Supattapone, Hydrogen peroxide-induced cell death in mammalian cells, *J. Cell. Signal.*, 2021, **2**(3), 206–211, DOI: [10.33696/signaling.2.052](https://doi.org/10.33696/signaling.2.052).

72 J. A. Imlay and S. Linn, Bimodal pattern of killing of DNA-repair-defective or anoxically grown *Escherichia coli* by hydrogen peroxide, *J. Bacteriol.*, 1986, **166**(2), 519–527, DOI: [10.1128/jb.166.2.519-527.1986](https://doi.org/10.1128/jb.166.2.519-527.1986).

73 E. Koh, R. Carmieli, A. Mor and R. Fluhr, Singlet Oxygen-Induced membrane disruption and Serpin-Protease balance in Vacuolar-Driven cell death, *Plant Physiol.*, 2016, **171**(3), 1616–1625, DOI: [10.1104/pp.15.02026](https://doi.org/10.1104/pp.15.02026).

74 A. E.-D. H. Sayed and H. A. M. Soliman, Developmental toxicity and DNA damaging properties of silver nanoparticles in the catfish (*Clarias gariepinus*), *Mutat. Res., Genet. Toxicol. Environ. Mutagen.*, 2017, **822**, 34–40, DOI: [10.1016/j.mrgentox.2017.07.002](https://doi.org/10.1016/j.mrgentox.2017.07.002).

75 “Oxidative stress in bacteria and protein damage by reactive oxygen species”, PubMed, Mar. 01, 2000. <https://pubmed.ncbi.nlm.nih.gov/10963327/>.

76 Z. Shen, W. Wu and S. L. Hazen, Activated Leukocytes Oxidatively Damage DNA, RNA, and the Nucleotide Pool through Halide-Dependent Formation of Hydroxyl Radical, *Biochemistry*, 2000, **39**(18), 5474–5482, DOI: [10.1021/bi992809y](https://doi.org/10.1021/bi992809y).

77 H. T. Endale, W. Tesfaye and T. A. Mengstie, ROS induced lipid peroxidation and their role in ferroptosis, *Front. Cell Dev. Biol.*, 2023, **11**, 1226044, DOI: [10.3389/fcell.2023.1226044](https://doi.org/10.3389/fcell.2023.1226044).

78 M. M. Gaschler and B. R. Stockwell, Lipid peroxidation in cell death, *Biochem. Biophys. Res. Commun.*, 2017, **482**(3), 419–425, DOI: [10.1016/j.bbrc.2016.10.086](https://doi.org/10.1016/j.bbrc.2016.10.086).

79 C. L. Simms and H. S. Zaher, Quality control of chemically damaged RNA, *Cell. Mol. Life Sci.*, 2016, **73**(19), 3639–3653, DOI: [10.1007/s00018-016-2261-7](https://doi.org/10.1007/s00018-016-2261-7).

80 M. Liu, X. Gong, R. K. Alluri, J. Wu, T. Sablo and Z. Li, Characterization of RNA damage under oxidative stress in *Escherichia coli*, *Biol. Chem.*, 2012, **393**(3), 123–132, DOI: [10.1515/hsz-2011-0247](https://doi.org/10.1515/hsz-2011-0247).

81 M. Tanaka and P. B. Chock, Oxidative modifications of RNA and its potential roles in biosystem, *Front. Mol. Biosci.*, 2021, **8**, 685331, DOI: [10.3389/fmolsb.2021.685331](https://doi.org/10.3389/fmolsb.2021.685331).

82 P. A. Küpfer and C. J. Leumann, in *Oxidative damage on RNA nucleobases*, RNA technologies, 2014, pp. 75–94, DOI: [10.1007/978-3-642-54452-1\\_5](https://doi.org/10.1007/978-3-642-54452-1_5).

83 A. Manke, L. Wang and Y. Rojanasakul, Mechanisms of Nanoparticle-Induced Oxidative stress and toxicity, *BioMed Res. Int.*, 2013, **2013**, 1–15, DOI: [10.1155/2013/942916](https://doi.org/10.1155/2013/942916).

84 L. Li, *et al.*, Trimethyltin chloride induces apoptosis and DNA damage via ROS/NF- $\kappa$ B in grass carp liver cells causing immune dysfunction, *Fish Shellfish Immunol.*, 2023, **142**, 109082, DOI: [10.1016/j.fsi.2023.109082](https://doi.org/10.1016/j.fsi.2023.109082).

85 N. Kandoth, *et al.*, Multimodal biofilm inactivation using a photocatalytic bismuth Perovskite-TIO2-RU(II) polypyridyl-Based multisite heterojunction, *ACS Nano*, 2023, **17**(11), 10393–10406, DOI: [10.1021/acsnano.3c01064](https://doi.org/10.1021/acsnano.3c01064).



86 S. Manori, *et al.*, Radical-Mediated photocatalytic dye degradation and antimicrobial properties of LA<sub>2</sub>NIMNO<sub>6</sub> nanoparticles, *New J. Chem.*, 2024, **49**(3), 807–824, DOI: [10.1039/d4nj04437a](https://doi.org/10.1039/d4nj04437a).

87 J. Schneider, M. Matsuoka, M. Takeuchi, J. Zhang, Y. Horiuchi, M. Anpo and D. W. Bahnemann, Understanding TiO<sub>2</sub> photocatalysis: mechanisms and materials, *Chem. Rev.*, 2014, **114**, 9919–9986.

88 R. Abe, Recent progress on photocatalytic and photoelectrochemical water splitting under visible light irradiation, *J. Photochem. Photobiol. C*, 2010, **11**, 179–209.

89 R. Prasanna, *et al.*, Band gap tuning via lattice contraction and octahedral tilting in perovskite materials for photovoltaics, *J. Am. Chem. Soc.*, 2017, **139**(32), 11117–11124, DOI: [10.1021/jacs.7b04981](https://doi.org/10.1021/jacs.7b04981).

90 A. Ummadisingu, S. Meloni, A. Mattoni, W. Tress and M. Grätzel, Crystal-Size-Induced Band gap tuning in perovskite films, *Angew. Chem., Int. Ed.*, 2021, **60**(39), 21368–21376, DOI: [10.1002/anie.202106394](https://doi.org/10.1002/anie.202106394).

91 S. A. Kulkarni, T. Baikie, P. P. Boix, N. Yantara, N. Mathews and S. Mhaisalkar, Band-gap tuning of lead halide perovskites using a sequential deposition process, *J. Mater. Chem. A*, 2014, **2**(24), 9221–9225, DOI: [10.1039/c4ta00435c](https://doi.org/10.1039/c4ta00435c).

92 S. M. H. Qaid, *et al.*, Band-gap tuning of lead halide perovskite using a single step spin-coating deposition process, *Mater. Lett.*, 2015, **164**, 498–501, DOI: [10.1016/j.matlet.2015.10.135](https://doi.org/10.1016/j.matlet.2015.10.135).

93 A. L. Abdelhady, *et al.*, Heterovalent dopant incorporation for bandgap and type engineering of perovskite crystals, *J. Phys. Chem. Lett.*, 2016, **7**(2), 295–301, DOI: [10.1021/acs.jpcllett.5b02681](https://doi.org/10.1021/acs.jpcllett.5b02681).

94 T. Htun, *et al.*, Lead-free iron-doped Cs<sub>3</sub>Bi<sub>2</sub>Br<sub>9</sub> perovskite with tunable properties, *RSC Adv.*, 2024, **14**(32), 23177–23183, DOI: [10.1039/d4ra04062g](https://doi.org/10.1039/d4ra04062g).

95 K. Guo, *et al.*, Modification of CS<sub>2</sub>AGBICl<sub>6</sub> Double-Perovskite photocatalytic activity by BR doping, *Inorg. Chem.*, 2025, **64**, 4339–4344, DOI: [10.1021/acs.inorgchem.4c04884](https://doi.org/10.1021/acs.inorgchem.4c04884).

96 Q. Chen, *et al.*, Planar heterojunction perovskite solar cells via Vapor-Assisted Solution Process, *J. Am. Chem. Soc.*, 2013, **136**(2), 622–625, DOI: [10.1021/ja411509g](https://doi.org/10.1021/ja411509g).

97 T. Tang, *et al.*, Enhancing the Photocatalytic Activity of Lead-Free Halide Perovskite Cs<sub>3</sub>Bi<sub>2</sub>I<sub>9</sub> by Compositing with Ti<sub>3</sub>C<sub>2</sub> MXene, *Molecules*, 2024, **29**(21), 5096, DOI: [10.3390/molecules29215096](https://doi.org/10.3390/molecules29215096).

98 E. Zhu, *et al.*, Heterojunction-Type Photocatalytic System Based on Inorganic Halide Perovskite CsPbBr<sub>3</sub>, *Chin. J. Chem.*, 2020, **38**(12), 1718–1722, DOI: [10.1002/cjoc.202000333](https://doi.org/10.1002/cjoc.202000333).

99 Y. Zhao, *et al.*, Anions-Exchange-Induced Efficient Carrier Transport at CsPbBr<sub>x</sub>Cl<sub>3-x</sub>/TiO<sub>2</sub> Interface for Photocatalytic Activation of C(sp<sup>3</sup>)–H bond in Toluene Oxidation, *ChemCatChem*, 2021, **13**(11), 2592–2598, DOI: [10.1002/cctc.202100223](https://doi.org/10.1002/cctc.202100223).

100 W. E. I. Sha, X. Ren, L. Chen and W. C. H. Choy, The Efficiency Limit of CH<sub>3</sub>NH<sub>3</sub>PbI<sub>3</sub> Perovskite Solar Cells, *Appl. Phys. Lett.*, 2015, **106**, 221104.

101 Y. Hu, *et al.*, Hybrid Perovskite/Perovskite heterojunction solar cells, *ACS Nano*, 2016, **10**(6), 5999–6007, DOI: [10.1021/acsnano.6b01535](https://doi.org/10.1021/acsnano.6b01535).

102 C. Mao, *et al.*, Enhanced Near-Infrared photocatalytic eradication of MRSA biofilms and osseointegration using oxide Perovskite-Based P–N heterojunction, *Adv. Sci.*, 2021, **8**(15), 2002211, DOI: [10.1002/advs.202002211](https://doi.org/10.1002/advs.202002211).

103 N. Kandoth, *et al.*, Harnessing Multi-Modal Exciton Migration in Hybrid Halide Perovskite for Photocatalytic Amplification of Nitric Oxide and Hydroxyl Radicals toward Bacterial Killing and Biofilm Disruption, *Adv. Funct. Mater.*, 2024, **34**(28), 2400998, DOI: [10.1002/adfm.202400998](https://doi.org/10.1002/adfm.202400998).

104 W. Fu, *et al.*, Stability of perovskite materials and devices, *Mater. Today*, 2022, **58**, 275–296, DOI: [10.1016/j.mattod.2022.06.020](https://doi.org/10.1016/j.mattod.2022.06.020).

105 S. N. Raja, *et al.*, Encapsulation of Perovskite Nanocrystals into Macroscale Polymer Matrices: Enhanced Stability and Polarization, *ACS Appl. Mater. Interfaces*, 2016, **8**(51), 35523–35533, DOI: [10.1021/acsami.6b09443](https://doi.org/10.1021/acsami.6b09443).

106 J. Zhao, *et al.*, Cesium immobilization in perovskite-type Ba<sub>1-x</sub>(La, Cs)<sub>x</sub>ZrO<sub>3</sub> ceramics by sol-gel method, *Ceram. Int.*, 2019, **46**(7), 9968–9971, DOI: [10.1016/j.ceramint.2019.12.219](https://doi.org/10.1016/j.ceramint.2019.12.219).

107 E. S. M. Mouele, *et al.*, Spin coating immobilisation of C–N-TIO<sub>2</sub> Co-Doped nano catalyst on glass and application for photocatalysis or as electron transporting layer for perovskite solar cells, *Coatings*, 2020, **10**(11), 1029, DOI: [10.3390/coatings10111029](https://doi.org/10.3390/coatings10111029).

108 Z. Balta and E. B. Simsek, Discovering of the photocatalytic performance of BiFeO<sub>3</sub>/BNQDs immobilized polyester filters for efficient continuous-flow elimination of recalcitrant antibiotic via PMS activated process, *Opt. Mater.*, 2022, **133**, 113015, DOI: [10.1016/j.optmat.2022.113015](https://doi.org/10.1016/j.optmat.2022.113015).

109 H. Ishihama, *et al.*, An antibacterial coated polymer prevents biofilm formation and implant-associated infection, *Sci. Rep.*, 2021, **11**(1), 3602, DOI: [10.1038/s41598-021-82992-w](https://doi.org/10.1038/s41598-021-82992-w).

110 M. B. Chabalala, N. N. Gumbi, B. B. Mamba, M. Z. Al-Abri and E. N. Nxumalo, Photocatalytic nanofiber membranes for the degradation of micropollutants and their antimicrobial activity: recent advances and future prospects, *Membranes*, 2021, **11**(9), 678, DOI: [10.3390/membranes11090678](https://doi.org/10.3390/membranes11090678).

111 N. Midoux, C. Roizard and J.-c. Andre, Industrial photochemistry XV: Interests and limits of the buckingham theorem for the design of industrial photoreactors, *J. Photochem. Photobiol. A*, 1989, **50**(1), 83–102, DOI: [10.1016/1010-6030\(89\)80023-1](https://doi.org/10.1016/1010-6030(89)80023-1).

112 Y. Yao, T. Ochiai, H. Ishiguro, R. Nakano and Y. Kubota, Antibacterial performance of a novel photocatalytic-coated cordierite foam for use in air cleaners, *Appl.*



*Catal., B*, 2011, **106**(3–4), 592–599, DOI: [10.1016/j.apcatb.2011.06.020](https://doi.org/10.1016/j.apcatb.2011.06.020).

113 J. Parmar, S. Jang, L. Soler, D.-P. Kim and S. Sánchez, Nano-photocatalysts in microfluidics, energy conversion and environmental applications, *Lab Chip*, 2015, **15**(11), 2352–2356, DOI: [10.1039/c5lc90047f](https://doi.org/10.1039/c5lc90047f).

114 S. Zou, X. Zhao, W. Ouyang and S. Xu, Microfluidic synthesis, doping strategy, and optoelectronic applications of nanostructured halide perovskite materials, *Micromachines*, 2022, **13**(10), 1647, DOI: [10.3390/mi13101647](https://doi.org/10.3390/mi13101647).

115 X. Fu, *et al.*, Critical review on modified floating photocatalysts for emerging contaminants removal from landscape water: problems, methods and mechanism, *Chemosphere*, 2023, **341**, 140043, DOI: [10.1016/j.chemosphere.2023.140043](https://doi.org/10.1016/j.chemosphere.2023.140043).

116 S.-M. Lam, J.-C. Sin and A. R. Mohamed, A newly emerging visible light-responsive  $\text{BiFeO}_3$  perovskite for photocatalytic applications: A mini review, *Mater. Res. Bull.*, 2017, **90**, 15–30, DOI: [10.1016/j.materresbull.2016.12.052](https://doi.org/10.1016/j.materresbull.2016.12.052).

117 N. Birben, E. Lale, R. Pelosato, C. Uyguner Demirel, I. Natali Sora and M. Bekbolet, Photocatalytic Bactericidal Performance of  $\text{LaFeO}_3$  under Solar Light: Kinetics, Spectroscopic and Mechanistic Evaluation, *Water*, 2021, **13**(9), 1135, DOI: [10.3390/w13091135](https://doi.org/10.3390/w13091135).

118 A. Akbari, M. Mehrabian, Z. Salimi, S. Dalir and M. Akbarpour, The comparison of antibacterial activities of  $\text{CsPbBr}_3$  and  $\text{ZnO}$  nanoparticles, *Int. Nano Lett.*, 2019, **9**(4), 349–353, DOI: [10.1007/s40089-019-0280-8](https://doi.org/10.1007/s40089-019-0280-8). <http://creativecommons.org/licenses/by/4.0/>.

119 Y. Zhu, H. Shen, Q. Ai, Y. Feng, B. Shin, M. Gonzales, Y. Yan, Z. He, X. Huang, X. Zhang, Y. Han, P. M. Ajayan, Q. Li and J. Lou, Double Layer  $\text{SiO}_2$ -Coated Water-Stable Halide Perovskite as a Promising Antimicrobial Photocatalyst under Visible Light, *Nano Lett.*, 2024, **24**, 13718–13726, DOI: [10.1021/ACS.NANOLETT.4C03793](https://doi.org/10.1021/ACS.NANOLETT.4C03793).

120 Y. Huang, J. Yu, Z. Wu, B. Li and M. Li, All-inorganic lead halide perovskites for photocatalysis: a review, *RSC Adv.*, 2024, **14**(7), 4946–4965, DOI: [10.1039/D3RA07998H](https://doi.org/10.1039/D3RA07998H).

121 M. Karami, M. Ghanbari, O. Amiri and M. Salavati-Niasari, Enhanced antibacterial activity and photocatalytic degradation of organic dyes under visible light using cesium lead iodide perovskite nanostructures prepared by hydrothermal method, *Sep. Purif. Technol.*, 2020, **253**, 117526, DOI: [10.1016/j.seppur.2020.117526](https://doi.org/10.1016/j.seppur.2020.117526).

122 C. Tedesco and L. Malavasi, Bismuth-Based Halide Perovskites for Photocatalytic  $\text{H}_2$  Evolution Application, *Molecules*, 2023, **28**(1), 339, DOI: [10.3390/molecules28010339](https://doi.org/10.3390/molecules28010339).

123 A. da Silva Júnior, *et al.*, Reviewing Perovskite Oxide-Based Materials for the Effective Treatment of Antibiotic-Polluted Environments: Challenges, Trends, and New Insights, *Surfaces*, 2024, **7**(1), 54–78, DOI: [10.3390/surfaces7010005](https://doi.org/10.3390/surfaces7010005).

124 Z. Yuan, J. Zhang, X. Feng and G. Zhao, Aqueous-phase stable  $\text{CsPbBr}_3$  nanocrystals and quaternary chitosan co-assembled by electrostatic interaction for synergistic photocatalytic antimicrobial, *J. Lumin.*, 2024, **271**, 120619, DOI: [10.1016/j.jlumin.2024.120619](https://doi.org/10.1016/j.jlumin.2024.120619).

125 Y. Cao, *et al.*, Pressure-Tailored Band Gap engineering and Structure evolution of cubic cesium lead iodide perovskite nanocrystals, *J. Phys. Chem. C*, 2018, **122**(17), 9332–9338, DOI: [10.1021/acs.jpcc.8b01673](https://doi.org/10.1021/acs.jpcc.8b01673).

126 K. S. Velu, *et al.*, Cesium lead iodide-decorated two-dimensional titanium dioxide/reduced graphene oxide nanofiber composites as photoanodes for inorganic perovskite solar cells, *Mater. Today Commun.*, 2023, **37**, 107281, DOI: [10.1016/j.mtcomm.2023.107281](https://doi.org/10.1016/j.mtcomm.2023.107281).

127 R. Waykar, *et al.*, Environmentally stable lead-free cesium bismuth iodide ( $\text{Cs}_3\text{Bi}_2\text{I}_9$ ) perovskite: Synthesis to solar cell application, *J. Phys. Chem. Solids*, 2020, **146**, 109608, DOI: [10.1016/j.jpcs.2020.109608](https://doi.org/10.1016/j.jpcs.2020.109608).

128 M. Miodyńska, *et al.*, Lead-free bismuth-based perovskites coupled with g-C3N4: A machine learning based novel approach for visible light induced degradation of pollutants, *Appl. Surf. Sci.*, 2022, **588**, 152921, DOI: [10.1016/j.apsusc.2022.152921](https://doi.org/10.1016/j.apsusc.2022.152921).

129 J. K. Pious, M. L. Lekshmi, C. Muthu, R. B. Rakhi and C. Vijayakumar, Zero-Dimensional methylammonium bismuth Iodide-Based Lead-Free perovskite capacitor, *ACS Omega*, 2017, **2**(9), 5798–5802, DOI: [10.1021/acsomega.7b00973](https://doi.org/10.1021/acsomega.7b00973).

130 B.-M. Bresolin, S. B. Hammouda and M. Sillanpää, Methylammonium iodo bismuthate perovskite ( $\text{CH}_3\text{NH}_3\text{Bi}_2\text{I}_9$ ) as new effective visible light-responsive photocatalyst for degradation of environment pollutants, *J. Photochem. Photobiol. A*, 2019, **376**, 116–126, DOI: [10.1016/j.jphotochem.2019.03.009](https://doi.org/10.1016/j.jphotochem.2019.03.009).

131 J. Liu, *et al.*, Self-assembled  $\text{LaCoO}_3/\text{Ag}_3\text{PO}_4$  nanocomposite with enhanced anti-bacterial performance, *Ceram. Int.*, 2024, **50**(17), 31051–31059, DOI: [10.1016/j.ceramint.2024.05.410](https://doi.org/10.1016/j.ceramint.2024.05.410).

132 S. S. Bhosale, S. Narra, E. Jokar, A. Manikandan, Y. L. Chueh and E. W. G. Diau, Functionalized hybrid perovskite nanocrystals with organic ligands showing a stable 3D/2D core/shell structure for display and laser applications, *J. Mater. Chem. C*, 2021, **9**(48), 17341–17348, DOI: [10.1039/D1TC04049A](https://doi.org/10.1039/D1TC04049A).

133 X. Qu, M. Liu, H. Zhai, X. Zhao, L. Shi and F. Du, Plasmonic Ag-promoted layered perovskite oxyhalide  $\text{Bi}_4\text{NbO}_8\text{Cl}$  for enhanced photocatalytic performance towards water decontamination, *J. Alloys Compd.*, 2019, **810**, 151919, DOI: [10.1016/J.JALLCOM.2019.151919](https://doi.org/10.1016/J.JALLCOM.2019.151919).

134 H. Fujito, *et al.*, Layered Perovskite Oxychloride  $\text{Bi}_4\text{NbO}_8\text{Cl}$ : A Stable Visible Light Responsive Photocatalyst for Water Splitting, *J. Am. Chem. Soc.*, 2016, **138**(7), 2082–2085, DOI: [10.1021/JACS.5B11191](https://doi.org/10.1021/JACS.5B11191).

135 H. Huang, L. Polavarapu, J. A. Sichert, A. S. Susha, A. S. Urban and A. L. Rogach, Colloidal lead halide perovskite nanocrystals: synthesis, optical properties and applications, *NPG Asia Mater.*, 2016, **8**(11), e328, DOI: [10.1038/am.2016.167](https://doi.org/10.1038/am.2016.167).

136 S. Ghosh and L. Manna, The Many ‘facets’ of Halide Ions in the Chemistry of Colloidal Inorganic Nanocrystals, *Chem.*



Rev., 2018, 118(16), 7804–7864, DOI: [10.1021/ACS.CHEMREV.8B00158/ASSET/IMAGES/LARGE/CR-2018-00158Z\\_0035.JPG](https://doi.org/10.1021/ACS.CHEMREV.8B00158/ASSET/IMAGES/LARGE/CR-2018-00158Z_0035.JPG).

137 R. Hailili, *et al.*, Oxygen vacancies induced visible-light photocatalytic activities of  $\text{CaCu}_3\text{Ti}_4\text{O}_{12}$  with controllable morphologies for antibiotic degradation, *Appl. Catal., B*, 2018, 221, 422–432, DOI: [10.1016/J.APCATB.2017.09.026](https://doi.org/10.1016/J.APCATB.2017.09.026).

138 A. Majumdar and A. Pal, Optimized synthesis of  $\text{Bi}_4\text{Nb}_8\text{O}_{31}$  perovskite nanosheets for enhanced visible light assisted photocatalytic degradation of tetracycline antibiotics, *J. Environ. Chem. Eng.*, 2020, 8(1), 103645, DOI: [10.1016/J.JECE.2019.103645](https://doi.org/10.1016/J.JECE.2019.103645).

139 R. Abirami, T. S. Senthil, S. Kalpana, L. Kungumadevi and M. Kang, Hydrothermal synthesis of pure  $\text{PbTiO}_3$  and silver doped  $\text{PbTiO}_3$  perovskite nanoparticles for enhanced photocatalytic activity, *Mater. Lett.*, 2020, 279, 128507, DOI: [10.1016/J.MATLET.2020.128507](https://doi.org/10.1016/J.MATLET.2020.128507).

140 Ö. Tuna, S. Karadirek and E. B. Simsek, Deposition of  $\text{CaFe}_2\text{O}_4$  and  $\text{LaFeO}_3$  perovskites on polyurethane filter: A new photocatalytic support for flowthrough degradation of tetracycline antibiotic, *Environ. Res.*, 2022, 205, 112389, DOI: [10.1016/J.ENVRES.2021.112389](https://doi.org/10.1016/J.ENVRES.2021.112389).

141 P. Zhou, *et al.*, Single-atom Pt-I<sub>3</sub> sites on all-inorganic  $\text{Cs}_2\text{Sn}_1\text{I}_6$  perovskite for efficient photocatalytic hydrogen production, *Nat. Commun.*, 2021, 12(1), 4412, DOI: [10.1038/S41467-021-24702-8](https://doi.org/10.1038/S41467-021-24702-8).

142 R. L. Milot, G. E. Eperon, H. J. Snaith, M. B. Johnston and L. M. Herz, Temperature-Dependent Charge-Carrier Dynamics in  $\text{CH}_3\text{NH}_3\text{PbI}_3$  Perovskite Thin Films, *Adv. Funct. Mater.*, 2015, 25(39), 6218–6227, DOI: [10.1002/ADFM.201502340](https://doi.org/10.1002/ADFM.201502340).

143 R. Hailili, *et al.*, Ionic liquid-mediated microstructure regulations of layered perovskite for enhanced visible light photocatalytic activity, *Front. Catal.*, 2022, 2, 890842, DOI: [10.3389/FCTLS.2022.890842](https://doi.org/10.3389/FCTLS.2022.890842).

144 A. O. Oluwole and O. S. Olatunji, Photocatalytic degradation of tetracycline in aqueous systems under visible light irradiation using needle-like  $\text{SnO}_2$  nanoparticles anchored on exfoliated g-C<sub>3</sub>N<sub>4</sub>, *Environ. Sci. Eur.*, 2022, 34(1), 1–14, DOI: [10.1186/S12302-021-00588-7/TABLES/2](https://doi.org/10.1186/S12302-021-00588-7/TABLES/2).

145 L. Yue, B. Yan, M. Attridge and Z. Wang, Light absorption in perovskite solar cell: Fundamentals and plasmonic enhancement of infrared band absorption, *Sol. Energy*, 2015, 124, 143–152, DOI: [10.1016/j.solener.2015.11.028](https://doi.org/10.1016/j.solener.2015.11.028).

146 V. Raval and T. Ghosh, Charge carrier dynamics and transient spectral evolutions in lead halide perovskites, *Chem. Commun.*, 2023, 59(94), 13939–13950, DOI: [10.1039/d3cc04297a](https://doi.org/10.1039/d3cc04297a).

147 L. M. Herz, Charge-Carrier mobilities in Metal halide perovskites: Fundamental mechanisms and limits, *ACS Energy Lett.*, 2017, 2(7), 1539–1548, DOI: [10.1021/acsenergylett.7b00276](https://doi.org/10.1021/acsenergylett.7b00276).

148 S. D. Stranks, *et al.*, Electron-Hole diffusion lengths exceeding 1 micrometer in an organometal trihalide perovskite absorber, *Science*, 2013, 342(6156), 341–344, DOI: [10.1126/science.1243982](https://doi.org/10.1126/science.1243982).

149 M. B. Johnston and L. M. Herz, Hybrid perovskites for photovoltaics: Charge-Carrier recombination, diffusion, and radiative efficiencies, *Acc. Chem. Res.*, 2015, 49(1), 146–154, DOI: [10.1021/acs.accounts.5b00411](https://doi.org/10.1021/acs.accounts.5b00411).

150 A. R. Bowman, M. T. Klug, T. A. S. Doherty, M. D. Farrar, S. P. Senanayak, B. Wenger, G. Divitini, E. P. Booker, Z. Andaji-Garmaroudi, S. Macpherson, E. Ruggeri, H. Sirringhaus, H. J. Snaith and S. D. Stranks, Microsecond carrier lifetimes, controlled P-Doping, and enhanced air stability in Low-Bandgap metal halide perovskites, *ACS Energy Lett.*, 2019, 4(9), 2301–2307, DOI: [10.1021/acsenergylett.9b01446](https://doi.org/10.1021/acsenergylett.9b01446).

151 S. A. Khan, C. Li, A. Jalil, X. Xin, M. Rauf, J. Ahmed, M. A. Majeed Khan, B. Dong, J. Zhu and S. Agathopoulos, Development of structure and tuning ability of the luminescence of lead-free halide perovskite nanocrystals (NCs), *Chem. Eng. J.*, 2020, 420, 127603, DOI: [10.1016/j.cej.2020.127603](https://doi.org/10.1016/j.cej.2020.127603).

152 S. Apergi, G. Brocks, S. Tao and S. Olthof, Probing the Reactivity of ZnO with Perovskite Precursors, *ACS Appl. Mater. Interfaces*, 2024, 16(12), 14984–14994, DOI: [10.1021/acsami.4c01945](https://doi.org/10.1021/acsami.4c01945).

153 C. Hu, J. Guo, J. Qu and X. Hu, Photocatalytic Degradation of Pathogenic Bacteria with AgI/TiO<sub>2</sub> under Visible Light Irradiation, *Langmuir*, 2007, 23(9), 4982–4987, DOI: [10.1021/la063626x](https://doi.org/10.1021/la063626x).

154 A. Góra, L. Tian, S. Ramakrishna and S. Mukherjee, Design of Novel Perovskite-Based Polymeric Poly(l-Lactide-Co-Glycolide) Nanofibers with Anti-Microbial Properties for Tissue Engineering, *Nanomaterials*, 2020, 10(6), 1127, DOI: [10.3390/nano10061127](https://doi.org/10.3390/nano10061127).

155 P. Raju, P. Arivalagan and S. Natarajan, One-pot fabrication of multifunctional catechin@ZIF-L nanocomposite: Assessment of antibiofilm, larvicidal and photocatalytic activities, *J. Photochem. Photobiol., B*, 2020, 203, 111774, DOI: [10.1016/j.jphotobiol.2019.111774](https://doi.org/10.1016/j.jphotobiol.2019.111774).

156 L. Zhang, P. Y. Tan, C. L. Chow, C. K. Lim, O. K. Tan, M. S. Tse and C. C. Sze, Antibacterial activities of mechanochemically synthesized perovskite strontium titanate ferrite metal oxide, *Colloids Surf., A*, 2014, 456, 169–175, DOI: [10.1016/j.colsurfa.2014.05.032](https://doi.org/10.1016/j.colsurfa.2014.05.032).

157 W. Bouch, F. Djani, D. E. Mazouzi, R. N. Elhoud, S. Makhlofi, C. Laiadi, A. Martínez-Arias, A. Aygün and F. Sen, Bi-doped  $\text{BaBiO}_3$  ( $x = 0\%$ , 5%, 10%, 15%, and 20%) perovskite oxides by a sol-gel method: comprehensive biological assessment and RhB photodegradation, *RSC Adv.*, 2024, 14(11), 7359–7370, DOI: [10.1039/D3RA06354B](https://doi.org/10.1039/D3RA06354B).

158 J. Wang, P. Li, Y. Zhao and X. Zeng, Nb/N Co-Doped Layered Perovskite  $\text{Sr}_2\text{TiO}_4$ : Preparation and Enhanced Photocatalytic Degradation Tetracycline under Visible Light, *Int. J. Mol. Sci.*, 2022, 23(18), 10927, DOI: [10.3390/IJMS231810927](https://doi.org/10.3390/IJMS231810927).

159 J. Kong, T. Yang, Z. Rui and H. Ji, Perovskite-based photocatalysts for organic contaminants removal: Current status and future perspectives, *Catal. Today*, 2019, 327, 47–63, DOI: [10.1016/J.CATTOD.2018.06.045](https://doi.org/10.1016/J.CATTOD.2018.06.045).



160 Y. Lu, R. Xiong, Y. Tang, N. Yu, X. Nie, X. Meng and Q. Ye, Recent advances in the stability-improved and performance-enhanced strategies to halide perovskites for the detection of food-harmful substances, *Chem. Eng. J.*, 2024, **488**, 150970, DOI: [10.1016/j.cej.2024.150970](https://doi.org/10.1016/j.cej.2024.150970).

161 Y. Li, Z. Cui, L. Shi, J. Shan, W. Zhang, Y. Wang, Y. Ji, D. Zhang and J. Wang, Perovskite Nanocrystals: Superior Luminogens for Food Quality Detection Analysis, *J. Agric. Food Chem.*, 2024, **72**(9), 4493–4517, DOI: [10.1021/acs.jafc.3c06660](https://doi.org/10.1021/acs.jafc.3c06660).

162 C. Singh and M. Rakesh, A new cost-effective potassium based LaFeO<sub>3</sub> perovskite for antimicrobial application, *Int. J. Chemtech. Res.*, 2019, **12**(05), 87–96, DOI: [10.20902/IJCTR.2019.120510](https://doi.org/10.20902/IJCTR.2019.120510).

163 Z. Jiang, H. Liu, J. Zou, Y. Huang, Z. Xu, D. Pustovyi and S. Vitusevich, Scale-up synthesis of high-quality solid-state-processed CsCuX (X = Cl, Br, I) perovskite nanocrystal materials toward near-ultraviolet flexible electronic properties, *RSC Adv.*, 2023, **13**(9), 5993–6001, DOI: [10.1039/d2ra07100b](https://doi.org/10.1039/d2ra07100b).

164 R. K. Raman, S. Ganesan, A. Alagumalai, V. S. Menon, S. Krishnan, S. A. Gurusamy Thangavelu and A. Krishnamoorthy, Facile and scalable bilayer polymer encapsulation to achieve long-term stability of perovskite solar cells under harsh humidity conditions, *Sustain. Energy Fuels*, 2024, **8**(9), 1953–1965, DOI: [10.1039/d3se01483e](https://doi.org/10.1039/d3se01483e).

165 M. Bonomo, B. Taheri, L. Bonandini, S. Castro-Hermosa, T. M. Brown, M. Zanetti, A. Menozzi, C. Barolo and F. Brunetti, Thermosetting polyurethane resins as Low-Cost, easily scalable, and effective oxygen and moisture barriers for perovskite solar cells, *ACS Appl. Mater. Interfaces*, 2020, **12**(49), 54862–54875, DOI: [10.1021/acsami.0c17652](https://doi.org/10.1021/acsami.0c17652).

166 J. A. Baker, Y. Mouhamad, K. E. A. Hooper, D. Burkitt, M. Geoghegan and T. M. Watson, From spin coating to roll-to-roll: investigating the challenge of upscaling lead halide perovskite solar cells, *IET Renew. Power Gener.*, 2016, **11**(5), 546–549, DOI: [10.1049/iet-rpg.2016.0683](https://doi.org/10.1049/iet-rpg.2016.0683).

167 P. W.-K. Fong and G. Li, The challenge of ambient Air-Processed organometallic halide perovskite: technology transfer from spin coating to meniscus blade coating of perovskite thin films, *Front. Mater.*, 2021, **8**, 635224, DOI: [10.3389/fmats.2021.635224](https://doi.org/10.3389/fmats.2021.635224).

168 J. H. Heo, M. H. Lee, M. H. Jang and S. H. Im, Highly efficient CH<sub>3</sub>NH<sub>3</sub>PbI<sub>3</sub>–xCl<sub>x</sub> mixed halide perovskite solar cells prepared by re-dissolution and crystal grain growth via spray coating, *J. Mater. Chem. A*, 2016, **4**(45), 17636–17642, DOI: [10.1039/c6ta06718b](https://doi.org/10.1039/c6ta06718b).

169 C.-F. Li, *et al.*, High-Performance Perovskite Solar Cells and Modules Fabricated by Slot-Die Coating with Nontoxic Solvents, *Nanomaterials*, 2023, **13**(11), 1760, DOI: [10.3390/nano13111760](https://doi.org/10.3390/nano13111760).

170 A. Babayigit, A. Ethirajan, M. Muller and B. Conings, Toxicity of organometal halide perovskite solar cells, *Nat. Mater.*, 2016, **15**(3), 247–251, DOI: [10.1038/nmat4572](https://doi.org/10.1038/nmat4572).

171 World Health Organization: WHO, “Lead Poisoning”, Sep. 27, 2024, <https://www.who.int/news-room/fact-sheets/detail/lead-poisoning-and-health>.

172 D. Patsiou, *et al.*, Exposure to Pb-halide perovskite nanoparticles can deliver bioavailable Pb but does not alter endogenous gut microbiota in zebrafish, *Sci. Total Environ.*, 2020, **715**, 136941, DOI: [10.1016/j.scitotenv.2020.136941](https://doi.org/10.1016/j.scitotenv.2020.136941).

173 Y. Zhu, *et al.*, Systematic evaluation of the biotoxicity of Pb-based perovskite materials and perovskite solar cells, *J. Mater. Chem. A*, 2023, **12**(5), 2916–2923, DOI: [10.1039/d3ta06303h](https://doi.org/10.1039/d3ta06303h).

174 X. Ding, *et al.*, Lung toxicity and molecular mechanisms of Lead-Based perovskite nanoparticles in the respiratory system, *ACS Appl. Mater. Interfaces*, 2023, **15**(36), 42139–42152, DOI: [10.1021/acsami.3c04255](https://doi.org/10.1021/acsami.3c04255).

175 G. Li, *et al.*, Biotoxicity of halide perovskites in mice, *Adv. Mater.*, 2024, **36**(2), 2306860, DOI: [10.1002/adma.202306860](https://doi.org/10.1002/adma.202306860).

176 C. Yang, *et al.*, Influences of lead-based perovskite nanoparticles exposure on early development of human retina, *J. Nanobiotechnol.*, 2025, **23**(1), 144, DOI: [10.1186/s12951-025-03245-w](https://doi.org/10.1186/s12951-025-03245-w).

177 I. Maietta, *et al.*, The toxicity of lead and Lead-Free perovskite precursors and nanocrystals to human cells and aquatic organisms, *Advanced Science*, 2025, **12**, 2415574, DOI: [10.1002/advs.202415574](https://doi.org/10.1002/advs.202415574).

178 A. Pramanik, *et al.*, Water-Soluble and bright luminescent Cesium–Lead–Bromide Perovskite Quantum Dot–Polymer composites for Tumor-Derived exosome imaging, *ACS Appl. Bio Mater.*, 2019, **2**(12), 5872–5879, DOI: [10.1021/acsabm.9b00837](https://doi.org/10.1021/acsabm.9b00837).

179 J. Zheng, W. Zhang, Y. Huang, J. Shao, M. S. Khan and Y. Chi, Encapsulation of Pure Water-Stable Perovskite Nanocrystals (PNCs) into Biological Environment-Stable PNCs for Cell Imaging, *Inorg. Chem.*, 2024, **63**(12), 5623–5633, DOI: [10.1021/acs.inorgchem.3c04620](https://doi.org/10.1021/acs.inorgchem.3c04620).

180 B. Lyu, Y. Ouyang, D. Gao, Y. Hou and A. Zhang, Antibacterial cotton fabric with fluorescent properties based on bismuth-based perovskite quantum dots with silica coating, *Colloids Surf., A*, 2024, **694**, 134153, DOI: [10.1016/j.colsurfa.2024.134153](https://doi.org/10.1016/j.colsurfa.2024.134153).

181 P. Kumar, M. Patel, C. Park, H. Han, B. Jeong, H. Kang, R. Patel, W.-G. Koh and C. Park, Highly luminescent biocompatible CsPbBr<sub>3</sub>@SiO<sub>2</sub> core–shell nanoprobes for bioimaging and drug delivery, *J. Mater. Chem. B*, 2020, **8**(45), 10337–10345, DOI: [10.1039/d0tb01833c](https://doi.org/10.1039/d0tb01833c).

182 Y. Jiang, Z. Wang, W. Yang, P. Yang, X. Feng, P. Qin and F. Huang, Lead-Free Cs<sub>2</sub>Ag<sub>2</sub>BiBr<sub>6</sub>/TiO<sub>2</sub> S-Scheme Heterojunction for Efficient Photocatalytic Antibiotic Rifampicin Degradation, *Nano Lett.*, 2024, **24**, 12597–12604, DOI: [10.1021/ACS.NANOLETT.4C03648](https://doi.org/10.1021/ACS.NANOLETT.4C03648).

183 T. Yang, Y. Mei, L. Chen, X. Xu and J. Zhu, Nanofibrous La<sub>0.95</sub>K<sub>0.05</sub>MnO<sub>3</sub> perovskite with improved photoelectrical properties for photocatalytic degradation of antibiotics, *Phys. Scr.*, 2024, **99**(7), 075003, DOI: [10.1088/1402-4896/ad65c8](https://doi.org/10.1088/1402-4896/ad65c8).



184 R. M. Williams and A. Farawar, *Perovskite Solar Cells: Stability, Design Architecture, Photophysical Properties, and Morphology of the...*, ResearchGate, Jan. 2016, DOI: [10.13140/RG.2.1.1406.8242](https://doi.org/10.13140/RG.2.1.1406.8242).

185 B. Kammlander, S. Svanström, D. Kühn, F. O. L. Johansson, S. Sinha, H. Rensmo, A. G. Fernández and U. B. Cappel, Thermal degradation of lead halide perovskite surfaces, *Chem. Commun.*, 2022, **58**(97), 13523–13526, DOI: [10.1039/d2cc04867a](https://doi.org/10.1039/d2cc04867a).

186 Z. Wang, Z. Zhang, L. X. S. Wang, C. Yang, C. Fang and F. Hao, Recent advances and perspectives of photostability for halide perovskite solar cells, *Adv. Opt. Mater.*, 2022, **10**(3), 2101822, DOI: [10.1002/adom.202101822](https://doi.org/10.1002/adom.202101822).

187 D. Bryant, N. Aristidou, S. Pont, I. Sanchez-Molina, T. Chotchunangatchaval, S. Wheeler, J. R. Durrantab and S. A. Haque, Light and oxygen induced degradation limits the operational stability of methylammonium lead triiodide perovskite solar cells, *Energy Environ. Sci.*, 2016, **9**(5), 1655–1660, DOI: [10.1039/c6ee00409a](https://doi.org/10.1039/c6ee00409a).

188 A. Alpay, Ö. Tuna and E. B. Simsek, Deposition of perovskite-type  $\text{LaFeO}_3$  particles on spherical commercial polystyrene resin: A new platform for enhanced photo-Fenton-catalyzed degradation and simultaneous wastewater purification, *Environ. Technol. Innov.*, 2020, **20**, 101175, DOI: [10.1016/j.eti.2020.101175](https://doi.org/10.1016/j.eti.2020.101175).

